Reprinted from:
SPIN LABELING
Theory and Applications
© [redacted]
ACADEMIC PRESS, INC.
New York San Francisco London

3

Theory of Slow Tumbling ESR Spectra for Nitroxides

JACK H. FREED

DEPARTMENT OF CHEMISTRY
CORNELL UNIVERSITY
ITHACA, NEW YORK

I. Introduction 53
II. Theory 55
A. General Method 55
B. Rotational Modulation in Isotropic Liquids 60
C. Anisotropic Liquids 63
D. Exchange and Slow Tumbling 67
E. Nitroxides 69
III. Applications 71
A. Isotropic Liquids: Experiments 71
B. Simplified Methods of Estimating τ_R 83
C. Very Anisotropic Rotational Reorientation 91
D. Anisotropic Liquids: Simulations 96
E. Anisotropic Liquids: Experiments 104
F. Saturation and Nonlinear Effects 109
Appendix A. General Solutions and Discussion of the Computer Program for Nitroxides 112
Appendix B. Computer Program for Slow Tumbling Nitroxides in Isotropic Liquids 121
References 130

I. INTRODUCTION

In this chapter we develop the theory for slow tumbling in ESR spectroscopy, with specific application to nitroxide free radical spectra. The slow tumbling region is that range of rotational reorientation times for which the

ESR spectrum can no longer be described as a simple superposition of Lorentzian lines, characteristic of the fast motional or motional narrowing region, for which the theory developed in the previous chapter applies. In this chapter we further take it to be the region for which the ESR spectrum still shows effects of the motion; i.e., the motion is not so slow as to yield a proper rigid-limit spectrum. For nitroxide free radicals, this usually means we are considering the range of rotational correlation times 10^{-9} sec $\leqq \tau_R \leqq 10^{-6}$ sec. This is an important range for nitroxide probes in viscous media or for nitroxide spin labels attached to large macromolecules.

In this region, the spectra are affected in a complicated way by both the motions and the magnetic spin interactions. As a result, a theory which can deal rigorously with describing this region must be both powerful and general. It is our objective to set forth this theory, which has been developed in the last few years, and to emphasize its general foundations. The general theory is presented in Section II.A. It is a characteristic of the slow motional region that it requires that we ask more intricate questions about the detailed nature of the molecular motions in order to properly analyze the spectra than is true for studies in the motional narrowing region. Thus in much of the remainder of Section II the dynamics of molecular motions is developed to an extent concomitant with the need to explain actual slow tumbling experiments.

It has also been our objective to demonstrate how the general theory can be applied to actual cases. Thus in Section III we give a detailed discussion of comparisons between the theoretical predictions and recent experimental studies. Wherever it appears reasonable, we have tried to indicate simplified approaches in the analysis of slow tumbling spectra short of running detailed computer simulations. Nevertheless, there are many cases where the researcher will need detailed simulations tailored to his specific needs. For that reason, we have, in Appendix B, supplied the computer program that is applicable to isotropic liquids.

The development of the theory and the specific examples given here draw most heavily on the recent work of the Cornell group, with which the author is most familiar. Detailed references to other work can be found in a recent review article (Freed, 1972b). Recently, Polnaszek (1975b) has reviewed our methods and compared them with the other approaches. It should be emphasized that the slow tumbling theory is in many ways based on a generalization of stochastic theories of jump models for magnetic resonance (Abragam, 1962; Kubo, 1962, 1969; Johnson, 1965) and we sometimes make use of the analogies when appropriate. A familiarity with motional narrowing theory, such as is discussed in Chapter 2, would be useful preparation for this chapter, and a familiarity with quantum mechanics and some statistical mechanics is assumed in Section II.

II. THEORY

A. General Method

A quantum mechanical wave function Ψ can be expanded in a complete set of orthonormal functions U_n as

$$\Psi(t) = \sum_n c_n(t)U_n \tag{1}$$

The density matrix is defined to be

$$\rho_{nm}(t) = \overline{c_n(t)c_m^*(t)} \tag{2}$$

where the bar indicates an average over a statistical ensemble. A useful property of the density matrix is the calculation of the expectation value of an operator O for a system described by the wave function Ψ. Thus

$$\langle\Psi|O|\Psi\rangle = \sum_{m,n}\langle\Psi|U_m\rangle\langle U_m|O|U_n\rangle\langle U_n|\Psi\rangle = \sum_{m,n} c_n(t)c_m^*(t)O_{mn} \tag{3a}$$

and for an average expectation value of an ensemble of such systems we have

$$\overline{\langle\Psi|O|\Psi\rangle} = \sum_{n,m}\rho_{nm}O_{mn} = \mathrm{Tr}\ \rho O \tag{3b}$$

where Tr is the trace. The trace is invariant to the choice of the complete orthonormal basis set. Thus all the information for calculating observable quantities is contained in the density matrix.

Since the wave function Ψ will vary with time, the coefficients $c_n(t)$ will be functions of time, and this time dependence can be obtained from the time-dependent Schrödinger equation. Then the density matrix equation of motion, assuming the same Hamiltonian $\hat{\mathscr{H}}(t)$ for all members of the ensemble, is given by the quantum mechanical Liouville equation

$$\partial\rho/\partial t = -i[\hat{\mathscr{H}}(t), \rho] \tag{4}$$

Now assume that the time dependence of the spin Hamiltonian $\hat{\mathscr{H}}(t)$ for a free radical arises from interactions with its environment such that $\hat{\mathscr{H}}(t)$ is fully determined by a complete set of random variables Ω. Also assume that this time dependence of Ω is described by a stationary Markov process, so that the probability of being in a state Ω_1 at time t, if in state Ω_2 at time $t - \Delta t$, is (a) independent of the value of Ω at any time earlier than $t - \Delta t$ and (b) depends only on Δt and not on t. A stationary Markov process can be described by a differential equation

$$\partial P(\Omega, t)/\partial t = -\Gamma_\Omega P(\Omega, t) \tag{5}$$

where $P(\Omega, t)$ is the probability of the free radical being in a state Ω at time t.

Since the process is assumed stationary, Γ_Ω is independent of time. The evolution operator Γ_Ω is an operator only on the random variables Ω and is independent of spin space. Γ_Ω includes such general Markov operators as the diffusion operators given by the Fokker–Planck equations and transition rate matrices among discrete states $\Omega_1, \Omega_2, \ldots, \Omega_n$. In this discussion, $\Omega \equiv \alpha, \beta, \gamma$ will represent Euler angles specifying orientation and Γ_Ω will be a rotational diffusion operator.

It is also assumed that the stochastic process has a unique equilibrium distribution $P_0(\Omega)$ characterized by

$$\Gamma_\Omega P_0(\Omega) = 0 \tag{6}$$

We can show (Kubo, 1969; Freed *et al.*, 1971; Freed, 1972a) that Eqs. (4)–(6) lead to the stochastic Liouville equation of motion

$$\partial\rho(\Omega, t)/\partial t = -i[\hat{\mathscr{H}}(\Omega), \rho(\Omega, t)] - \Gamma_\Omega \rho(\Omega, t) \tag{7}$$

where $\rho(\Omega, t)$ is now understood to be the value of ρ associated with a particular value of Ω, hence of $\hat{\mathscr{H}}(\Omega)$. Thus, instead of looking at the explicit time dependence of the spin Hamiltonian $\hat{\mathscr{H}}(t)$ involving the interaction with its environment, the spin Hamiltonian is written in terms of random angle variables Ω and its modulation (due to rotational motions) is expressed by the time dependence of Ω.

The steady-state spectrum in the presence of a single rotating microwave frequency field is determined by the power absorbed from this field. We find for the λth hyperfine line at an orientation specified by Ω

$$P_\lambda(\Omega) = 2N\hbar\omega d_\lambda Z_\lambda^{(1)''}(\Omega) \tag{8}$$

where P_λ is the power absorbed, N is the concentration of electron spins, d_λ is a "transition moment" given by $d_\lambda = \frac{1}{2}\gamma_e H_1 \langle \lambda^- | \hat{S}_- | \lambda^+ \rangle$ (where $\hat{S}_-$ is the electron spin-lowering operator and $\lambda^\pm$ are the $M_S = \pm\frac{1}{2}$ states of the electron spin for the λth transition), and $Z_\lambda^{(1)''}$ is defined by the series of equations

$$(\rho - \rho_0)_\lambda = \chi_\lambda \tag{9}$$

$$\chi_\lambda = \sum_{n=-\infty}^{\infty} [\exp(in\omega t)] Z_\lambda^{(n)} \tag{10}$$

and

$$Z_\lambda^{(n)} = Z_\lambda^{(n)'} + iZ_\lambda^{(n)''} \tag{11}$$

(Actually, the experimentally observed signal is proportional to $Z_\lambda^{(1)''}$ and not to $d_\lambda Z_\lambda^{(1)''}$.)

In Eq. (9), $\rho_0(\Omega)$ is the equilibrium spin density matrix. Equation (8) displays the fact that it is the $n = 1$ harmonic, i.e., the component rotating with the microwave field, that is directly observed. In the case of simple lines we can identify $Z_\lambda^{(1)'}$ and $Z_\lambda^{(1)''}$ with the magnetization components M_x and M_y for the λth line in the rotating frame.

The notation for a matrix element of an operator O is

$$O_{ab} = \langle a | O | b \rangle \tag{12a}$$

$$O_\lambda = \langle \lambda^- | O | \lambda^+ \rangle \tag{12b}$$

$$O_{\lambda\pm} = \langle \lambda^\pm | O | \lambda^\pm \rangle \tag{12c}$$

where a, b are eigenstates and λ^+, λ^- are, respectively, the upper and lower electron spin states between which the λth ESR transition occurs. For a nitroxide there are three allowed ESR transitions.

The total absorption is then obtained as the equilibrium average of Eq. (8) over all Ω. Thus averages are introduced such as

$$\overline{Z_\lambda^{(n)}} = \int d\Omega Z_\lambda^{(n)}(\Omega) P_0(\Omega) \tag{13}$$

so that

$$P_\lambda = 2N\hbar\omega d_\lambda \overline{Z_\lambda^{(1)''}} \tag{14}$$

where d_λ has been taken to be independent of orientation. The total spin Hamiltonian $\hat{\mathscr{H}}(t)$, expressed in angular frequency units, is now separated into three components,

$$\hat{\mathscr{H}}(\Omega) = \hat{\mathscr{H}}_0 + \hat{\mathscr{H}}_1(\Omega) + \hat{\varepsilon}(t) \tag{15}$$

In the high-field approximation

$$\hbar\hat{\mathscr{H}}_0 = g_s\beta_e H_0 \hat{S}_z - \hbar \sum_i \gamma_i \hat{I}_{z_i} H_0 - \hbar\gamma_e \sum_i a_i \hat{S}_z \hat{I}_{z_i} \tag{16}$$

yields the zeroth-order energy levels and transition frequencies (cf. Chapter 2). $\hat{\mathscr{H}}_1(\Omega)$ is the perturbation depending on the orientation angles Ω, and, being a scalar, can be expressed as the scalar product of two tensors. That is, in general, we write $\hat{\mathscr{H}}_1(\Omega)$ as [in the notation of Freed and Fraenkel (1963)]

$$\hat{\mathscr{H}}_1(\Omega) = \sum_{L, m, m', \mu, i} \mathscr{D}^L_{-m, m'}(\Omega) F'^{(L, m)}_{\mu, i} A^{(L, m')}_{\mu, i} \tag{17}$$

where the $F'^{(L, m)}_{\mu, i}$ and $A^{(L, m')}_{\mu, i}$ are irreducible tensor components of rank L and component m, with the F' being spatial functions in molecule-fixed coordinates, while A consists only of spin operators quantized in the laboratory axis system. The subscripts μ and i refer to the type of perturbation and

to the different nuclei, respectively. The Wigner rotation matrix elements $\mathcal{D}^{(L)}_{-m,m'}(\Omega)$ include the transformation from the molecule-fixed axis system (x', y', z') into the laboratory axis system (x, y, z). We shall be concerned with the **A** and **g** tensors, for which $L = 2$. [It has been found that effects of the ^{14}N quadrupole tensor is negligible (Goldman *et al.*, 1972a; Goldman, 1973).] In addition,

$$\hat{\varepsilon}(t) = \tfrac{1}{2}\gamma_e H_1[\hat{S}_+ \exp(-i\omega t) + \hat{S}_- \exp(i\omega t)] \tag{18}$$

is the interaction of the electron spin with the oscillating magnetic radiation field. [When more than one oscillating field, e.g. ELDOR or ENDOR, is present and/or when field modulation effects are to be explicitly incorporated then Eq. (18) may be appropriately modified to include these effects.]

When we take the $\langle\lambda^-|\ |\lambda^+\rangle$ matrix elements of Eq. (7) and utilize Eqs. (9)–(11), we find the steady-state equation for $Z^{(n)}_\lambda$ to be

$$(n\omega - \omega_\lambda)Z^{(n)}_\lambda(\Omega) + [\hat{\mathscr{H}}_1(\Omega), Z^{(n)}(\Omega)]_\lambda - i[\Gamma_\Omega Z^{(n)}]_\lambda + d_\lambda[\chi^{(n-1)}_{\lambda+} - \chi^{(n-1)}_{\lambda-}] = q\omega_\lambda d_\lambda \tag{19}$$

[The superscripts to $\chi_{\lambda\pm}$ refer to harmonics in the sense of Eq. (10). The harmonic components of any other oscillating fields present may be introduced in a similar manner.] For reasonable temperatures and typical ESR field strengths we may write $\rho_0 = N'^{-1} - q\mathscr{H}_0$, where N' is the number of spin eigenstates of $\mathscr{H}_0$ and $q = \hbar/N'kT$. Also, $\hbar\omega_\lambda = E_{\lambda+} - E_{\lambda-}$ and the $Z^{(n)}_\lambda(\Omega)$ are spin matrices defined by Eqs. (9)–(11), and the $E_{\lambda\pm}$ are the eigenenergies of $\mathscr{H}_0$ for the $\lambda^\pm$ states.

It is convenient at this point to introduce a "symmetrizing" transformation for the evolution operator. It is not needed for isotropic liquids but becomes useful for anisotropic liquids.
Thus

$$\tilde{\Gamma}_\Omega = P_0^{-1/2}\Gamma_\Omega P_0^{1/2} \tag{20}$$

and similarly

$$\tilde{Z}^{(n)}_\lambda(\Omega) = P_0^{-1/2}[Z^{(n)}_\lambda(\Omega)P_0] \tag{21}$$

This transformation usually renders Γ_Ω Hermitian. Now, Eqs. (6) and (20) combine to give

$$\tilde{\Gamma}_\Omega P_0^{1/2} = 0 \tag{22}$$

Equations (21) and (13) yield

$$\overline{Z^{(n)}_\lambda} = \int d\Omega P_0^{1/2}\tilde{Z}^{(n)}_\lambda(\Omega) \tag{23}$$

and Eq. (19) with Eqs. (20)–(21) becomes

$$(n\omega - \omega_\lambda)\tilde{Z}^{(n)}_\lambda(\Omega) + [\hat{\mathscr{H}}_1(\Omega), \tilde{Z}^{(n)}(\Omega)]_\lambda - i[\tilde{\Gamma}_\Omega Z^{(n)}]_\lambda + d_\lambda[\tilde{\chi}^{(n-1)}_{\lambda+} - \tilde{\chi}^{(n-1)}_{\lambda-}] = q\omega_\lambda d_\lambda P_0^{1/2} \tag{24}$$

In order to solve for the absorption, Eq. (23), we first solve the diffusion equation (5). As in quantum mechanics, the solution of such a partial differential equation can be expressed in terms of a complete orthonormal set of eigenfunctions, call them $G_m(\Omega)$, such that

$$\tilde{\Gamma}_\Omega G_m(\Omega) = \tau_m^{-1} G_m(\Omega) \tag{25}$$

where τ_m^{-1} is the mth "eigenvalue." We generally find

$$G_0(\Omega) = P_0^{1/2} \tag{25a}$$

Then we expand matrix elements of $\tilde{Z}^{(n)}_\lambda(\Omega)$ in the complete orthonormal set $G_m(\Omega)$:

$$\tilde{Z}^{(n)}_\lambda(\Omega) = \sum_m [C^{(n)}_m(\omega)]_\lambda G_m(\Omega) \tag{26}$$

where the coefficient $C^{(n)}_m(\omega)$ is an operator in spin space and is a function of ω, but is independent of Ω.

Substituting Eq. (26) into Eq. (24), premultiplying the resulting equation by $G^*_m(\Omega)$, and then integrating over Ω and taking advantage of the orthonormal properties of $G_m(\Omega)$, we obtain

$$[(n\omega - \omega_\lambda) - i\tau_m^{-1}][C^{(n)}_m]_\lambda + \sum_{m'}\int d\Omega G^*_m(\Omega)[\hat{\mathscr{H}}_1(\Omega), C^{(n)}_{m'}]_\lambda C_{m'}(\Omega) + d_\lambda([C^{(n-1)}_m]_{\lambda+} - [C^{(n-1)}_m]_{\lambda-}) = q\omega_\lambda d_\lambda\ \delta(m, 0)\,\delta(n, 1) \tag{27}$$

Since the absorption, Eq. (14), depends only on $Z^{(1)}_\lambda$, then solving Eq. (27) for $[C^{(1)}_0]_\lambda$ for all allowed transitions will give the spectral line shapes.

In the absence of saturation we can set $d_\lambda = 0$ on the left-hand side of Eq. (27) and then let $n = 1$, to obtain the needed expression.

A rotationally invariant Lorentzian linewidth T_2^{-1} can be included in Eq. (19) or Eq. (27) by letting

$$\omega_\lambda \to \omega_\lambda + iT_2^{-1} \tag{28}$$

In the near-rigid limit, this linewidth corresponds to the linewidth in a single crystal, or more precisely to a residual linewidth in a powder spectrum. More generally, an angular variation of the width can be introduced. For simplicity, this variation is allowed to take the form

$$T_2^{-1}(\theta) = \alpha + \beta\cos^2\theta \tag{29}$$

where θ is the angle between the magnetic field axis and the molecular z axis.

The above equations yield coupled complex algebraic equations for the coefficients $[C_m^{(n)}]_\lambda$, and we attempt to solve for these equations utilizing only a finite number of coefficients. (The complete orthonormal set includes an infinite number of such eigenfunctions.) The convergence depends essentially on the ratio $|\mathscr{H}_1(\Omega)|/\tau_m^{-1}$. The larger the value of this ratio of off-diagonal to diagonal terms, the more terms $[C_m^{(n)}]_\lambda$ that are needed. The results obtained by relaxation theory valid in the fast motional limit (cf. Chapter 2) are recovered when only one order beyond $[C_0^{(1)}]_\lambda$ is included.

B. Rotational Modulation in Isotropic Liquids

When the general method of the previous section is applied to rotational modulation, Ω refers to the Euler angles for a tumbling molecular axis with respect to a fixed laboratory axis system. For a molecule undergoing many collisions, causing small random angular reorientations, the resulting isotropic Brownian rotational motion is a Markov process, which can be described by the rotational diffusion equation (Freed *et al.*, 1971; Freed, 1972a,b)

$$\partial P(\Omega, t)/\partial t = R\,\nabla_\Omega^2 P(\Omega, t) \tag{30}$$

where ∇_Ω^2 is the Laplacian operator on the surface of a unit sphere and R is the rotational diffusion coefficient. If the molecule is approximated by a rigid sphere of radius a rotating in a medium of viscosity η, then a rotational Stokes–Einstein relationship yields

$$R = kT/8\pi a^3\eta \tag{31}$$

In an isotropic liquid, the equilibrium probability $P_0(\Omega)$ of Eq. (6) will be equal for all orientations, so that $P_0(\Omega) = 1/8\pi^2$. Here the Markov operator Γ_Ω, Eq. (5), for isotropic Brownian rotation, Eq. (30), is $-R\nabla_\Omega^2$, which is formally the Hamiltonian for a spherical top whose orthonormal eigenfunctions are the normalized Wigner rotation matrices or generalized spherical harmonics:

$$G_m \rightarrow \phi_{KM}^L(\Omega) = [(2L+1)/8\pi^2]^{1/2}\mathscr{D}_{K,M}^L(\Omega) \tag{32}$$

with eigenvalues $RL(L+1)$ (Freed, 1964, 1972a). Note that for $K = 0$, $\mathscr{D}_{0M}^L(\alpha, \beta, \gamma) = [4\pi/(2L+1)]^{1/2}Y_{LM}(\beta, \gamma)$, where Y_{LM} is the well-known spherical harmonic (Rose, 1954; Edmonds, 1957).

Similarly, the Markov operator for axially symmetric Brownian rotation about a molecule-fixed z axis is formally the Hamiltonian for a symmetric top whose symmetry axis is the z axis. The orthonormal eigenfunctions are again the normalized Wigner rotation matrices with eigenvalues given by

$$\Gamma_\Omega\phi_{KM}^L = [R_\perp L(L+1) + (R_\parallel - R_\perp)K^2]\phi_{KM}^L \tag{33}$$

where $R_\perp$ and $R_\parallel$ are the rotational diffusion constants about the x, y axes and z axis, respectively (Freed, 1964; Favro, 1965). The "quantum numbers" K and M of the Wigner rotation matrices refer to projections along the body-fixed symmetry axis and along a space-fixed axis, respectively.

For completely asymmetric Brownian rotation (Freed, 1964, 1972a; Favro, 1965) $R_x \neq R_y \neq R_z$, where R_x, R_y, and R_z are the respective rotational diffusion constants about the x, y, and z axes, the Markov operator Γ_Ω has more complex solutions (see below). Also, for fast rotation about one axis (e.g., the z axis, so that $R_z \gg R_x, R_y$), the completely asymmetric rotation can be treated as axially symmetric with eigenvalues $R_+ L(L+1) + (R_z - R_+)K^2$, where $R_\pm = \frac{1}{2}(R_x \pm R_y)$.

In the fast rotational motion region, all rotational reorientation processes yield the same ESR line shapes, which, as predicted by earlier relaxation theories, yields Lorentzian lines (Abragam, 1961; Freed and Fraenkel, 1963). Naturally, in the very slow rotational motion region all models should tend to the rigid-limit powder line shape of the equilibrium distribution. However, in the intermediate slow rotational region $|\mathscr{H}_1(t)|\tau_R \lesssim 1$, the ESR line shapes are found to be sensitive to the details of the molecular reorientation process.

A number of different models for rotational reorientation can be proposed. Some useful ones are: (a) Brownian rotational diffusion; (b) free diffusion in which a molecule rotates freely for time τ (i.e., inertial motion with $\tau = I/B$, with I the moment of inertia and B the friction coefficient) and then reorients instantaneously; and (c) jump diffusion in which a molecule has a fixed orientation for time τ and then "jumps" instantaneously to a new orientation (Goldman *et al.*, 1972; Egelstaff, 1970). For isotropic reorientation, we can summarize the results for these models as

(a) $$\tau_L^{-1} = L(L+1)R \tag{34}$$

(b) $$\tau_L^{-1} = L(L+1)R/[1 + L(L+1)R\tau]^{1/2} \tag{35}$$

and

(c) $$\tau_L^{-1} = \tau^{-1}\left\{1 - (2L+1)^{-1}\int_0^\pi d\varepsilon W(\varepsilon)[\sin(L+\tfrac{1}{2})\varepsilon/\sin(\tfrac{1}{2}\varepsilon)]\right\} \tag{36}$$

where $W(\varepsilon)$ is the distribution function for diffusive steps by angle ε and is normalized so that

$$\int_0^\pi W(\varepsilon)\,d\varepsilon = 1 \tag{37}$$

One convenient form for $W(\varepsilon)$ is

$$W(\varepsilon) = A \sin(\tfrac{1}{2}\varepsilon) \exp(-\varepsilon/\theta) \tag{38}$$

where A is a normalization constant. For $\theta \ll \pi$, we obtain

$$\tau_L^{-1} = L(L+1)R/[1 + R\tau L(L+1)] \tag{39}$$

and

$$(\varepsilon^2)_{avg} = 6\theta^2 \tag{40}$$

where $R\tau$ is proportional to the size of a mean diffusive step when the diffusion coefficient is defined as

$$R = (\varepsilon^2)_{avg}/6\tau \tag{41}$$

Other possible choices for $W(\varepsilon)$ are summarized elsewhere (Goldman *et al.*, 1972). A good formal theoretical discussion of jump diffusion as has been employed here is given by Cukier and Lakatos-Lindenberg (1972); also the basic work of Ivanov on jump diffusion has recently been reviewed by Valiev and Ivanov (1973).

It should be noted that Eq. (35) is only an approximate expression for free diffusion. Since free diffusion includes inertial effects, the orientation of the molecule is not properly described as a simple Markovian process. A more accurate treatment of free diffusion must include angular momentum as well as orientational degrees of freedom, but recent work by Bruno and Freed (1974b) shows that the results for the more complete formulation of free diffusion are similar to those obtained using the simple model.

A comparison of Eqs. (34)–(36) shows that the L dependence of τ_L depends on the choice of reorientational model. Thus in the slow motional region, where the line shape is simulated in terms of an expansion in $\mathscr{D}^L_{K,M}$ with eigenvalues $\tau^{-1}_{L,K}$, the ESR spectra will be model sensitive. We can summarize these equations with the simple expression

$$\tau_L^{-1} = B_L L(L+1)R \tag{42}$$

with the "model parameter" $B_L = 1$ for Brownian motion; $B_L = [1 + L(L+1)]^{-1}$ for strong jump diffusion with $R\tau = 1$; and $B_L = [1 + L(L+1)]^{-1/2}$ for free diffusion and $R\tau = 1$. For purposes of comparison, the definition of τ_R is generalized to

$$\tau_R \equiv (6B_2R)^{-1} \tag{43}$$

where B_2 is the appropriate model parameter for $L = 2$. Thus in the motionally narrowed region, where only the $L = 2$ term is important, it follows from Eqs. (42) and (43) that all models yield the same Lorentzian width for the same value of τ_R.

For anisotropic rotational diffusion, there are no convenient solutions for the jump and free diffusion models. The most straightforward course then is to generalize the equations for spherically symmetric rotation. Thus we let

$$\tau^{-1}_{L,K} = (B_L/R_\perp)[R_\perp L(L+1) + (R_\parallel - R_\perp)K^2] \tag{44}$$

where B_L is the same model parameter as in Eq. (42). In effect, it is assumed in Eq. (44) that although the L dependence of $\tau^{-1}_{L,K}$ is model dependent, the "quantum number" K plays the same role in all models (Goldman *et al.*, 1972a). Other interpretations of the model dependence in terms of more fundamental analyses of microscopic molecular dynamics have been discussed by Hwang *et al.* (1975).

C. Anisotropic Liquids

Suppose now that the liquid has a preferred axis of orientation, i.e., the director axis (cf. Chapter 8). We now write the perturbing Hamiltonian (17) as (Polnaszek *et al.*, 1973) [with the $(-1)^K$ which was included into the $F'^{(L,K)}_{\mu,i}$ of Eq. (17) now explicitly displayed]:

$$\mathscr{H}_1(\Omega, \Psi) = \sum_{\substack{L,M,M' \\ K,\mu,i}} (-1)^K \mathscr{D}^L_{-KM'}(\Omega)\mathscr{D}^L_{M'M}(\Psi)F'^{(L,K)}_{\mu,i}A^{(L,M)}_{\mu,i} \tag{45}$$

Equation (45) is based on two sets of rotations of the coordinate systems: first from the molecular axis system (x', y', z') into the director axis system (x'', y'', z'') with Euler angles $\Omega = (\alpha\beta\gamma)$; and then into the laboratory axis system (x, y, z) with Euler angles Ψ. The orientation of the director relative to the laboratory frame can be specified by the two polar angles θ' and ϕ' such that $\Psi = (0, \theta', \phi')$. More precisely, one means by the molecular coordinate system (x', y', z') the principal axis system for the orientation of the molecule in the mesophase. It may also be necessary to transform from the principal axis system of the magnetic interactions (x''', y''', z''') to the (x', y', z') system with Euler angles Θ, according to

$$F'^{(L,K)}_{\mu,i} = \sum_{K'} \mathscr{D}^L_{K,K'}(\Theta)F'''^{(L,K')}_{\mu,i} \tag{46}$$

where $\Theta = (\alpha', \beta', \gamma')$.

The diffusion equation for a particle undergoing Brownian rotational diffusion in the presence of a potential V is given by (Favro, 1965; Polnaszek and Freed, 1975; Polnaszek, 1975a)

$$\frac{\partial P(\Omega, t)}{\partial t} = -\nabla \cdot \left[\mathbf{R} \cdot \frac{\nabla V(\Omega)}{kT} + \mathbf{R} \cdot \nabla\right] P(\Omega, t) \equiv -\Gamma_\Omega P(\Omega, t) \tag{47}$$

where $V(\Omega)$ can be taken to be the orienting pseudopotential for a liquid crystal, $\cdot\mathcal{M}$ is the vector operator, which generates an infinitesimal rotation, and is identified with the quantum mechanical angular momentum operator for a rigid rotator, and $\mathbf{R}$ is the diffusion tensor of the molecule. Both $\mathbf{R}$ and $\cdot\mathcal{M}$ are defined in the (x', y', z') molecular coordinate system. The angular momentum operator $\cdot\mathcal{M}$ is defined by

$$\mathcal{M}^2\phi^L_{KM}(\Omega) = L(L+1)\phi^L_{KM}(\Omega) \tag{48a}$$

$$\mathcal{M}_\pm\phi^L_{KM}(\Omega) = [(L \mp K)(L \pm K + 1)]^{1/2}\phi^L_{K\pm1,M}(\Omega) \tag{48b}$$

$$\mathcal{M}_{z'}\phi^L_{KM}(\Omega) = K\phi^L_{KM}(\Omega) \tag{48c}$$

where the $\phi^L_{KM}(\Omega)$ are the eigenfunctions of $\mathcal{M}^2$ and $\mathcal{M}_{z'}$, given by Eq. (32), and

$$\mathcal{M}_\pm = \mathcal{M}_{x'} \pm i\mathcal{M}_{y'} \tag{49}$$

When $V = 0$, Eq. (47) is simply the equation for (asymmetric) Brownian rotational diffusion in isotropic liquids. [Simpler expressions have been given for special cases by Nordio and Busolin (1971), Nordio *et al.* (1972), and Polnaszek *et al.* (1973).] Equation (47) is based on the assumption that the external torque $\mathbf{T}$ is derived from the potential $V(\Omega)$:

$$\mathcal{T} = -i\cdot\mathcal{M}V(\Omega) \tag{50}$$

[Cf. Eq. (30), where we have set $\nabla^2_\Omega = -\mathcal{M}^2$.] The equilibrium solution to Eq. (47) is given by

$$P_0(\Omega) = \frac{\exp[-V(\Omega)/kT]}{\int d\Omega \exp[-V(\Omega)/kT]} \tag{51}$$

When the symmetrized forms of Eqs. (20)–(22) are used, we obtain the diffusion equation

$$\partial\tilde{P}(\Omega, t)/\partial t = -\tilde{\Gamma}_\Omega\tilde{P}(\Omega, t) \tag{52}$$

where

$$\tilde{\Gamma}_\Omega = \cdot\mathcal{M}\cdot\mathbf{R}\cdot\cdot\mathcal{M} + \frac{(\cdot\mathcal{M}\cdot\mathbf{R}\cdot V)}{2kT} + \frac{\mathcal{T}\cdot\mathbf{R}\cdot\mathcal{T}}{(2kT)^2} \tag{53}$$

The restoring potential for liquid crystals can be written in its most general form as

$$V(\Omega) = \sum_{L,K,M}\varepsilon^L_{KM}\mathcal{D}^L_{KM}(\alpha, \beta, \gamma) \tag{54}$$

The assumption of cylindrical symmetry about the director axis $\mathbf{n}$ implies that all averages taken over the angle γ vanish unless $M = 0$ (Glarum and

Marshall, 1966, 1967). The uniaxial property of nematic liquid crystals (i.e. $\mathbf{n} \equiv -\mathbf{n}$) implies that L must be even. It is useful to use the linear combinations of the $\mathcal{D}^L_{KM}$ that are of definite parity, i.e., the real linear combination

$$V(\Omega) = \sum_{\text{even } L}^{\infty}\left(\varepsilon^L_0\mathcal{D}^L_{00}(\Omega) + \sum_{K>0}^{L}\varepsilon^L_{K\pm}[\mathcal{D}^L_{K0}(\Omega) \pm \mathcal{D}^L_{-K0}(\Omega)]\right) \tag{55}$$

These have simpler properties for molecular symmetries less than cylindrical.

Usually we consider only the leading term $\varepsilon^2_0\mathcal{D}^2_{00}(\Omega)$, i.e., the Meier-Saupe (1958) potential. The cylindrically symmetric case when $\varepsilon^4_0 \neq 0$ has also been considered (Polnaszek *et al.*, 1973) and it was shown that typical ESR spectral predictions are not very sensitive to having $\varepsilon^4_0 \neq 0$. In general however, we expect the terms for $L > 2$ to be less important than those for $L = 2$, and we can approximate

$$V(\Omega) \simeq \varepsilon^2_0\mathcal{D}^2_{00}(\Omega) + \sum_{K>0}^{2}\varepsilon^2_{K\pm}[\mathcal{D}^2_{K0}(\Omega) \pm \mathcal{D}^2_{-K0}(\Omega)] \tag{56}$$

The ε^2_0 and $\varepsilon^2_{K\pm} = \varepsilon^2_K \pm \varepsilon^2_{-K}$ (with the upper sign for $K > 0$, and the lower sign for $K < 0$) are themselves second-rank irreducible tensor components, so that, in the principal axis of molecular orientation system (x', y', z') their Cartesian components ε^2_{ij} are diagonalized, with $\mathrm{Tr}_i\,\varepsilon^2_{ii} = 0$, and complete specification is given by just ε^2_0 and ε^2_{2+}. [Equation (56) can be thought of as the scalar product of second-rank irreducible tensors.] The ordering tensor is defined by

$$\langle\mathcal{D}^L_{KM}(\Omega)\rangle = \int d\Omega P_0(\Omega)\mathcal{D}^L_{KM}(\Omega) \tag{57}$$

where $L = 2$ and $M = 0$. It is also a second-rank irreducible tensor whose symmetry properties are related to those of the $\varepsilon^2_{K\pm}$. Thus from Eqs. (51) and (56) and the orthogonality of the $\mathcal{D}^L_{KM}(\Omega)$ terms it follows that in the (x', y', z') system only $\langle\mathcal{D}^2_{00}(\Omega)\rangle$ and $\langle\mathcal{D}^2_{20} + \mathcal{D}^2_{-20}\rangle$ are nonzero, i.e., $\langle\mathcal{D}^2_{KM}(\Omega)\rangle$ is also diagonalized. Thus the "diagonalized" potential (retaining only $L = 2$ terms) becomes

$$V(\Omega) = \varepsilon^2_0\mathcal{D}^2_{00}(\Omega) + \varepsilon^2_{2+}[\mathcal{D}^2_{20}(\Omega) + \mathcal{D}^2_{-20}(\Omega)] \tag{58}$$

or equivalently

$$V(\alpha, \beta) = \gamma_2\cos^2\beta + \varepsilon\sin^2\beta\cos 2\alpha \tag{58'}$$

where $\varepsilon^2_0 = 2\gamma_2/3$ and $\varepsilon^2_{2+} = 2\varepsilon(6)^{-1/2}$. For molecules in which the molecular x' and y' axes are aligned to different extents, ε is nonzero. If we choose the orientation coordinate system such that the z' axis tends to align to a

greater degree either parallel or perpendicular to the director than does the x' axis or the y' axis, we have $|\gamma_2| > |\varepsilon|$. The case $\varepsilon < 0$ corresponds to the y' axis being ordered preferential to the x' axis along the direction of $\mathbf{n}$ and/or to the x' axis being ordered to a greater degree perpendicular to the $\mathbf{n}$ than is the y' axis.

We can utilize Eqs. (50), (48b) and (48c) to obtain $\mathscr{T}$ from the potential in Eq. (58) in terms of its components in the (x', y', z') coordinate system:

$$\mathscr{T}_{\pm} \equiv \mathscr{T}_{x'} \pm i\mathscr{T}_{y'} = \pm i(\sin 2\beta)(\varepsilon e^{\mp i\alpha} - \gamma_2 e^{\pm i\alpha}) \tag{59a}$$

$$\mathscr{T}_{z'} = -2\varepsilon \sin^2\beta \sin 2\alpha \tag{59b}$$

We assume axially symmetric rotation about z' such that $R_{x'x'} = R_{y'y'} = R_\perp$ and $R_{z'z'} = R_\parallel$. Further, we introduce the definitions

$$\lambda \equiv -\gamma_2/kT \tag{60a}$$

and

$$\rho \equiv -\varepsilon/kT \tag{60b}$$

Then the symmetrized Markov operator defined in Eq. (52) becomes (Polnaszek and Freed, 1975; Polnaszek, 1975a)

$$\tilde{\Gamma} = .\mathscr{M} \cdot \mathbf{R} \cdot .\mathscr{M} - f(R_\perp, R_\parallel, \lambda, \rho, \Omega) \tag{61a}$$

where

$$f(R_\perp, R_\parallel, \lambda, \rho, \Omega) = \sum_{L=0,2,4} [X^L_{00}\mathscr{D}^L_{00} + \sum_{0<K\le L} X^L_{K0}(\mathscr{D}^L_{K0} + \mathscr{D}^L_{-K0})] \tag{61b}$$

with

$$X^0_{00} = -(2/15)[R_\perp(\lambda^2 + \rho^2) + 2R_\parallel\rho^2] \tag{62a}$$

$$X^2_{00} = 2\{R_\perp\lambda - [R_\perp(\lambda^2 + \rho^2) - 4R_\parallel\rho^2]/21\} \tag{62b}$$

$$X^4_{00} = 4[2R_\perp(\lambda^2 + \rho^2) - R_\parallel\rho^2]/35 \tag{62c}$$

$$X^2_{20} = 6^{1/2}\rho[\tfrac{1}{3}(R_\perp + 2R_\parallel) + \tfrac{2}{7}R_\perp\lambda] \tag{62d}$$

$$X^4_{20} = 4(10)^{1/2}R_\perp\rho\lambda/35 \tag{62e}$$

$$X^4_{40} = (8/35)^{1/2}R_\parallel\rho^2 \tag{62f}$$

and $.\mathscr{M} \cdot \mathbf{R} \cdot .\mathscr{M}$ is just the Γ_Ω of Eq. (33) with its associated eigenvalues.

We can also write the diffusion equation in terms of the general angular momentum operator $\mathscr{N}$ referred to the director frame (Favro, 1965). This is appropriate when $\mathbf{R}$ is diagonal in this frame, i.e., one has anisotropic viscosity. We then generate an analogous set of expressions (Polnaszek, 1975a;

Polnaszek and Freed, 1975). It is now assumed that $R_{xx} = R_{yy} = R_\perp$, $R_{zz} = R_\parallel$. The result is

$$\Gamma_\Omega = \mathscr{N} \cdot \mathbf{R}_n \cdot \mathscr{N} - \hat{R}_\perp \hat{f}(\lambda, \rho, \Omega) \tag{(}$$

where

$$\hat{f}(\lambda, \rho, \Omega) = \sum_{L=0,2,4} \left[\hat{X}^L_{00}\mathscr{D}^L_{00}(\Omega) + \sum_{0<K\le L} \hat{X}^L_{K0}(\mathscr{D}^L_{K0}(\Omega) + \mathscr{D}^L_{-K0}(\Omega))\right] \tag{(}$$

with

$$\hat{X}^0_{00} = -2(\lambda^2 + 3\rho^2)/15 \tag{6}$$

$$\hat{X}^2_{00} = 2[\lambda - (\lambda^2 - 3\rho^2)/21] \tag{6}$$

$$\hat{X}^4_{00} = 4(2\lambda^2 + \rho^2)/35 \tag{6}$$

$$\hat{X}^2_{20} = 6^{1/2}\rho[1 + (2\lambda/7)] \tag{6}$$

$$\hat{X}^4_{20} = 4(10)^{1/2}\lambda\rho/35 \tag{6}$$

$$\hat{X}^4_{40} = (8/35)^{1/2}\rho^2 \tag{6}$$

and

$$\mathscr{N} \cdot \mathbf{R} \cdot \mathscr{N} \cdot \phi^L_{KM} = [\hat{R}_\perp L(L+1) + (\hat{R}_\parallel - \hat{R}_\perp)M^2]\phi^L_{KM} \tag{(}$$

It is shown in Appendix A how the slow tumbling equations for isotro liquids can be simply modified to deal with anisotropic liquids in the sim case of a Meier–Saupe potential and with $\Psi = (0, 0, 0)$ and $\Theta = (0, 0,$ (except that permutation of the labeling of the molecular axis system permitted). The more complex expressions for the general cases are given Polnaszek (1975a).

Finally, note that when $|\lambda| \gg 1$, and the eigenfunction expansion $\Phi^L_{KM}(\Omega)$ is only slowly convergent for solutions of the diffusion equati then there are other types of eigenfunction expansions, specifically tailo to these limiting cases, which become very useful (Polnaszek *et al.*, 197

D. Exchange and Slow Tumbling

In cases where the concentration of nitroxide spin probes is high, we a have to consider the effects of Heisenberg spin exchange. This phenomer involves bimolecular collisions of radicals during which time an excha integral J' is turned on, and, because of the Pauli principle, can be written an added term in the spin Hamiltonian:

$$\mathscr{H}_{SS} = J(t)\mathbf{S}_1 \cdot \mathbf{S}_2 \tag{(}$$

where $J = 2J'$ and is time dependent due to the relative motion of the radical pairs. Its effect (viewed from an ESR point of view) is to cause the electron spins to exchange their nuclear environments.

A rigorous analysis of exchange (cf. Freed, 1967; Eastman *et al.*, 1969) shows that we can add to the left side of Eq. (19) for the allowed transitions λ, the terms:

$$-i\omega_{SS}\left(1 - \frac{2D_\lambda}{N'}\right)Z_\lambda + i\omega_{SS}\sum_{\eta\neq\lambda}\frac{2D_\eta}{N'}Z_\eta \tag{68}$$

where D_λ and D_η are the degeneracies of the λth and ηth allowed ESR transitions, respectively. That is, for nitroxides $D_\lambda = D_\eta = 1$ and $N' = 6$. The sum in Eq. (68) is over all allowed transitions η not equal to λ. Also, the effective exchange frequency ω_{SS} obeys

$$\omega_{SS} = \tau_2^{-1}[J^2\tau_1^2/(1 + J^2\tau_1^2)] \tag{69}$$

where τ_2 is the mean time between successive new bimolecular encounters of radicals, and τ_1 is the lifetime of the interacting pair. In the case of simple Brownian diffusion of uncharged radicals in solution we can write (Eastman *et al.*, 1969; Pedersen and Freed, 1973a, b):

$$\tau_2^{-1} = 4\pi dDN \tag{70}$$

$$\tau_1^{-1} = D/d\Delta r_J \tag{71}$$

where N is the density of radicals, d is the "interaction distance" for $J(r)$ which is nonzero (and equal to J) only in the range of $d < r < d + \Delta r_J$, and the diffusion coefficient in a Stokes–Einstein model is

$$D = kT/6\pi a\eta \tag{72}$$

Expression (68) is only appropriate for the allowed transitions, which then couple together by this mechanism. For each forbidden ESR transition (see below), we have instead of (68) to add the term to the left side of Eq. (19)

$$-i\omega_{SS}Z_\kappa \tag{73}$$

If we make the simplifying assumption that ω_{SS} is independent of any orientational effects [i.e., $J(r)$ is taken as a function only of the relative internuclear separation of the radical pair], then (68) and (73) can be added to the LHS of Eq. (27), where we let $Z_\lambda(\Omega) \rightarrow [C_m^{(n)}]_\lambda$, etc.

Expressions (69) and (70) are based on a simple contact-exchange model (Eastman *et al.*, 1969). More complex models of the motional modulation of $J(\mathbf{r}_1, \mathbf{r}_2)$ can also be dealt with (Pedersen and Freed, 1973a,b). Effects of radical charge and/or electrolyte concentration on Eqs. (70) and (71) must also be considered (Eastman *et al.*, 1970). Expressions (68) and (73) are also

useful for two-dimensional motions, but Eqs. (69)–(72) would have to modified. Also, in general, effects of intermolecular electron-spin dipo interactions become important at higher concentrations as the motions sl down (Eastman *et al.*, 1969).

E. Nitroxides

For nitroxides, there are three allowed ESR transitions and six forbidd transitions which must be considered in a rigorous solution of Eq. (27). Th are illustrated in Fig. 1a. The asymmetric g tensor $\mathbf{g}$ and the hyperfine tens $\mathbf{A}$ yield an $\hat{\mathscr{H}}_1(\Omega)$ given by

$$\begin{aligned}\hat{\mathscr{H}}_1(\Omega) = {} & \mathscr{D}^2_{0,0}(\Omega)[F_0 + D'\hat{I}_z]\hat{S}_z + [\mathscr{D}^2_{-2,0}(\Omega) + \mathscr{D}^2_{2,0}(\Omega)] \\ & \times (F_2 + D^{(2)\prime}\hat{I}_z)\hat{S}_z + [\mathscr{D}^2_{0,1}(\Omega)\hat{I}_+ - \mathscr{D}^2_{0,-1}(\Omega)\hat{I}_-]D\hat{S}_z \\ & + [\mathscr{D}^2_{-2,1}(\Omega) + \mathscr{D}^2_{2,1}(\Omega)]D^{(2)}\hat{I}_+\hat{S}_z \\ & - [\mathscr{D}^2_{-2,-1}(\Omega) + \mathscr{D}^2_{2,-1}(\Omega)]D^{(2)}\hat{I}_-\hat{S}_z \end{aligned} \tag{7}$$

where

$$F_i = \sqrt{\tfrac{2}{3}}g^{(i)}\hbar^{-1}\beta_e H_0 \tag{75}$$

$$g^{(0)} = 6^{-1/2}[2g_{z'} - (g_{x'} + g_{y'})] \tag{75}$$

$$g^{(2)} = \tfrac{1}{2}[g_{x'} - g_{y'}] \tag{75}$$

$$D = (|\gamma_e|/2\sqrt{6})(A_{x'} + A_{y'} - 2A_{z'}) \tag{76}$$

$$D^{(2)} = \tfrac{1}{4}|\gamma_e|(A_{y'} - A_{x'}) \tag{76}$$

with $D' = -(8/3)^{1/2}D$ and $D^{(2)\prime} = -(8/3)^{1/2}D^{(2)}$. The forbidden transitio 4–9 of Fig. 1a are coupled into the expressions for the allowed transitio because of the pseudosecular terms in Eq. (74), i.e., the terms involving $\hat{I}_\pm$ (where $\hat{I}_\pm$ are the nuclear spin raising and lowering operators). The Eul angles $\Omega \equiv \alpha, \beta, \gamma$ define the rotation between the laboratory coordina system (x, y, z) and the principal axis system in the molecular frame which the g and hyperfine tensors are diagonal. We assume they are dia onal in the same axis system [which is rigorously the x''', y''', z''' system, b

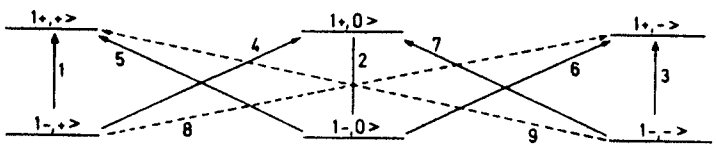

Fig. 1a. Energy levels and transitions for a nitroxide in high fields. Here $S = \frac{1}{2}$ and $I =$ and the notation is $|M_S, M_I\rangle$.

Eqs. (75a)–(75c) and (76a) and (76b) are written as though they correspond to the x', y', z' system].

It can be shown that the nuclear Zeeman term (which appears in the resonance frequencies of the forbidden transitions) makes a negligible contribution, so one can neglect it. Then it is only necessary to consider forbidden transitions 4 and 5, 6 and 7, and 8 and 9 in pairs, and this simplifies the expressions (see Appendix A).

We can now evaluate Eq. (27) (for $n = 1$) and the resulting expressions, neglecting saturation [i.e., set $d_\lambda = 0$ on the LHS of Eq. (27)], are given in Appendix A. They define an infinite set of coupled algebraic equations coupling the allowed and forbidden transitions. Only even values of the "quantum number" L appear for the allowed transitions for which $M = 0$. Also, one has the general restriction

$$0 \leqq K \leqq L \qquad \text{with } K \text{ even} \tag{77}$$

while $M = 1$ for the coefficients C^L_{KM} representing the "single forbidden" transition pairs (4, 5) and (6, 7) and $M = 2$ for the "doubly forbidden" pair (8, 9).

Approximations to the complete solution can be obtained by terminating the coupled equations at some finite limit by letting $C^L_{KM}(i) = 0$ for all $L > n_L$. While the number of equations needed to obtain a satisfactory convergent solution depends on the value of τ_R (the larger is τ_R, the greater is the value of n_L needed) the convergence also depends on the rotational reorientation model. The model that yields eigenvalues with the greatest dependence on L value in Eqs. (34)–(40) will have the fastest convergence. Therefore, in general, the convergence becomes poorer as one progresses from Brownian to simple free and intermediate jump, to strong collisional jump diffusion. For Brownian rotational diffusion with $\tau_R \sim 2 \times 10^{-8}$ sec, $n_L = 6$ is sufficient; with $\tau_R \sim 2 \times 10^{-7}$ sec, $n_L = 12$ is sufficient; and with $\tau_R \sim 2 \times 10^{-6}$ sec, $n_L = 24$ is sufficient. However, for simple free diffusion and $\tau_R \sim 2 \times 10^{-8}$ sec, $n_L = 10$ is needed and for a strong jump model $n_L = 16$ is needed. It is also often useful to terminate K at some value considerably less than n_L (i.e., for $n_K < n_L$). This would be especially applicable for isotropic or for axially symmetric reorientation about an axis parallel to the 2p π orbital of nitrogen, because in such a principal axis system, the **A** tensor is almost axially symmetric. Typical values for the nitroxide radical in this coordinate frame (cf. Table I) are $|F_0| \simeq 4.8$ G and $|D| \simeq 10.4$ G, while the asymmetric values are $|F_2| \simeq 1.6$ G and $|D^{(2)}| = 0.4$ G. These smaller terms are the coefficients for coupling the variable $\bar{C}^L_{KM}(i)$ with $K \neq 0$ into the problem, so their smallness guarantees faster convergence (cf. Appendix A). Also, if $R_\parallel \gg R_\perp$ or R_+, then this will greatly improve the convergence in K relative to that in L.

The computer program in Appendix B has provision for separate termi ating values for K and L. The number of coupled equations is then found be

$$r = 3 + \tfrac{9}{4}(n_L - \tfrac{1}{2}n_K + 1)n_K + \tfrac{3}{2}n_L, \qquad n_L \geq n_K, \quad n_K \geq 2 \tag{78}$$

or

$$r = 9 + 3(n_L - 2) \qquad \text{if } n_K = 0 \quad \text{and} \quad n_L \geqq 2 \tag{78}$$

A further reduction in the number of equations can be made by disti guishing between the allowed and forbidden transition coefficients. That is the coefficients for the allowed transitions $C^L_{K0}(i)$ are terminated at $L = r$ then the coefficients for the singly forbidden transitions $C^L_{K1}(j, k)$ are t minated at $L = n'$ and the doubly forbidden $C^L_{K2}(8, 9)$ at $L = n''$, whe $n', n'' \leqq n_L$. We have found that for convergence usually $n' \simeq n_L$ or $n_L -$ but n'' may be truncated at values significantly below n_L (e.g., wh $n_L = n' = 16$ was needed, $n'' = 8$ was sufficient). Also the terms of odd which exist only for the forbidden transitions, may be truncated at valu of $L \ll n_L$. The computer program in Appendix B also provides for the truncations.

III. APPLICATIONS

A. Isotropic Liquids: Experiments

The validity of the slow tumbling theory has now been carefu confirmed in studies on model systems of PADS (peroxylamine disulfona and PD-TEMPONE (perdeuterated 2,2,6,6-tetramethyl-4-piperidone oxyl) (cf. Fig. 1b) in viscous media (Goldman *et al.*, 1972a; Goldman, 19 Hwang *et al.*, 1975).

One of the most important requirements in analyzing a slow tumbli spectrum is to have accurate values for the magnetic tensors **A** and **g**. The are best obtained from viscous solutions in the same solvent as is the sl tumbling spectrum. This is because, in general, nitroxides will exhibit ma netic parameters which are rather solvent dependent. Figure 2 shows o

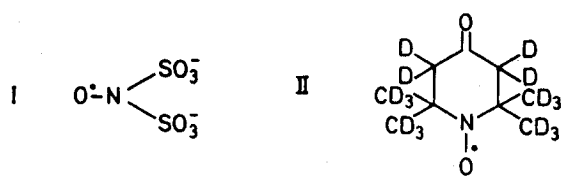

Fig. 1b. (I) Peroxylamine disulfonate anion (PADS). (II) Perdeuterated 2,2,6 tetramethyl-4-piperidone-1-oxyl (PD-TEMPONE).

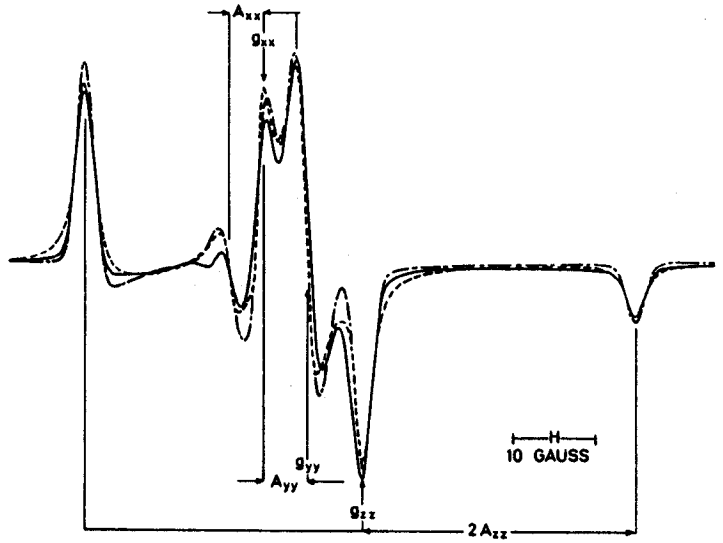

Fig. 2. Rigid limit spectrum (——) and simulations using Lorentizan (- - -) and Gaussian (· - - -) line shapes to the very well-resolved spectrum for PD-TEMPONE (cf. Fig. 1b) in toluene-d_8. See Table I for magnetic parameters. [Reprinted with permission from Hwang *et al., J. Phys. Chem.* **79**, 489–511 (1975). Copyright by the American Chemical Society.]

such rigid-limit spectrum from PD-TEMPONE in toluene-d_8 (Hwang *et al.*, 1975). This is a convenient case, where the solution can be cooled sufficiently without any changes in phase until a rigid-limit spectrum is achieved. This is a particularly well-resolved spectrum because the effects of magnetic interactions of intra- and intermolecular protons on the ESR have been replaced with much weaker deuteron interactions. Note that while A_z and g_z can be read from the spectrum, accurate determination of the other principal values of the hyperfine tensor requires careful computer simulation. The rigid-limit computer simulations were performed according to standard methods; a program listing for nitroxides appears in Polnaszek's thesis (1975a). Note that a Lorentzian line shape gives an overall better fit in this case. (Other cases show line shapes ranging from near Lorentzian to intermediate between Lorentzian and Gaussian.)

Table I gives accurate sets of magnetic parameters determined for PD-TEMPONE and PADS in a variety of solvents, as well as other nitroxide magnetic parameters.† In Table I the x axis is taken as being along the N–O bond, the z axis along the 2p π orbital of the nitrogen, and the y

† Editor's note: See also Appendix II (page 564) and Chapter 6, Table II (p. 247) for additional **g** and **A** data.

TABLE I

MAGNETIC PARAMETERS[a]

	PADS in frozen D_2O[b]	PADS in 85% glycerol-H_2O[b]	DTBN[c]	PADS in $(KSO_3)_2NOH$[d]	^{17}O PADS in 85% glycerol-H_2O[e]
g_x	2.0081 ± 0.0002	2.00785 ± 0.0002	2.00872 ± 0.00005	2.0094 ± 0.0004	—
g_y	2.0057 ± 0.0002	2.00590 ± 0.0002	2.00616 ± 0.00005	2.0055 ± 0.0004	—
g_z	2.0025 ± 0.0001	2.00265 ± 0.0001	2.00270 ± 0.00005	2.0026 ± 0.0004	—
$\langle g \rangle^f$	2.00543 ± 0.000017	2.00547 ± 0.00017	2.00586 ± 0.00005	2.0058 ± 0.0004	—
g_e[g]	2.00545 ± 0.00002	2.00548 ± 0.00001	—	—	—
$g(0)^h\|_{z'=z}$	−3.61 ± 0.15 × 10^{-3}	−3.47 ± 0.13 × 10^{-3}			
$\|_{z'=y}$	3.1 ± 1.5 × 10^{-4}	5.3 ± 1.4 × 10^{-4}	—	—	—
$g(2)^i\|_{z'=z}$	1.2 ± 0.1 × 10^{-3}	9.8 ± 1.0 × 10^{-4}			
$\|_{z'=y}$	−2.8 ± 0.1 × 10^{-3}	−2.6 ± 0.1 × 10^{-3}			
A_x (G)	5.5 ± 0.5	5.5 ± 0.5	—	—	—
A_y (G)	4.0 ± 0.5	5.0 ± 0.5	7.59 ± 0.05	7.7 ± 0.2	−8.7
A_z (G)	29.8 ± 0.3	28.7 ± 0.3	5.95 ± 0.05	5.5 ± 0.2	−8.7
$\langle A \rangle^j$ (G)	13.1 ± 0.4	13.1 ± 0.4	31.78 ± 0.05	27.5 ± 0.2	80.2 ± 0.8
$a_N{}^k$ (G)	13.11 ± 0.03	13.03 ± 0.04	15.11 ± 0.05	13.6 ± 0.2	—
$-D/2\pi\|_{z'=z}$	28.6 ± 0.6		—	—	20.92 ± 0.06
$\|_{z'=y}$	−15.6 ± 0.9	−13.8 ± 0.9			
$-D^{(2)}/2\pi\|_{z'=z}$	1.05 ± 0.7	0.35 ± 0.7	—	—	—
$\|_{z'=y}$	17.0 ± 0.6	16.2 ± 0.6			
$-D^{(2)}/2\pi\|_{z'=z}$			—	—	—
$\|_{z'=y}$					

TABLE I (*cont.*)

	PD-TEMPONE[p] in toluene-d_8	PD-TEMPONE[p] in 85% glycerol-d_3–D_2O	PD-TEMPONE[p] in Acetone-d_6	PD-TEMPONE[p] in Ethanol-d_6	PD-TEMPONE[p] in phase V^q
g_x	2.0096 ± 0.0002	2.0084 ± 0.0002	2.0095 ± 0.0003	2.0092 ± 0.0004	2.0097 ± 0.0002
g_y	2.0063 ± 0.0002	2.0060 ± 0.0002	2.0062 ± 0.0003	2.0061 ± 0.0004	2.0062 ± 0.0002
g_z	2.0022 ± 0.0001	2.0022 ± 0.0001	2.0022 ± 0.0002	2.0022 ± 0.0003	2.00215 ± 0.0001
$\langle g\rangle^f$	2.0060 ± 0.00017	2.0055 ± 0.00017	2.0060 ± 0.00027	2.0058_5 ± 0.0037	2.0060 ± 0.00017
g_s^g	2.00602 ± 0.00005	2.00570_5 ± 0.00005	2.00598 ± 0.00005	2.00589 ± 0.00005	2.00601 ± 0.00005
$g(0)^h$, $z' = z$	−4.68 ± 0.18 × 10^{-3}	−4.29 ± 0.18 × 10^{-3}	−4.63 ± 0.31 × 10^{-3}	−4.52 ± 0.43 × 10^{-3}	−4.74 ± 0.18 × 10^{-3}
$g(0)^h$, $z' = y$	3.4 ± 1.8 × 10^{-4}	3.6 ± 1.8 × 10^{-4}	2.7 ± 3.1 × 10^{-4}	2.6 ± 4.3 × 10^{-4}	2.2 ± 1.8 × 10^{-4}
$g(2)^i$, $z' = z$	1.65 ± 0.1 × 10^{-3}	1.2 ± 0.1 × 10^{-3}	1.7 ± 0.2 × 10^{-3}	1.6 ± 0.3 × 10^{-3}	1.75 ± 0.1 × 10^{-3}
$g(2)^i$, $z' = y$	−3.7 ± 0.1 × 10^{-3}	−3.1 ± 0.1 × 10^{-3}	−3.7 ± 0.2 × 10^{-3}	−3.5 ± 0.3 × 10^{-3}	−3.77 ± 0.1 × 10^{-3}
A_x (G)	4.1 ± 0.5	5.5 ± 0.5	4.8 ± 0.5	4.7_5 ± 0.6	5.61 ± 0.2
A_y (G)	6.1 ± 0.5	5.7 ± 0.5	5.4 ± 0.5	5.6_5 ± 0.6	5.01 ± 0.2
A_z (G)	33.4_5 ± 0.2	35.8 ± 0.3	34.0 ± 0.3	35.9 ± 0.4 (66%), 33.6_5 ± 0.4 (34%) } 35.1 ± 0.4	33.7 ± 0.3
$\langle A\rangle^m$ (G)	14.5_5 ± 0.4	15.7 ± 0.4	15.2 ± 0.4		14.77 ± 0.3
a_N^g (G)	14.572 ± 0.015	15.740 ± 0.015	14.742 ± 0.015	15.173 ± 0.015	14.78 ± 0.02
α^l	1.2,[n] 2.15	1.8, 2.9[n]	2.45, 3.1	1.54	2.2
β^l	0.2, 0.0[o]	0.3, 0.5	0.5, 0.7	0.0	0.2
$-D/2\pi$, $z' = z$	32.4 ± 0.4	34.4 ± 0.4	33.1 ± 0.4	34.2 ± 0.7	32.5 ± 0.2
$-D/2\pi$, $z' = y$	−14.5 ± 0.9	−17.2 ± 0.9	−16.0 ± 0.9	−16.3 ± 1.1	−16.8 ± 0.5
$-D^{(2)}/2\pi$, $z' = z$	−1.39 ± 0.7	−0.105 ± 0.7	−0.441 ± 0.7	−0.631 ± 0.8	−0.420 ± 0.4
$-D^{(2)}/2\pi$, $z' = y$	20.6 ± 0.5	21.2 ± 0.6	20.5 ± 0.6	21.3 ± 0.7	19.7 ± 0.3
a_D (mG)	20.5 ± 0.2	16.0 ± 0.2	22.4 ± 0.2	20.2 ± 0.2	−21.5 ± 0.5
$A_{z,D}$ (mG)	—	—	—	—	−93 ± 7

	Tempone[r]	[s]	[t]	Tempol[u]	Tempane[v]
g_x	—	2.0089 ± 0.001	2.00783 ± 0.0002	2.0095	2.0103
g_y	—	2.0058 ± 0.001	2.00604 ± 0.0002	2.0064	2.0069
g_z	—	2.0021 ± 0.001	2.00270 ± 0.0002	2.0027	2.0030
$\langle g\rangle$	—	—	—	2.0062	2.0067
A_x (G)	5.2	5.8 ± 0.5	9.96 ± 1.07	—	—
A_y (G)	5.2	5.8 ± 0.5	7.94 ± 1.07	—	—
A_z (G)	31	30.8 ± 0.5	32.6 ± 1.07	—	—

[a] The magnetic parameters are given in their principal axis system (x''', y''', z'''), but the triple primes have been dropped for convenience. The (x', y', z') axes are the principal axes for the rotational diffusion.

[b] From Goldman *et al.* (1972a), PADS = peroxylamine disulfonate; cf. Fig. 1b.

[c] From Libertini and Griffith (1970).

[d] From Hamrick *et al.* (1972).

[e] From Goldman *et al.* (1973); entries give ^{17}O hyperfine entries. Note that it is assumed here that $A_x = A_y$.

[f] $\langle g\rangle = \frac{1}{3}(g_x + g_y + g_z)$.

[g] Measured in motionally narrowed region. Error limits reflect total range of observed values.

[h] $g(0) = 6^{-1/2}[2g_{z'} - (g_{x'} + g_{y'})]$

[i] $g^{(2)} = \frac{1}{2}(g_{x'} - g_{y'})$.

[j] $\langle A\rangle = \frac{1}{3}(A_x + A_y + A_z)$.

[k] $-D/2\pi = (|\gamma_e|/2\pi)(2\sqrt{6})^{-1}[2A_{z'} - (A_{x'} + A_{y'})]$ in MHz.

[l] $-D^{(2)}/2\pi = \frac{1}{4}(|\gamma_e|/2\pi)(A_{x'} - A_{y'})$ in MHz.

[m] Numbers are for Lorentzian and Gaussian fits, respectively.

[n] Lorentzian fit is best for PD-TEMPONE in toluene-d_8 and Gaussian fit is best for PD-TEMPONE in 85% glycerol-D_2O.

[o] Note that a small β would help the relative amplitude of $\tilde{M}(\pm 1)/\tilde{M}(0)$ but gives too much resolution in the central region.

[p] Perdeuterated 2,2,6,6-tetramethyl-4-piperidone-1-oxyl; cf. Fig. 1b, from Hwang *et al.* (1975).

[q] Cf. Fig. 1b, from Polnaszek and Freed (1975).

[r] 2,2,6,6-Tetramethyl-4-piperidone-1-oxyl in tetramethyl-1,3-cyclobutadione crystal, from Griffith *et al.* (1965).

[s] *N*-oxyl-4′,4′-dimethyloxazolidine derivative of 5-α-cholestan-3-one in cholesteryl chloride, from Hubbell and McConnell (1971).

[t] Nitroxide maleimide spin-labeled horse oxyhemoglobin crystal, from Ohnishi *et al.* (1966).

[u] 2,2,6,6-Tetramethyl-4-piperidinol-1-oxyl in crystal, from D. Bordeaux *et al.* (1973).

[v] 2,2,6,6-Tetramethyl piperidine-1-oxyl in crystal, from D. Bordeaux *et al.* (1973).

axis perpendicular to the other two. [These axes should more rigorously be written as x''', y''', z''', cf. Eq. (46), but the primes have been dropped for convenience, since there should be no confusion with the laboratory axes.] The x', y', z' axes are the principal axes of the diffusion tensor $\mathbf{R}$ and they are assumed in Table I to be either the same as the x, y, z axes or else to be a cyclic permutation of them. It should be clear from this tabulation that (1) nitroxides do exhibit significant solvent dependences in their magnetic parameters and (2) the different nitroxides will exhibit some difference in their magnetic parameters. One interesting observation in this context is the result for PD-TEMPONE (cf. Fig. 1b) in ethanol-d_6. It exhibits two distinct values of A_z, the larger one characteristic of the values in hydrogen-bonding solvents, while the smaller one is characteristic of the values in non-hydrogen-bonding solvents. In general, one must expect some variation in the magnetic parameters from site to site in a given solvent, and this will be an important source of the [orientation-dependent, cf. Eq. (29)] rigid-limit intrinsic width. These matters are discussed elsewhere (Hwang *et al.*, 1975).

Another source of valuable information for the analysis of the slow tumbling spectrum is the relaxation results from the fast motional spectrum in less viscous media, if it is at all available.

Figure 3 shows the results for PADS (cf. Fig. 1b) in D_2O (Goldman *et al.*, 1972a) where the derivative width $\delta(\tilde{M})$ is plotted as

$$\delta(\tilde{M}) = A + B\tilde{M} + C\tilde{M}^2 \tag{79}$$

The analysis of motional narrowing spectra is discussed by Nordio in Chapter 2. Suffice it to say here, that the motional narrowing theory, coupled with experimental values of B and C and *accurate* values of the magnetic parameters, is sufficient to determine $R_\parallel$ and $R_\perp$ at each temperature. It is important to note that in Fig. 3 the curves for B and C are very nearly parallel. This fact and the temperature insensitivity of a_N and g_s provide strong evidence against competing relaxation mechanisms affecting the interpretation. Figures 4a and 4b are plots of C versus B for PADS in glycerol–H_2O and for PD-TEMPONE in toluene-d_8, respectively. These results can be analyzed to yield

$$\tau_R \equiv (6\bar{R})^{-1} \tag{80}$$

$$\bar{R} \equiv (R_z R_\perp)^{1/2} \tag{80'}$$

and

$$N \equiv R_z/R_\perp \tag{81}$$

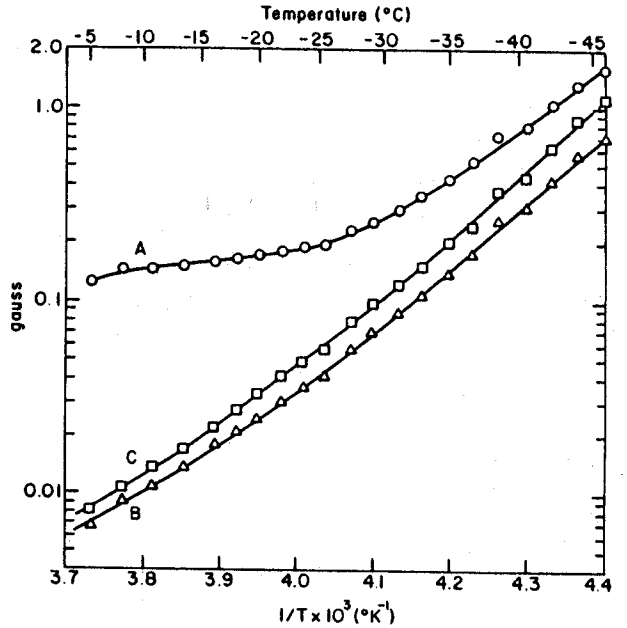

Fig. 3. The linewidth parameters A, B, and C [cf. Eq. (79)] versus $1/T$ for PADS Fig. 1b) in frozen water. [From Goldman *et al.* (1972a).]

It is found that the PADS system exhibits anisotropic rotational diffusi ($N = 4.7$ in aqueous glycerol solvents) where the z axis for the rotatio diffusion tensor is parallel to the line through the two sulfur atoms, while t PD-TEMPONE system rotates isotropically (within experimental erro An interesting sidelight to this result is that, if we were to interpret t PD-TEMPONE motional narrowing results in glycerol solvent in terms the magnetic parameters from toluene solvent, we would obtain $N \approx 3$ with fastest rotation about the molecular y axis, but when we use the corr magnetic parameters for glycerol, we again obtain $N = 1$.

The value of these motional narrowing results for the slow tumbli studies is that one can extrapolate the information obtained on τ_R and into the slow motional region. That is, $\log \tau_R$ is found to have a nearly line dependence on $1/T$, as expected for an activation process. More precise for PD-TEMPONE in toluene, it is linear in η/T, as shown in Fig. 5. This expected from Eq. (31) for Stokes–Einstein-type behavior. Also, N is fou to be temperature independent. Figure 6 shows one such comparison of experimental spectrum with computer simulated results utilizing the valu of τ_R and N extrapolated from the motional narrowing region. This is t case of PADS in D_2O, where $N = 3$, and is one of incipient slow tumbli

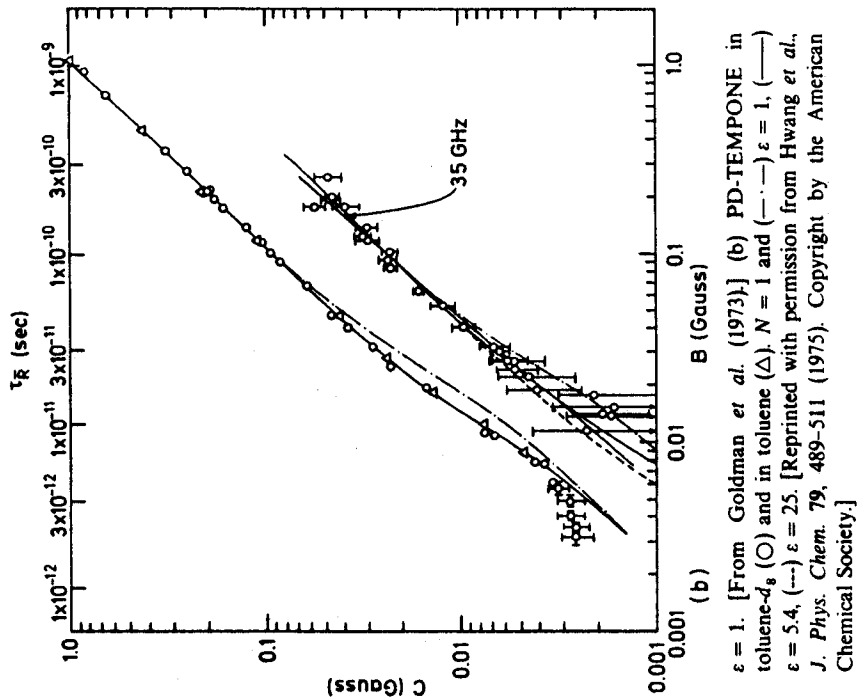

$\varepsilon = 1$. [From Goldman *et al.* (1973).] (b) PD-TEMPONE in toluene-d_8 (○) and in toluene (△). $N = 1$ and (— · —) $\varepsilon = 1$, (——) $\varepsilon = 5.4$, (- - -) $\varepsilon = 25$. [Reprinted with permission from Hwang *et al.*, *J. Phys. Chem.* **79**, 489-511 (1975). Copyright by the American Chemical Society.]

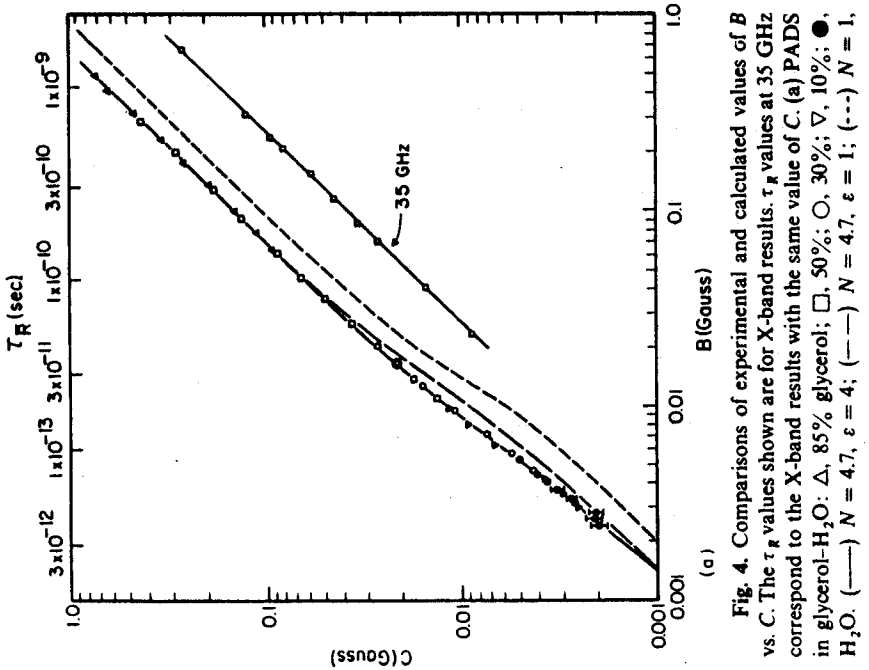

Fig. 4. Comparisons of experimental and calculated values of B vs. C. The τ_R values shown are for X-band results. τ_R values at 35 GHz correspond to the X-band results with the same value of C. (a) PADS in glycerol-H_2O: △, 85% glycerol; □, 50%; ○, 30%; ▽, 10%; ●, H_2O. (——) $N = 4.7$, $\varepsilon = 4$; (— —) $N = 4.7$, $\varepsilon = 1$; (- - -) $N = 1$,

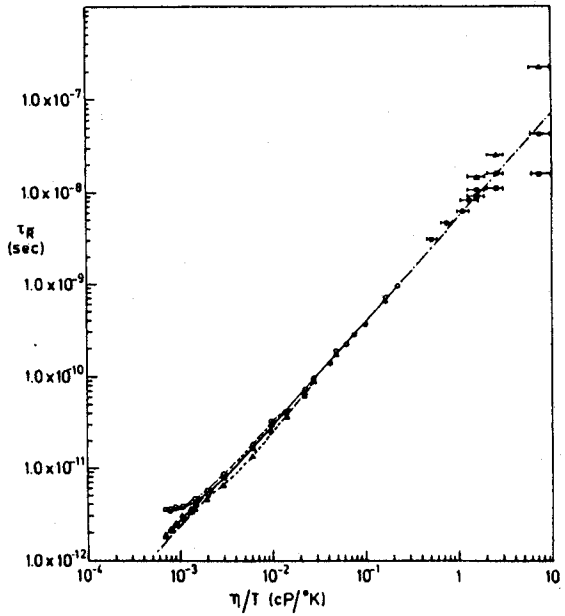

Fig. 5. τ_R versus $1/T$ for PD-TEMPONE in toluene-d_8. Motional narrowing results designated by △ (τ_R from B values) and ○ (τ_R from C values). They are extrapolated to the sl tumbling region (- — -) and are compared to best fits for the different models: (●) free diffusi (▲) Brownian diffusion, (■) strong jump diffusion. (——) $N = 1$, $\varepsilon = 5.4$. (- - -) $N = 1$, $\varepsilon =$ [Reprinted with permission from Hwang *et. al.*, *J. Phys. Chem.* 79, 489-511 (1975). Copyri by the American Chemical Society.]

($\tau_R = 4 \times 10^{-9}$ sec). A comparison is given for different values of N, anc clearly shows that the best fit is for $N = 3$. These simulations were p formed for a Brownian diffusion model, with the model parameter $B_L =$ When slower motional spectra were obtained ($\tau_R \gtrsim 10^{-8}$ sec), it was fou that a Brownian motion model was not yielding good simulations for small spin probes PADS and PD-TEMPONE. Therefore other models w tried, i.e., the strong jump diffusion of Eq. (39) with $R\tau = 1$ and the f diffusion of Eq. (35) also with $R\tau = 1$. A typical comparison for the th models is shown in Fig. 7, from which it is clear that the best experimenta is obtained with the free diffusion result. In this context, it is important recognize that the values of B_L for this free diffusion model are not uniq For $\tau_R \lesssim 10^{-8}$ sec the simulated spectrum is determined mainly coefficients of $L = 2, 4, 6$, and 8. Over this range of values of L, it is possi to reproduce the values of B_L of the free diffusion case reasonably well by jump diffusion models given by Eq. (36) [and the special case of Eq. (. with $R\tau \approx 0.13$ corresponding to an rms jump angle of 50°]. In fact, co

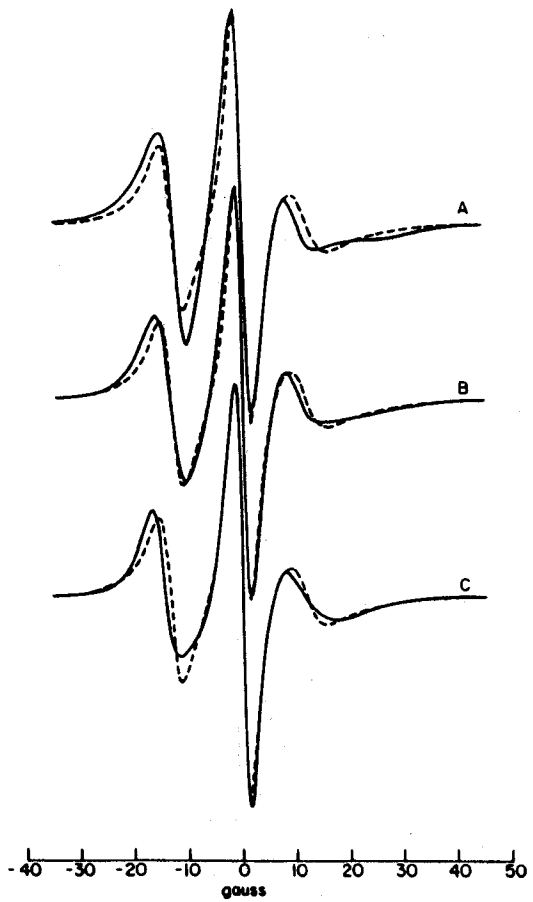

Fig. 6. A comparison of simulated and experimental spectra for PADS in frozen D_2O at $T = -50°C$: (---) experimental spectrum, (——) calculated for Brownian diffusion with $\tau_R = 4 \times 10^{-9}$ sec, $A' = 0.2$ G, and A, $N = 1$; B, $N = 3$; and C, $N = 6$. [From Goldman *et al.* (1972a).]

puter simulations of such jump models do yield virtually identical results. Figure 8 shows the results for PADS in D_2O in the model-sensitive region of τ_R for free diffusion and a range of values of N. This is also a case where free diffusion fits best.

Another way of testing the model dependence of the results is to extrapolate the τ_R values obtained in the motional narrowing region and to compare them with the "best" τ_R values obtained for each model. (This is associated with the S parameter discussed in Section III.B.) It is seen in Fig. 5 that the

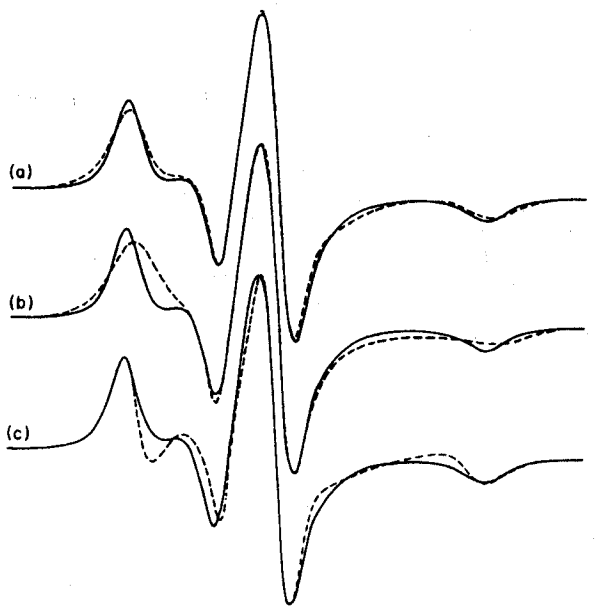

Fig. 7. A comparison of simulated (---) and experimental (——) spectra for P TEMPONE in toluene-d_8 at $\eta/T = 1.4$ cP/°K. The simulations are for: (a) the free diffusi model, $\tau_R = 1.0 \times 10^{-8}$ sec, $A' = 0.6$ G; (b) the strong jump diffusion model, $\tau_R = 8.7 \times 10$ sec, $A' = 0.8$ G; (c) the Brownian diffusion model, $\tau_R = 1.4 \times 10^{-8}$ sec, $A' = 0.4$ G. [Reprint with permission from Hwang *et al.*, *J. Phys. Chem.* 79, 489–511 (1975). Copyright by t American Chemical Society.]

free diffusion model gives good agreement, but the others do not, especial for the slower values of $\tau_R > 10^{-8}$ sec.

The parameters τ_R and N are not the only ones that can be extrapolate from the motional narrowing region. Another is the parameter A' in G (c Fig. 7), which is that part of A in Eq. (79) that is not attributable to **g**- c **A**-tensor sources. (It is given as $T_{2,a}^{-1} = \frac{1}{2}\sqrt{3}\,|\gamma_e|\,A'$ in sec^{-1} in the con puter programs.) The best A' for free diffusion again falls closest to th values extrapolated from the motional narrowing region, although the di tinction here is not so clear (cf. Mason *et al.*, 1974).

An important point to emphasize at this stage is that the mode dependent studies summarized above were greatly aided by the very wel resolved spectra obtained from PADS and PD-TEMPONE in deuterate solvents. In general, the added intrinsic widths of typical spin labels due t the unresolved proton superhyperfine splitting will tend to obscure many c the spectral details in the slow motional and rigid-limit spectra. The analysi of the motional narrowing spectra would be particularly seriously affecte

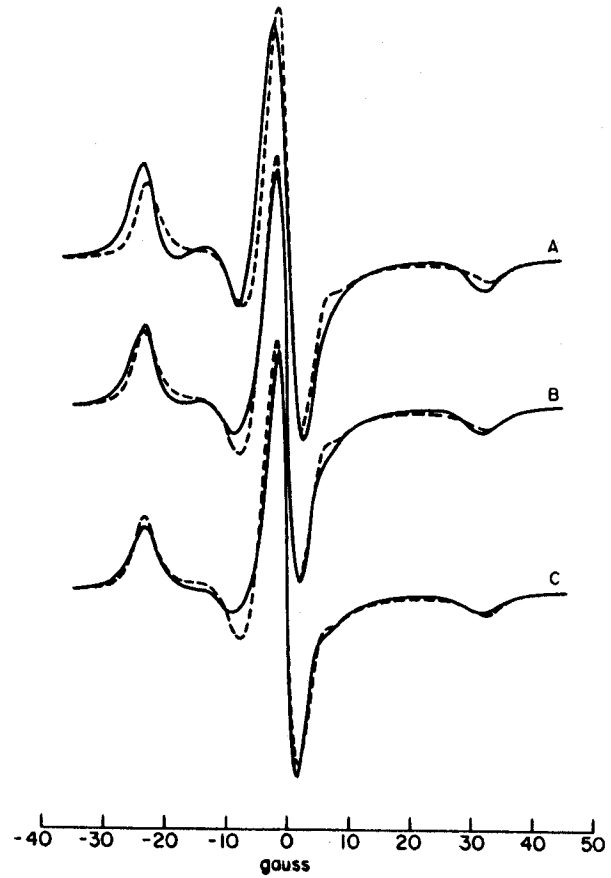

Fig. 8. A comparison of simulated (——) and experimental (- - -) spectra for PADS in frozen D_2O at $T = -60°C$. The simulated spectra are calculated for free diffusion with $\tau_R = 2 \times 10^{-8}$ sec, $A' = 0.6$ G, and A, $N = 1$; B, $N = 3$; and C, $N = 6$. [From Goldman *et al.* (1972a).]

It is interesting to note, however, that the ESR spectra obtained by McCalley *et al.* (1972)† from spin-labeled oxyhemoglobin in H_2O at $\tau_R \cong 2.6 \times 10^{-8}$ sec show many of the features that are characteristic of Brownian diffusion (cf. Fig. 7). This is an important confirmation of the theory, because one would expect that a macromolecule (unlike the small spin probes) would obey simple Brownian motion.

† Editor's note: Appendix I (p. 562) contains simulated spectra calculated by this model for a broad range of τ_R values.

B. Simplified Methods of Estimating τ_R

An important characteristic of a typical nitroxide slow motional spectrum is that it has two well-separated outer hyperfine extrema with an overlapped central region. It has been found that a useful parameter for describing these spectra is $S = A'_z/A_z$, where A_z has already been defined in Fig. 2 as one-half the separation of the outer hyperfine extrema, and A'_z is the slow tumbling value for the same spectral feature (Goldman *et al.*, 1972b). McCalley *et al.* (1972) have discussed the separate deviations of high-field and low-field positions from their rigid-limit values. Figure 9 compares the

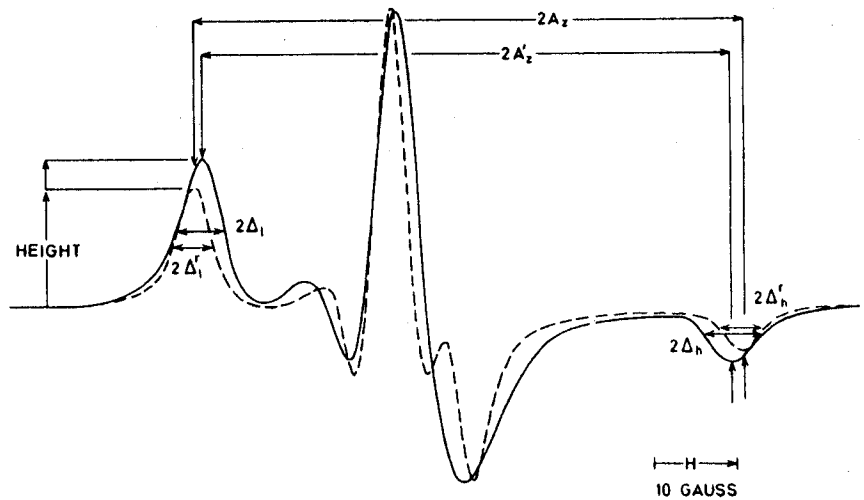

Fig. 9. Superposition of computed rigid-limit nitroxide spectrum with a computed slow tumbling spectrum at $\tau_R = 5.0 \times 10^{-8}$ sec, demonstrating the measurements required for th parameters $S = A'_z/A_z$, $W_l = \Delta_l/\Delta'_l$, and $W_h = \Delta_h/\Delta'_h$. In an actual experiment, it is ofte necessary to estimate the Δ'^{est}_l in place of the Δ'_l as described in the text. The magnetic parameter utilized are $\delta = 3.0$ G, $g_x = g_y = 2.0075$, $g_z = 2.0027$, $A_x = A_y = 6.0$ G, $A_z = 32.0$ G, an $B_0 = 3.300$ G. [Reprinted with permission from Mason and Freed, *J. Phys. Chem.* 78, 1321-132 (1974). Copyright by the American Chemical Society.]

quantities A_z and A'_z. Note that A'_z decreases monotonically from its rigid limit value of A_z as the motion becomes more rapid. Thus S is a sensitive monotonically increasing function of τ_R. Furthermore, simulations per formed for axial and asymmetric **A** and **g** tensors show that for a given valu of A_z, the value of S is insensitive to changes in A_x, A_y, and the g-tenso components. Changes in the magnitude of A_z, however, do affect the valu of S. This is expected, of course, since, as can be seen from Fig. 2, A_x, A_y, an **g** only contribute to the central regions of the rigid limit spectrum. Thi

dependence can be approximately expressed in the functional form $S = S(\tau_R A_z)$, where S is simply dependent on the product $\tau_R A_z$. This functional dependence permits the scaling of results for one value of A_z to the range of values of A_z typical for nitroxides (27–40 G) with an error of less than 3%. Thus, if we know how S is affected by changes in the linewidth and rotational diffusion model, then it is possible to estimate τ_R without the necessity of making detailed line-shape calculations and comparisons. This is particularly useful for nitroxides that are broadened by inhomogeneous intramolecular or intermolecular (solvent) hyperfine and dipolar interactions. As already noted, this line broadening decreases the spectral resolution and obscures other τ_R-dependent line-shape changes.

The variation of S with τ_R is shown in Fig. 10 for Brownian, free, and strong jump diffusion models and isotropic diffusion, with $A_z = 32$ G and peak-to-peak derivative Lorentzian linewidths $[\delta = (2/\sqrt{3})|\gamma_e|^{-1}T_{2,a}^{-1}]$ of 0.3 and 3.0 G. It can be seen that S is model sensitive, and for an equivalent value of τ_R, S increases from a Brownian to a free to a jump reorientational model. (This is consistent with the analysis we have already given for the best τ_R fit as a function of model; cf. Fig. 7.) These curves can be fit to the expression

$$\tau_R = a(1 - S)^b \tag{82}$$

to within 2, 3, or 5% in the value of τ_R for a given S for jump, Brownian, or free diffusion, respectively, with the values of a and b given in Table II

TABLE II

PARAMETERS[a] FOR FITTING $\tau_R = a(1 - S)^b$

Diffusion model[b]	Linewidth[c] (G)	a	b	$\tau_R(S = 0.99)$[d] (sec)
Brownian diffusion	0.3	2.57×10^{-10}	−1.78	9×10^{-7}
	3.0	5.4×10^{-10}	−1.36	3×10^{-7}
	5.0	8.52×10^{-10}	−1.16	2×10^{-7}
	8.0	1.09×10^{-9}	−1.05	2×10^{-7}
Free diffusion	0.3	6.99×10^{-10}	−1.20	3×10^{-7}
	3.0	1.10×10^{-9}	−1.01	1×10^{-7}
Strong diffusion	0.3	2.46×10^{-9}	−0.589	4×10^{-8}
	3.0	2.55×10^{-9}	−0.615	5×10^{-8}

[a] These values are calculated for an axial nitroxide with $A_\parallel = 32$ G, $A_\perp = 6$ G, $g_\perp - g_\parallel = 0.0041$, and isotropic reorientation. (From Goldman *et al.*, 1972b.)

[b] These models are discussed in detail in the text.

[c] Peak-to-peak derivative Lorentzian width: δ.

[d] For this τ_R value, $1 - S = 0.01$.

(Goldman *et al.*, 1972b; Goldman, 1973). The parameters for Brownia diffusion with linewidths of 5 and 8 G are also given. It should be noted tha for $\tau_R < 7 \times 10^{-9}$ sec, S is undefinable since the outer lines begin to con verge to the motionally narrowed spectrum. For longer τ_R's than shown i Fig. 10, the spectrum approaches the rigid limit, and the value of $1 -$ become comparable to experimental uncertainties. The value of τ_R for whic $1 - S = 0.01$ is given in Table II. The least squares fit to Eq. (82) was cal culated for 7×10^{-9} sec $\leqq \tau_R \leqq \tau_R(S = 0.99)$.

The effect of linewidth on the value of S is also shown in Fig. 10. Fo Brownian and free diffusion models, S increases with increasing linewidt while for jump diffusion a decrease in S is observed. The uncertainty i estimating τ_R due to an uncertainty in intrinsic linewidth, for a given value o S, increases for longer τ_R. Thus for a Brownian diffusion model and a 1.5 C uncertainty in the intrinsic width, the uncertainty in calculating τ_R for given value of S increases from about 5% for $\tau_R \approx 1 \times 10^{-8}$ sec to abou 50% for $\tau_R \approx 1 \times 10^{-7}$ sec to an order of magnitude for $\tau_R \gtrsim 1 \times 10^{-6}$ sec Linear interpolations along the vertical line between the curves A and B (o

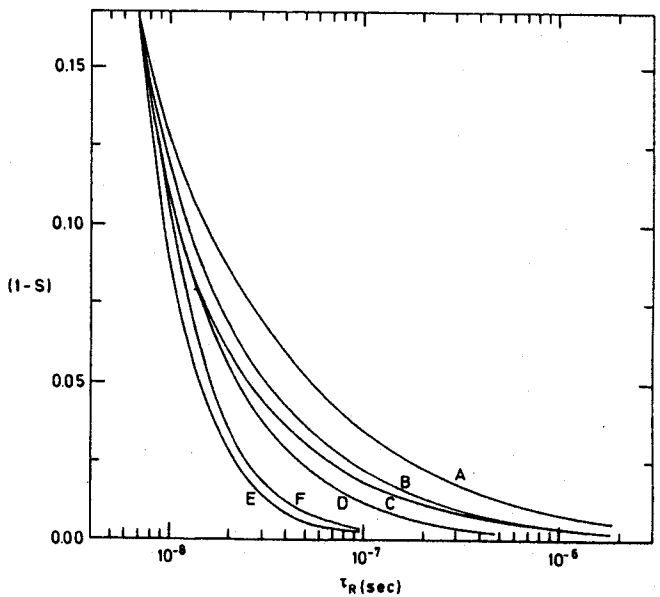

Fig. 10. Graph of $1 - S$ vs. τ_R. A, B: Brownian diffusion and derivative width $\delta = 0.3$ and 3.0 G, respectively; C, D: Free diffusion and $\delta = 0.3$ and 3.0 G, respectively; E, F: strong jump diffusion and $\delta = 0.3$ and 3.0 G, respectively. Values are calculated for isotropic reorientation with $A_z = 32$ G. See also Table II. [Reprinted with permission from Goldman *et al.*, *J. Phys Chem.* **76**, 1858–1860 (1972b). Copyright by the American Chemical Society.]

(Goldman *et al.*, 1972b; Goldman, 1973). The parameters for Brownian diffusion with linewidths of 5 and 8 G are also given. It should be noted that for $\tau_R < 7 \times 10^{-9}$ sec, S is undefinable since the outer lines begin to converge to the motionally narrowed spectrum. For longer τ_R's than shown in Fig. 10, the spectrum approaches the rigid limit, and the value of $1 - S$ become comparable to experimental uncertainties. The value of τ_R for which $1 - S = 0.01$ is given in Table II. The least squares fit to Eq. (82) was calculated for 7×10^{-9} sec $\leqq \tau_R \leqq \tau_R(S = 0.99)$.

The effect of linewidth on the value of S is also shown in Fig. 10. For Brownian and free diffusion models, S increases with increasing linewidth, while for jump diffusion a decrease in S is observed. The uncertainty in estimating τ_R due to an uncertainty in intrinsic linewidth, for a given value of S, increases for longer τ_R. Thus for a Brownian diffusion model and a 1.5 G uncertainty in the intrinsic width, the uncertainty in calculating τ_R for a given value of S increases from about 5% for $\tau_R \approx 1 \times 10^{-8}$ sec to about 50% for $\tau_R \approx 1 \times 10^{-7}$ sec to an order of magnitude for $\tau_R \gtrsim 1 \times 10^{-6}$ sec. Linear interpolations along the vertical line between the curves A and B (or

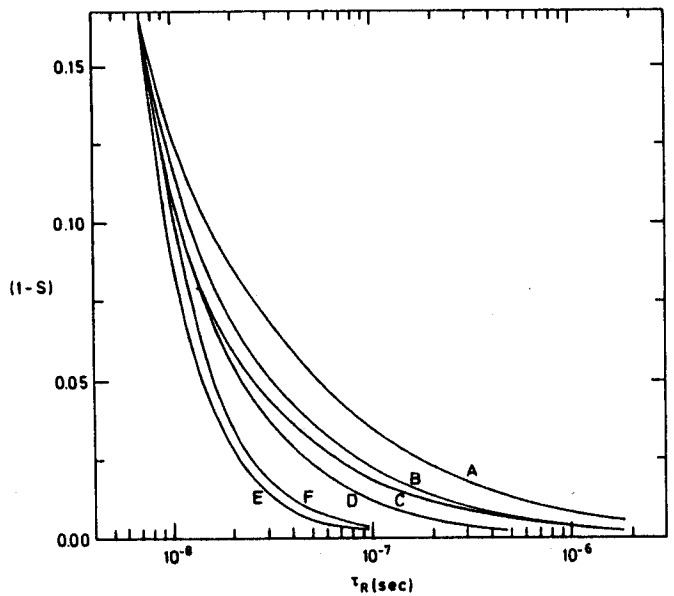

Fig. 10. Graph of $1 - S$ vs. τ_R. A, B: Brownian diffusion and derivative width $\delta = 0.3$ and 3.0 G, respectively; C, D: Free diffusion and $\delta = 0.3$ and 3.0 G, respectively; E, F: strong jump diffusion and $\delta = 0.3$ and 3.0 G, respectively. Values are calculated for isotropic reorientation with $A_z = 32$ G. See also Table II. [Reprinted with permission from Goldman *et al.*, *J. Phys. Chem.* **76**, 1858–1860 (1972b). Copyright by the American Chemical Society.]

which very simple equations exist (Johnson, 1965), we find that the separation of the lines decreases by the factor $[1 - 2(\tau s)^{-2}]^{1/2}$ $[\approx 1 - (\tau s)^{-2}$ wh the line shifts are small], where $\tau/2$ and $2s$ are the lifetime in one state and t separation between peaks, respectively. If we now draw the analogy betwe the rotational motion (carrying the nitroxide radical between different orie tations corresponding to substantially different ESR frequencies) at a rate the order of τ_R^{-1} and the τ^{-1} of the two jump model, and we use the furth analogy between A_z and s, then the result noted above, that $S = S(\tau_R A_z)$ seen to follow. If we employ the two-jump expression for small shifts to t present case, then we would predict the form of Eq. (82) w $a = 1.78 \times 10^{-9}$ sec (for $A_z = 32$ G) and $b \approx -\frac{1}{2}$. We see from Table that these results are of the correct order for strong jump diffusion, where t analogy is probably the best, but are substantially different than the Brov ian diffusion results.

However, the analogy between τ_R^{-1} and τ^{-1} suggests that we examine incipient line broadening of the outer hyperfine extrema, which should roughly correspond to τ_R^{-1} and (2) be a more sensitive function of motion than the shifts in position. Indeed, accurate computer simulatic have confirmed these suggestions as being theoretically correct (Mason a Freed, 1974). In fact, the residual width is found to be given by τ_R^{-1} to wit a factor of ~ 2 (or $\frac{1}{2}$) over most of the range of interest. This is about as gc an agreement as we might hope for, when we recognize that the analog incomplete, because in the slow tumbling case, the rotational motion modulates the ESR frequency over a continuous range, (and not betw discrete values) and (b) induces nuclear spin flips as well because the qua zation axis of the nuclear spins is orientation dependent; this is known a nonadiabatic effect (Freed, 1972a). However, a recent approximate tr ment, for small pseudosecular terms in Eq. (74), has shown that this la effect is roughly proportional to τ_R^{-1} (Freed, 1974).

We give now a more quantitative discussion of this width effect (Ma and Freed, 1974). The average of the measured half-widths at half-heights for the two outer extrema of a rigid-limit spectrum is found from simulati to be equal, to a very good approximation, to $\frac{1}{2}\sqrt{3}\,\delta = |\gamma_e|^{-1} T_{2,a}^{-1}$. heights of the hyperfine extrema are measured from the true baseline Fig. 9). More precisely, we have

$$2\Delta_l^r = 1.59\delta \tag{8}$$

$$2\Delta_h^r = 1.81\delta \tag{8}$$

where the subscripts l and h refer to the low- and high-field lines, resp tively, and the superscript r refers to the rigid-limit value. This result is fo to be independent of δ over the range $1.0 \leqq \delta \leqq 4.0$ G and virtu

independent of A_z over the range $27 \leqq A_z \leqq 40$ G. It is, of course, essentially independent of variations in the other nitroxide rigid-limit parameters. Equations (83a) and (83b) are valid for the assumption of Lorentzian inhomogeneous broadening. (No calculations for non-Lorentzian broadening have yet been performed for the method discussed.)

In the slow motional region, near the rigid limit, the linewidth Δ for Lorentzian line shapes can be decomposed into two contributions (cf. Abragam, 1961): (1) the Lorentzian inhomogeneous component given by Eqs. (83a) and (83b) and (2) the excess motional width (of order of magnitude τ_R^{-1}). (It is convenient to think in terms of this decomposition even though it is not necessary for the method.) A useful dimensionless parameter for describing these spectra is then

$$W_i \equiv \Delta_i/\Delta_i^r, \qquad W_i - 1 = (\Delta_i - \Delta_i^r)/\Delta_i^r \tag{84}$$

where $i = l$, h. In general, $W_i - 1$ is about an order of magnitude larger than $1 - S$ for a particular value of τ_R (cf. Fig. 11), and furthermore, it can be measured to *at least* comparable accuracy ($\sim 1\%$; cf. Fig. 9). The results in Fig. 11 were calculated utilizing the computer program in Appendix B. A study of how W_i is affected by changes in (1) the spin parameters, (2) linewidth, and (3) rotational diffusion model has been made. It was found that W_i, like S, is insensitive to deviations from axial **A** and **g** tensors, as well as to variations in $A_\perp$ and **g** typical of a nitroxide. However, in contrast to S, which is dependent on the product $\tau_R A_z$, W_i is virtually independent of A_z over the range $27 \leqq A_z \leqq 40$ G; (we have used $A_z = 32$ G in obtaining the results in Fig. 11), as expected from our simple analogy. However, W_i is found to depend on δ. Generally, a smaller δ implies a larger $\Delta_i - \Delta_i^r$ for a given τ_R. In particular, $\delta = 1$ G yields values of $\Delta_i - \Delta_i^r$ ranging from 1.3 to 2.5 times greater than those for $\delta = 3$ G. We can try to explain this observation qualitatively. The rigid-limit extrema of finite width Δ_i^r arise from those nitroxide radicals whose 2p π N-atom orbitals lie within a cone of angle Ω about the applied field direction, and the size of the cone increases rapidly with an increase in the rigid-limit δ (McConnell and McFarland, 1970). If we roughly identify the excess width $\Delta_i - \Delta_i^r$ with the rate at which radicals reorient out of the cone, then extrema from the larger cones (which result from greater values of δ) will be less broadened, since it takes longer for the radicals to leave the cone. The observation that $\Delta_h - \Delta_h^r$ is always significantly larger than $\Delta_l - \Delta_l^r$ at a given τ_R could be explained in a similar manner. It is known that the high-field resonance for a single-crystal spectrum changes with angle more rapidly than the low-field resonance; thus the range of Ω contained in the observed cone (from a polycrystalline sample) must be smaller for the high-field line. Reorientations out of the high-field cone thus occur at a more rapid rate, and, in general, W_h is a more sensitive function of τ_R than is W_l, as can be seen from Fig. 11.

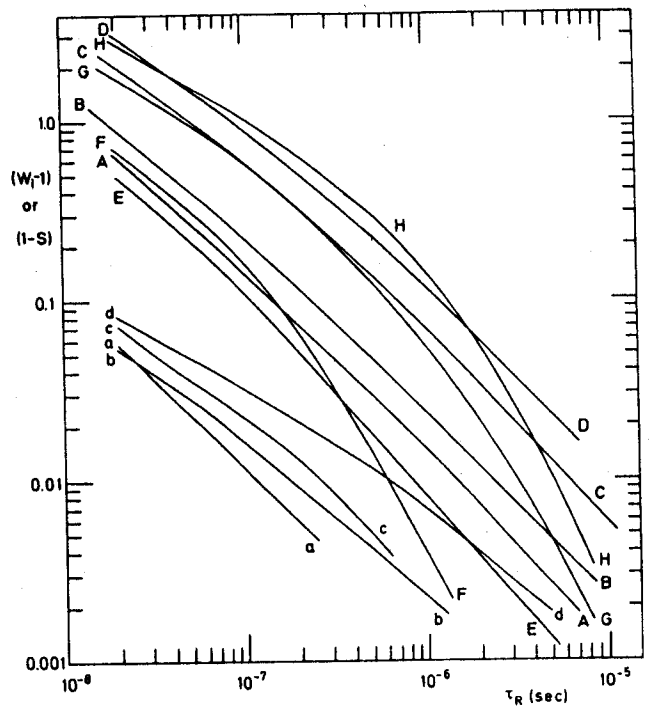

Fig. 11. Graph of $W_i - 1$ (curves A–H); and $1 - S$ (curves a–d) vs., τ_R for nitroxide isc tropic rotational reorientation. Curves a and b are for free diffusion and $\delta = 3.0$ and 1.0 C respectively; curves c and d are for Brownian diffusion and $\delta = 3.0$ and 1.0 G, respectivel Curves A and B are for free diffusion, $\delta = 3.0$ G, and the low- and high-field extrema, respe tively, and curves C and D are the same as A and B, respectively, except $\delta = 1.0$ G. Curves E, G, and H correspond respectively to curves A, B, C, and D except that they are for Brownia diffusion. See also Table III. [Reprinted with permission from Mason and Freed, *J. Phys. Che* **78**, 1321–1323 (1974). Copyright by the American Chemical Society.]

The choice of a proper δ is clearly at the heart of the method. Near t rigid limit, an appropriate estimate of δ can be deduced from the Δ_i^r. T narrowest rigid-limit δ found in our laboratory is 1.5 G, which correspon to $2\Delta_l^r = 2.4$ G. Hubbell and McConnell (1971) reported values of 4.6 an 5.5 G for $2\Delta_l^r$ for pseudoaxial "rigid-limit" spectra, corresponding to δ of 2 and 3.5 G, respectively. The rigid limit spectrum of t *N*-oxyl-4′,4′-dimethyloxazolidine derivative of 5α-androstan-3-one appea to have $2\Delta_l^r \approx 5.0$ G, which corresponds to a δ of 3.1 G (McConnell an McFarland, 1970). The motional broadening can easily double the widths the outer extrema when the separation of the hyperfine extrema is not muc different from the rigid-limit value (i.e., $S > 0.95$). Thus, very near the rig limit, where δ can be determined from the rigid-limit extrema widths, tw independent determinations of τ_R can be made using Fig. 11.

As has been noted, the major contributions to the Δ_i^r are electron nuclear hyperfine interactions between the electron and the protons of the spin label and host, while heterogeneity of the environment also contributes to Δ_i^r. These interactions will be quickly averaged with the onset of molecular motion, resulting in a decrease in the appropriate δ. When this is the case, it becomes necessary to estimate a single δ such that the rotational correlation times obtained from Fig. 11 for both the low- and high-field extrema are equal within experimental error. For this process we can define "effective inhomogeneous widths" Δ_i^{er}, which obey Eqs. (83a) and (83b) and which generally obey the relation $\Delta_i^{er} \leqq \Delta_i^r$. Then we should rewrite Eq. (84) as

$$W_i \equiv \Delta_i/\Delta_i^{er} \tag{84'}$$

with the W_i given by Fig. 11. This procedure should then yield both τ_R and δ.

As noted, the uncertainty in δ can result in serious errors when τ_R's of $> 3 \times 10^{-8}$ sec are determined from S. Once δ has been determined from the W_i, another estimate of τ_R may (when feasible) be obtained from a measurement of S. In other words, τ_R and δ could be obtained as a function of three experimental parameters, S and the W_i.

The model-dependent results shown in Fig. 11 were obtained for Brownian diffusion and free diffusion, as before. The free diffusion model results in a more nearly linear dependence (in a log-log plot) of $W_i - 1$ versus τ_R in Fig. 11 than the Brownian motion model. The plots in Fig. 11 have been fitted to the form

$$\tau_R = a'(W_i - 1)^{-b'} \tag{85}$$

for the region $W_i - 1 > 0.01$, and the coefficients are given in Table III. The maximum variation between the curves and the results predicted from Eq. (85) is also given. It is clear that the use of Eq. (85) is a less accurate means of estimating τ_R than the curves. However, the fact that $b' \cong 1$ (except for the anomalous curve F, which is presumably affected by overlap) is consistent with the interpretation of $\Delta_i - \Delta_i^r$ as a lifetime broadening.

When there is axially symmetric rotational diffusion about the molecular z axis with $R_\parallel > R_\perp$, it should mean that $\tau_{R_\perp}$ is again obtained. Also, the introduction of an angle-dependent rigid-limit width given by Eq. (29) should have no effect on the outer hyperfine extrema, except that now

$$\delta = (2/\sqrt{3})\,|\gamma_e|^{-1}(T_{2,a}^{-1} + T_{2,b}^{-1}) = (2/\sqrt{3})\,|\gamma_e|^{-1}(\alpha + \beta) \tag{86}$$

It is very important in the experimental application of this method to avoid distortion of the true linewidth by overmodulation of the magnetic field and/or power saturation. Experimental applications of this method have not yet been reported.

TABLE III

PARAMETERS[a] FOR FITTING $\tau_R = a'(W_i - 1)^{b'}$

Curve	$a' \times 10^8$ sec	b'	Maximum deviation (%)[b]
A	1.29	1.033	3
B	1.96	1.062	6
C	5.32	1.076	18
D	7.97	1.125	18
E	1.15	0.943	5
F	2.12	0.778	18
G	5.45	0.999	30
H	9.95	1.014	55

[a] Table is based on approximate fit of Fig. 11 data to Eq. (85) for $W_i - 1 > 0.01$. See Fig. 11 for explanation of the different curves. [Reprinted with permission from Mason and Freed, *J. Phys. Chem.* 78, 1321–1323 (1974). Copyright by the American Chemical Society.]

[b] Based on comparing values in Fig. 11 with Eq. (85).

The simplified methods discussed above are based on the relatively simple to analyze behavior of the outer extrema. While it is true that the central region of the nitroxide spectrum is very sensitive to motional effects it is also very sensitive to the deviations of the nitroxide magnetic parameters from cylindrical symmetry and this can vary considerably (cf Table I). Thus it would be difficult to develop general methods based on the central region; computer simulation with accurate magnetic parameters is probably required.

C. Very Anisotropic Rotational Reorientation

The simplified methods discussed in the previous section have an important failing in that they are not really applicable to spectra arising from highly anisotropic motion, especially when the molecular z axis is not itself a principal axis. The phenomenon of spin labels undergoing very rapid anisotropic rotational reorientation is a common one. In fact, the Stanford group (Hubbell and McConnell, 1969a,b, 1971; McConnell and McFarland, 1970; McFarland and McConnell, 1971) have developed a simple analysis in terms of an effective time-independent spin Hamiltonian $\mathcal{H}_{eff}$ to account for rapid anisotropic motion.

Suppose that there is very rapid motion about some molecular axis while motion perpendicular to that axis is very slow. This is the case, for example, if the nitroxide spin label rotates about a single bond while the overall motion is that of the macromolecule to which it is attached. Then we

can introduce effective $\mathbf{g}'$ and $\mathbf{A}'$ tensors that are axially symmetric about $\mathbf{v}$, and this yields an effective rigid-limit Hamiltonian to predict the spectrum. The use of such an effective Hamiltonian implies (1) a large enough $R_\parallel$ (representing rotational reorientation about $\mathbf{v}$) that residual time-dependent effects of the averaging process, which could lead to line broadening, are negligible; and (2) motion about axes perpendicular to $\mathbf{v}$, described by an effective $R_\perp$, is so slow that its effects on the spectrum are negligible.

Suppose that either of these conditions is not fulfilled, and that motional effects assert themselves in the spectrum. If condition 1 is fulfilled, but $R_\perp$ becomes fast enough to affect the spectrum, then one can simulate spectra using the program in Appendix B but with the effective axial tensors $\mathbf{A}'$ and $\mathbf{g}'$. The tensor $\mathbf{A}'$ is given in terms of the true $\mathbf{A}$ and the direction cosines α_i ($i = x'''$, y''', or z''', but we drop the triple primes for convenience in this section) of $\mathbf{v}$, in the molecular principal axis system as

$$A'_\parallel = \sum_i \overline{\alpha_i^2} A_i \tag{87}$$

$$A'_\perp = \frac{1}{2} \sum_i (1 - \overline{\alpha_i^2}) A_i \tag{88}$$

The simplified methods of the previous section would only apply in modified form if $A'_\parallel$ and $A'_\perp$ are not much different from typical nitroxide values (see below).

If, however, condition 1 is relaxed somewhat, then a motional narrowing theory can be applied to consider how the motion represented by $R_\parallel$ yields line broadening, etc., from the deviations between $\hat{\mathscr{H}}_{\text{eff}}$ and the true $\hat{\mathscr{H}}$. However, using our example above, the relaxation effects are a function of the orientation of the macromolecule, and we would have to compute such effects from $R_\parallel$ for each orientation.

However, the general theory given here can be rigorously applied to this example, including effects from both types of motion simultaneously. A series of simulations in which $R_\perp$ is just large enough to show incipient slow motional effects, namely $\tau_{R_\perp} = 5 \times 10^{-8}$ sec, were performed where $\tau_{R_\parallel}$ is allowed to vary from 5×10^{-8} to 6×10^{-11} sec (Mason *et al.*, 1974). This series of simulations, shown in Fig. 12b, was motivated by experimental results (cf. Fig. 12a) of Wee and Miller (1973) on a spin-labeled polybenzyl glutamate in DMF solution (cf. Fig. 13). These simulations required that the principal axes of $\mathbf{R}$ (i.e., x', y', and z') be tilted relative to the principal axes of the magnetic tensors (x''', y''', z'''). In this modified computer program, $\mathbf{A}$ and $\mathbf{g}$ are expressed in the x', y', z' coordinate system (cf. Polnaszek, 1975a). The spectra were calculated for a spatially isotropic distribution of spin labels with a tilt angle between respective z axes of 41.7°. The simulated spectra of

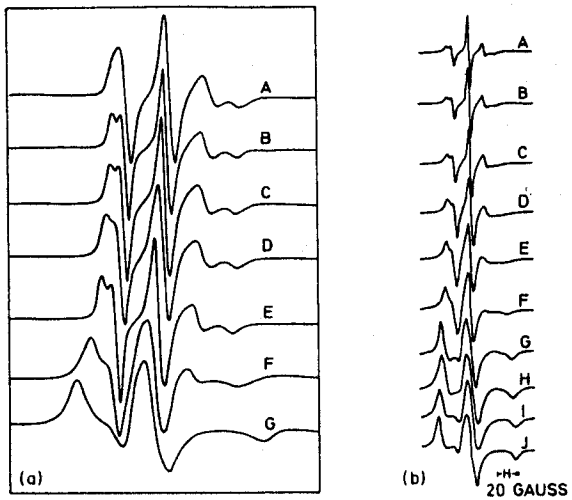

Fig. 12. (a) ESR spectra of polybenzyl glutamate labeled with 2,2,6,6-tetramethyl aminopiperidine-1-oxyl (TEMP-NH_2) in DMF solutions of varying concentrations at roc temperature. The polymer concentration (volume fraction) was A, 0.008; B, 0.0917; C, 0.128; 0.148; E, 0.200; F, 0.42 (0.5 weight fraction); and G, 1.0 (solid polymer). [Reprinted wi permission from Wee and Miller, *J. Phys. Chem.* 77, 182–189 (1973). Copyright by the Americ Chemical Society.] (b) Simulations computed with the magnetic parameters of the TEMP-NI spin label: $A_z = 30.8$ G, $A_x = A_y = 5.8$ G, $g_x = 2.0089$, $g_y = 2.0058$, $g_z = 2.0021$. The sy metry axis of the rotational diffusion tensor is defined in the molecular axis system by the ang $\cos^{-1}(\overline{\alpha_x^2})^{1/2} = 48.3°$, $\cos^{-1}(\overline{\alpha_y^2})^{1/2} = 90°$, $\cos^{-1}(\overline{\alpha_z^2})^{1/2} = 41.7°$. $\tau_{R_\perp}$ is 5.0×10^{-8} sec and o $\tau_{R_\parallel}$ is varied in this series, except for the rigid-limit simulation J. See Table IV for values of and δ used. [Reprinted with permission from Mason *et al.*, *J. Phys. Chem.*, 78, 1324–13 (1974). Copyright by the American Chemical Society.]

Fig. 12b for $\tau_{R_\parallel}$ of the same order of magnitude as $\tau_{R_\perp}$ appear similar to tl isotropic and near-isotropic motional spectra already shown, and for whi the simplified approaches already apply. But for $\tau_{R_\parallel} \ll \tau_{R_\perp}$ there are mark qualitative differences. (Note that this is an ideal case for K truncation, i. $n_K < n_L$.) The general progression of spectra in Fig. 12b from A to I, whe $\tau_{R_\parallel}$ is increasing bears considerable resemblance to the progression of e perimental spectra in Fig. 12a from A to G, where the polymer concentr tion, and hence the solution viscosity, is increasing. Rather close agreeme is found between pairs 12b-I and 12a-G (the near-rigid limit), 12b-B a 12a-B (where $\tau_{R_\parallel}$ is very fast), and 12b-F and 12a-F (an intermediate cas These results provide evidence that there is fast motion of the piperidine ri about the NH–CH bond, and no observable motion of the overall polym (i.e., $\tau_R > 10^{-7}$ sec).

The question now remains of the range of validity of the effective t independent Hamiltonian in terms of $\mathbf{g}'$ and $\mathbf{A}'$. Its use by Hubbell

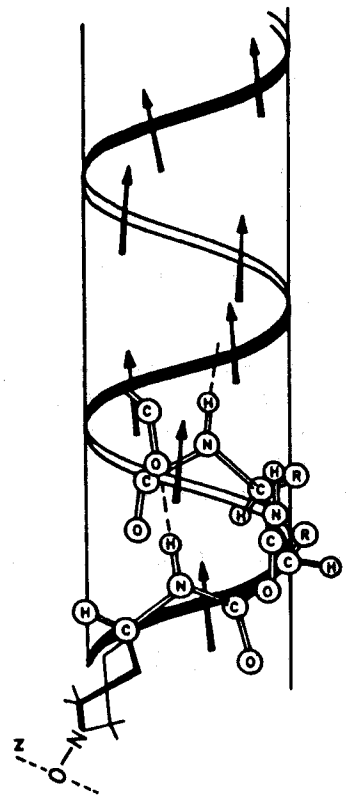

Fig. 13. End-labeled polybenzyl glutamate (cf. Fig. 12b), right-handed α-helix. [Reprinted with permission from Wee and Miller *J. Phys. Chem.* 77, 182–189 (1973). Copyright by the American Chemical Society.]

McConnell (1969a,b, 1971) is based by analogy with liquid crystalline spectra, on a so-called order parameter S_o given by

$$S_o = \tfrac{1}{2}(3\overline{\alpha_z^2} - 1) \approx (A'_{\parallel} - A'_{\perp})/(A_z - A_x) \tag{89}$$

where the bar implies a time average and the second equality is based on letting $A_x = A_y$ as is the case in many nitroxides. S_o is a measure of the extent of the motion leading to $\hat{\mathcal{H}}_{eff}$. We then have

$$A'_{\parallel} = A_o + \tfrac{2}{3}(A_z - A_x)S_o \tag{90a}$$

$$A'_{\perp} = \tfrac{1}{2}(3A_o - A'_{\parallel}) \tag{90b}$$

and

$$A_o = \tfrac{1}{3}\,\mathrm{Tr}\,A = \tfrac{1}{3}\,\mathrm{Tr}\,A' = A'_o \tag{91}$$

TABLE IV[a]

Spectrum index	$\tau_{R_\perp}$ (nsec)	$A'_{\parallel}$ (G)	$A'_{\perp}$ (G)	$\Delta A'$ (G)	A'_o[e]	$\cos^{-1}(\alpha_z^2)^{1/2}$ (deg)[f]	$g'_{\parallel} - g'_{\perp}$	S_o[f]	$g'_{\parallel}$	$g'_{\perp}$	g'_o[h]	$\cos^{-1}(\alpha_z^2)^{1/2}$ (deg)[i]
A[b]	0.06	18.9	11.5	7.4	14.0	43.2	−.0008	0.296[k]	2.0051	2.0059	2.0056	55[j]
B[b]	0.10	18.9	11.3	7.6	13.8	42.9	−.0008	0.304	2.0051	2.0059	2.0056	55
C[b]	0.20	19.2	11.1	8.1	13.8	42.2	−.0010	0.324	2.0050	2.0060	2.0057	57
D[b]	0.40	20.2	10.7	9.5	13.9	40.0	−.0014	0.380	2.0047	2.0061	2.0056	60
E[b]	0.67	22.6	10.3_5	12.2_5	14.4	35.7	−.0025	0.490	2.0037	2.0062	2.0054	80
F[b]	1.00	24.1	10.9	13.2	15.3	34.1	−.0017	0.528	2.0033	2.0058	2.0050	47
G[b]	6.00	27.3	[d]	—	—	—	—	—	2.0030	[d]	—	—
H[c]	10.0	27.7	[d]	—	—	—	—	—	2.0028	[d]	—	—
I[c]	50.0	29.7_5	[d]	—	—	—	—	—	2.0025	[d]	—	—
J[c]	∞[g]	30.8	[d]	—	—	—	—	—	2.0021	[d]	—	—

[a] Reprinted with permission from Mason *et al.*, *J. Phys. Chem.* 78, 1324–1329 (1974). Copyright by the American Chemical Society.
[b] Peak-to-peak residual derivative width δ of 1.0 G was used.
[c] Peak-to-peak residual derivative width δ of 3.0 G was used.
[d] The inner hyperfine extrema are not resolved.
[e] $R_\perp$ and $R_\parallel$ are zero.
[f] S_o and α_z are defined by Eq. (89).
[g] A_o is defined by Eq. (91).
[h] g'_o is defined as $\frac{1}{3}(g'_x + g'_y + g'_z)$.
[i] From construction $\cos^{-1}(\alpha_y^2)^{1/2} = \pi/2$.
[j] If $S_o = 0.336$ is used. $\cos^{-1}(\alpha_z^2)^{1/2}$ equals 50°; see text.
[k] If correction is made for the finite $\tau_{R_\perp} = 5 \times 10^{-8}$ sec. then $S_o = 0.338$ (cf. Mason *et al.*, 1974).

A check on the validity of using $\mathcal{H}_{eff}$ for interpreting a spectrum in terms of the "pseudoaxial" rigid limit is that one must have Tr A = Tr A', which follows directly from the rotational invariance of the trace of a tensor. The simulated spectra of Fig. 12b have been analyzed just as though they were experimental results from anisotropically immobilized spin labels, and the results are summarized in Table IV (Mason *et al.*, 1974). These results are in fact very similar to those obtained by Wee and Miller (1973) and in spin label studies in membrane models and membranes (Hubbell and McConnell, 1969a,b, 1971; McConnell and McFarland, 1970; McFarland and McConnell, 1971). Note that (1) A'_0 does vary slightly from A_0 = 14.13 G but (2) the apparent S_0 varies considerably even though the calculated spectra were from a tilt angle of 41.7°, corresponding to a constant true value of S_0 = 0.336. The results for A and B in Fig. 12b, where $\tau_{R_\parallel}$ is very fast, are reasonable; the only discrepancy with the true results probably arises from the residual motional effects on the spectrum of having $\tau_{R_\perp} = 5 \times 10^{-8}$ sec. However, for spectra such as E and F, where $\tau_{R_\parallel} \sim 5\text{–}10 \times 10^{-10}$ sec, the motional effects for the fast motion about a single bond are already slow enough for us to utilize the simple time-independent $\mathcal{H}_{eff}$. Thus the invariance of S_0 is a necessary but not really sufficient condition for the simple approach.

Thus we note that a change in S_0 can arise from a real change in the angle between **v** and z or a change in the rotational rate about **v**, as is the predominant phenomenon in the spectra of Fig. 12a (the spectrum A, however, has a shorter τ_R than the other spectra) (Mason *et al.*, 1974). In general, these two phenomena cannot be distinguished unless the rotational rate about **v** slows to where A'_0 is clearly anomalous and/or the slowed motion manifests itself in the other spectral characteristics shown in Fig. 12a.

Note that the analysis in terms of a single $R_\perp$ and $R_\parallel$ represents a considerable simplification of the complex dynamics of polymer motion including localized bond motions and internal rotations. However, (1) as long as the internal rotation is much faster than the overall motion, it can be treated as uncoupled from the latter, and (2) if the overall motion is only showing marginal spectral effects, it would be difficult to obtain anything more precise than an effective $\tau_{R_\perp}$.

D. Anisotropic Liquids: Simulations

Some examples will now be given for nitroxides oriented in nematic liquid crystals (Polnaszek *et al.*, 1973; Polnaszek, 1975a). For convenience, the Meier–Saupe potential, coincidence of the magnetic and orientation principal axes, and axial magnetic parameters were used, unless otherwise noted. In all cases the director was assumed parallel to the static magnetic field.

First, the effect of keeping the rotational correlation time $\tau_R \equiv (6R)^{-1}$ constant but varying the ordering by changing the potential parameter λ is considered. Figure 14 shows such a case for an oblate nitroxide, i.e., one that

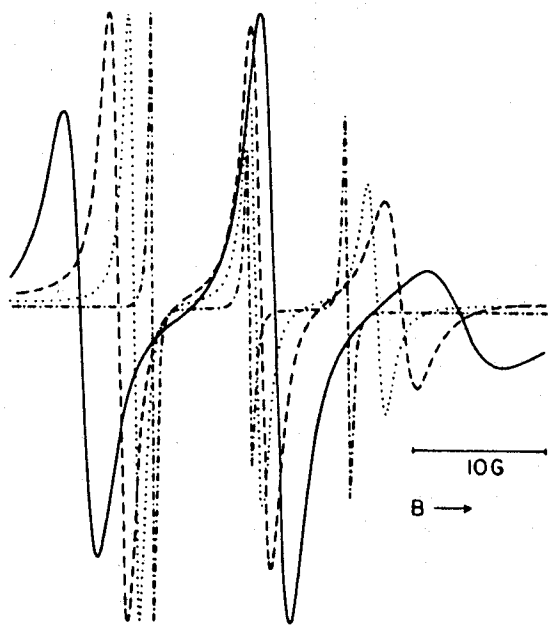

Fig. 14. First derivative line shapes for a nitroxide as a function of λ for Brownian diffusion. The different λ values are (——) 0, (– – –) −2.0, (···) −3.5, (–·–) −7.5. All correspond to $\tau_R = 1.84 \times 10^{-9}$, $g_\parallel = 2.0027$, $g_\perp = 2.0075$, $A_\parallel = 33.4$ G, $A_\perp = 5.42$ G, and $\delta = 0.1$ G. [From Polnaszek *et al.* (1973).]

tends to orient with its z axis perpendicular to the magnetic field. The rotational correlation time was held constant at a value of 1.84×10^{-9} sec which is in the incipient slow motional region for nitroxides. One sees that the effect of increasing the absolute magnitude of the orienting potential is (1) to decrease linewidths considerably, and (2) to introduce larger shifts in the positions of the lines. The first effect is due to the fact that the effective $[\mathcal{H}_1(t) - \langle\mathcal{H}_1\rangle]$ is reduced as the sample is being ordered, while $\langle\mathcal{H}_1\rangle$, the average part of the perturbation, which causes the line shifts, departs more from its isotropic value of zero. It appears that the slow tumbling spectra begin to resemble motional narrowing results as $|\lambda|$ is increased at a constant τ_R, although the shift of line positions is characteristic of liquid crystals in the nematic range. However, the observed line shifts are not predicted correctly by expressions appropriate for the motional narrowing region (cf

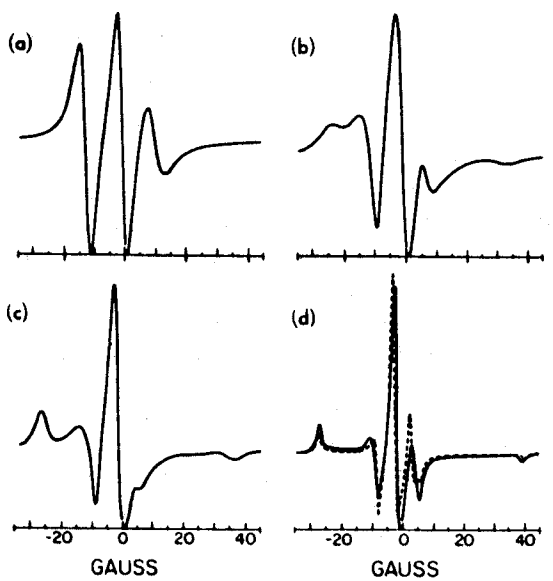

Fig. 15. First derivative line shapes for a nitroxide in the case of low ordering as a function of τ_R for Brownian diffusion: (a) $\tau_R = 3 \times 10^{-9}$ sec, IF = 5.08 (IF is the intensity factor, a measure of the relative integrated intensity); (b) $\tau_R = 10^{-8}$ sec, IF = 3.48; (c) $\tau_R = 3 \times 10^{-8}$ sec, IF = 4.38; (d) $\tau_R = 3 \times 10^{-7}$ sec, IF = 10.02; (---) rigid limit. Here $g_\parallel = 2.0024$, $g_\perp = 2.0078$, $A_\parallel = 33.75$ G, $A_\perp = 5.34$, and $\delta = 1.0$ G. All spectra are normalized to the same total height. [From Polnaszek *et al.* (1973).]

Chapter 10). We can use these shifts as an indication of slow motion in the mesophase. For $\lambda > 0$ a prolate top (a nitroxide that tends to orient with its z axis parallel to the field) similar linewidth behavior is observed, except that the spectrum spreads out and shifts to higher fields. In Fig. 15, λ is held constant at a value of -0.975, corresponding to a low degree of ordering typical of small nitroxides. Comparison with figures for isotropic liquids (cf. Figs. 6–8) shows that the trends are quite similar in both cases, but that there are distinct quantitative differences in the details of the line shapes at comparable τ_R's.

In Figs. 16a and b, λ is held constant (at -7.5 and 8.5, respectively) for large ordering parameters, with the correlation time varying over several orders of magnitude. They correspond respectively to large disklike and rodlike nitroxide molecules, which tend to be very well ordered. They show that spectra with correlation times $< 3 \times 10^{-8}$ sec will be fairly insensitive to changes in τ_R. In fact the observed ordering parameter for the oblate top nitroxide is nearly equal to the theoretical value for $\tau_R \lesssim 10^{-8}$ sec, and it is found that the rigid limit is not approached until $\tau_R \approx 10^{-6}$ (cf. Fig. 16c),

compared to $\tau_R \approx 3 \times 10^{-7}$ for the low ordering case in Fig. 15. Thus f a very highly ordered nitroxide, we can extend the upper limit of rotation correlation times obtainable from the unsaturated slow motional line shape

For values of the potential parameter λ that lead to intermediate orde ing (e.g., $\lambda = -3.5$, corresponding to $\langle \mathscr{D}^2_{00} \rangle = -0.30$), it has been foun that the deviations from symmetric lines and from the theoretical orderir parameter begin to occur at somewhat longer values of τ_R in the incipie slow tumbling region than for isotropic liquids, but that the linewidth asyn metry starts to be appreciable at somewhat shorter τ_R's than those for whi the apparent ordering parameter deviates significantly from the corre value. Therefore the linewidth asymmetry can be used as an indication slow tumbling in nematics. This can also be seen from Fig. 16 for high ordered nitroxides.

The effect of using different models of rotational reorientation has al been studied. For weakly ordered systems, one again sees the same qualit tive behavior of spectral changes as the rotational model is changed, b there are qualitative differences between the spectral changes for the isotro ic and nematic phases. As has been usually done for isotropic liquids, t correlation times for the non-Brownian models were determined to be tho that gave the same values for the separation of the outer hyperfine extrer (i.e., S) as observed in the Brownian diffusion case. For liquid crystals S expected to be a function of λ as well as of τ_R and A_z, thus complicating a attempts to use it as a quantitative measure of τ_R's in nematic phases. T was found to be true for weakly ordered systems. For the strongly orde cases, the parameter S is meaningless since no outer extrema are observe

Figure 17 gives an example in which the principal axis of orientation permuted among the three principal axes of the nitroxide magnetic tenso The hyperfine tensor is taken as axially symmetric, but the g tensor is asy metric, as is typical for nitroxides. The rotational correlation time 10^{-8} sec and λ was adjusted to make the S values nearly equal. The x- a y-axis spectra are cases where the molecule tends to align parallel to tho axes, respectively, while the z axis tends to be perpendicular to the field. O sees significant changes in the line shapes as the principal axis of orientati is changed, even for this weakly ordered system. There are also "apparen shifts in $\Delta g_\parallel$. The g shifts persist in the motional narrowing region for t case of three different orientations. Thus, especially when using any cyli drically symmetric potential, one must be careful to choose the principal a of orientation correctly. However, when an asymmetric potential such that given in Eq. (58) is used, the potential is invariant to permutation of t principal axes (i.e., the relabeling of x''', y''', z''' to obtain x', y', z'). Since t coefficients of the potential transform as the components of an irreducib tensor, we can transform the potential parameters for a principal axis syste

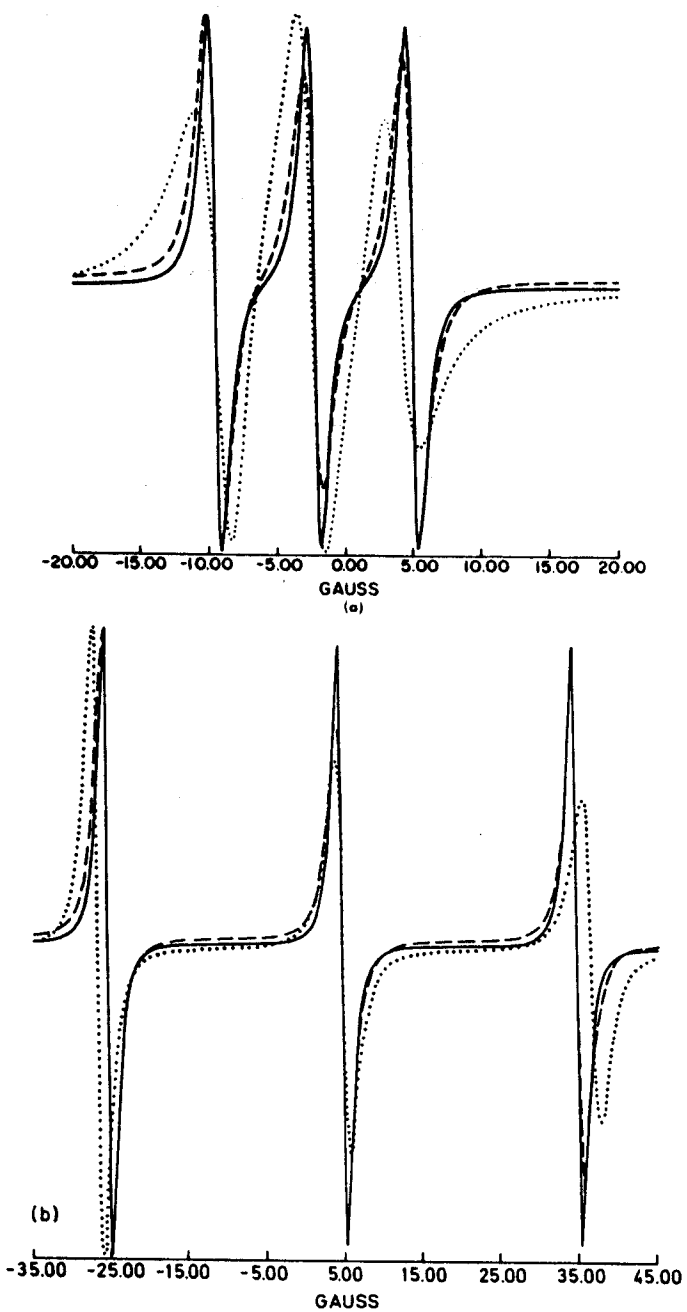

Fig. 16a, b.

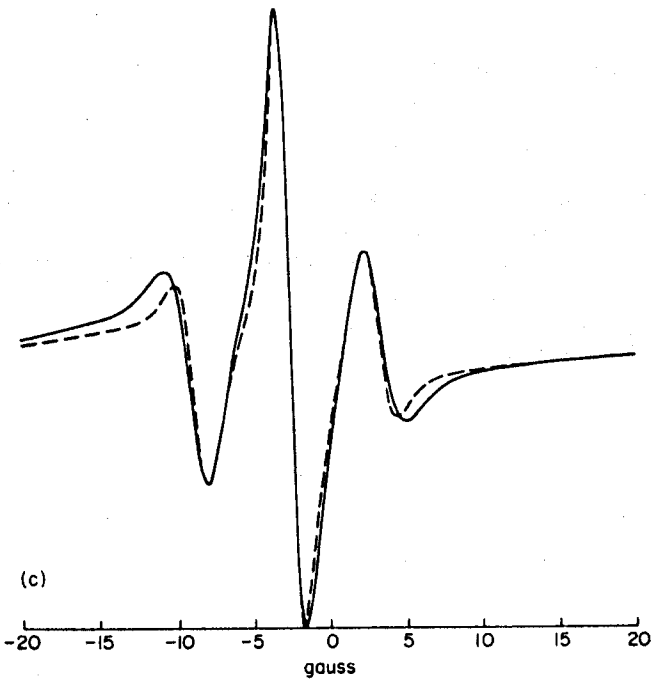

Fig. 16. First derivative line shapes for nitroxides in highly ordered cases as a function of for Brownian diffusion: (——) $\tau_R = 3 \times 10^{-10}$ sec, IF = 77.9; (- - -) $\tau_R = 3 \times 10^{-9}$ se IF = 52.9; (···) $\tau_R = 3 \times 10^{-8}$ sec, IF = 16.3. (a) $\lambda = -7.5$; (b) $\lambda = +8.5$. (c) $\lambda = -7.5$ a (——) $\tau_R = 3 \times 10^{-7}$ sec, IF = 29.8; (- - -) $\tau_R = 1 \times 10^{-6}$ sec, IF = 41.0. All other paramet as in Fig. 15. [From Polnaszek *et al.* (1973) and Polnaszek (1975a).]

in the molecule into those for another molecular axis system. For the pote tial given by Eq. (58), one has for a permutation of axes such that the axis → z' axis

$$\lambda_y = -(\lambda_z - 3\rho_z)/2 \tag{92}$$

and

$$\rho_y = -(\lambda_z + \rho_z)/2 \tag{92}$$

where the subscripts refer to the principal axis of orientation of the molecul We can also determine λ_x and ρ_x from the relation

$$\sum_i \lambda_i = \sum_i \rho_i = 0 \tag{9}$$

which follows from the fact that the ordering tensor is traceless.

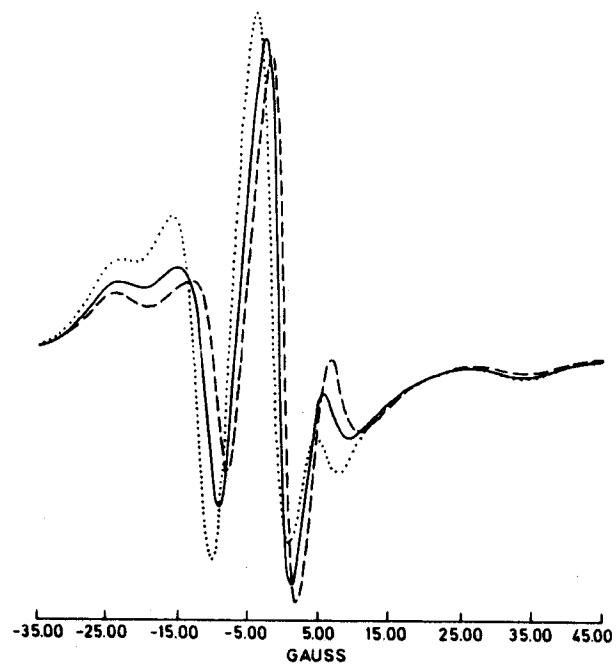

Fig. 17. First derivative line shapes for nitroxides with cylindrically symmetric potentials relative to the different principal axes of the magnetic tensor for Brownian diffusion. (——) The molecular z''' axis as the principal orientation axis with $\lambda = -0.975$; (···) the x''' axis as the principal orientation axis with $\lambda = 1.6$; (- - -) the y''' axis as the principal orientation axis with $\lambda = 1.6$. In all cases $\tau_R = 1 \times 10^{-8}$ sec, $A_z = 33.75$ G, $A_x = A_y = 5.34$ G, $g_x = 2.0094$, $g_y = 2.0062$, $g_z = 2.0024$. [From Polnaszek (1975a).]

It is well known that liquid crystals exhibit an anisotropic viscosity when oriented in a magnetic field (Miesowicz, 1946). The effects of anisotropic viscosity on nitroxide slow tumbling spectra are shown in Fig. 18. In this figure $\tau_{R_\perp} = (6R_\perp)^{-1}$ is kept constant at 1×10^{-8} sec, the potential parameter λ is -0.975, and $\tau_{R_\parallel}$ is varied. The effect of keeping $R_\perp$ constant is to keep the value of S virtually constant. However, there are gross changes in the central region of the spectrum as $R_\parallel$ is increased relative to $R_\perp$. Note from Eq. (66) that the terms that contain the effect of anisotropic viscosity have $M \neq 0$. It is seen from Eq. (74) that such terms are the pseudosecular terms in $\mathscr{H}_1(\Omega)$. Thus we must include them in the Hamiltonian in order to see the effects of anisotropic viscosity. The effects of anisotropic viscosity on the slow motional line shapes are negligible when the ordering parameter is large or if the molecule tends to be aligned with its z axis, the axis of cylindrical symmetry of the hyperfine tensor, parallel to the field. Note that

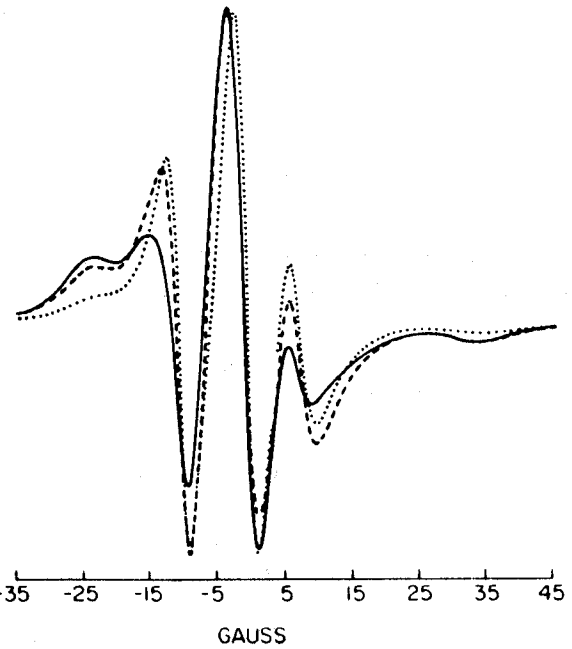

Fig. 18. First derivative line shapes for nitroxides as a function of the anisotropic viscosity parameter $\tilde{N} = \hat{R}_\parallel/\hat{R}_\perp$ for Brownian diffusion. (——) $\tilde{N} = 1$, IF = 3.48; (- - -) $\tilde{N} = 6$ IF = 3.30; (···) $\tilde{N} = 24$, IF = 5.33. All correspond to $\tau_{R_\perp} = 1 \times 10^{-8}$ sec. All other parameters as in Fig. 15. [From Polnaszek *et al.* (1973).]

the effects of anisotropic molecular reorientation on slow tumbling spectra from nitroxides are not as dramatic as the effects of anisotropic reorientation with respect to the director axis. Birrell *et al.* (1973) observed a system that can be thought of in terms of a highly anisotropic viscosity. Nitroxide free radicals were oriented in tubular cavities in inclusion crystals in which the molecule is free to rotate about the long axis but with its rotation hindered about the other two axes because of the cavity geometry. The system behaves as a highly ordered liquid crystal, which, as has already been noted, is fairly insensitive to the dynamics of the motion.

In all the preceding discussion, it has been assumed that $\mathbf{n}$ is fixed along the laboratory z axis, so that $\Psi = (0, 0, 0)$. When $\mathbf{n}$ is tilted relative to the axis, then Eq. (45) must be used to expand $\mathscr{H}_1(\Omega, \Psi)$, but otherwise the same diffusion equations in terms of Ω are applicable. If there are random static distributions of directors, then, in principle, one must solve the problem for each value of Ψ and then integrate over the correct static distribution to predict the spectrum. When there is residual motion of the director, the

the stochastic Liouville equation can be augmented to deal effectively with the simultaneous motions of Ψ and Ω (Polnaszek, 1975a; Polnaszek and Freed, 1975).†

E. Anisotropic Liquids: Experiments

Experiments have now been carried out to test the applicability of the slow tumbling theory to anisotropic liquids using the same general approach as has already been described for studies in isotropic liquids (Polnaszek, 1975a; Polnaszek and Freed, 1975). In particular, the PD-TEMPONE probe has been studied in several viscous nematic solvents. The study was limited by the fact that before very large viscosities could be reached, the nematics would freeze. However, in the case of phase V solvent, it was possible to reach the slow motional region (cf. Fig. 19). Note in Fig. 20 how the apparent $\langle \mathscr{D}^2_{00} \rangle$ changes markedly when the slow motional region is approached.

In the isotropic studies, the motional narrowing line shapes were carefully corrected for the residual inhomogenous broadening effects of the deuteron splittings given in Table I. In the nematic phase, the splittings were found to vary with temperature as a result of the increase of $\langle \mathscr{D}^2_{K0} \rangle$ with decreasing temperature. This added factor had to be corrected for in order to adequately deal with the line shapes.

Furthermore, careful measurements of the a_N and g shifts clearly demonstrated that the radical ordering required the use of the two-parameter potential of Eq. (58). For most cases (including phase V solvent), if the choice $x''' = x'$, $y''' = y'$, and $z''' = z'$ is made, then $|\lambda| > |\rho|$, with typical values for phase V being $\lambda_z = -0.8$ and $\rho = 0.3$. The higher temperature spectra from the isotropic phase again showed $N = 1$ for the anisotropic diffusion parameter, corresponding to isotropic rotation. However, in the nematic phase, only if the correct ordering potential involving *both* λ and ρ were used could the linewidth results be fit to isotropic rotational diffusion.

The appropriate values of τ_R, $N = 1$, λ, and ρ were then extrapolated to the slow motional region to obtain parameters to predict the slow motional spectrum. A typical comparison is shown in Fig. 21a, where $\tau_R = 3.6 \times 10^{-9}$ sec at $-25°$. There are serious discrepancies between experiment and prediction, unlike the good agreement (cf. Fig. 16) for isotropic liquids. This incipient slow tumbling region has been found to be rather model insensitive. However, careful analysis of the motional narrowing region for $\tau_R > 2 \times 10^{-10}$ sec showed that the discrepancy was developing

† Editor's note: Further and more expanded discussions of order parameters and the anisotropic motion of spin labels in liquid crystals and bilayer model membrane systems are found in Appendix IV and Chapters 10–12, respectively.

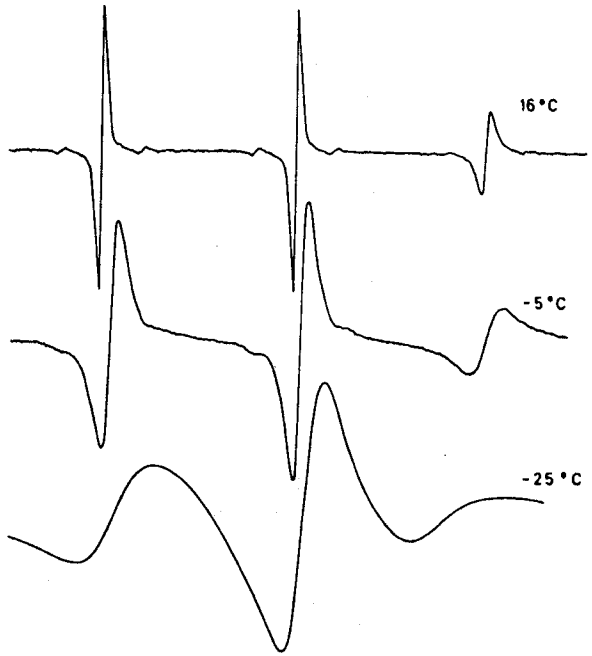

Fig. 19. ESR spectra of PD-TEMPONE in liquid crystal: phase V, at different temperatures. The scan range is 40 G. [From Polnaszek (1975a).]

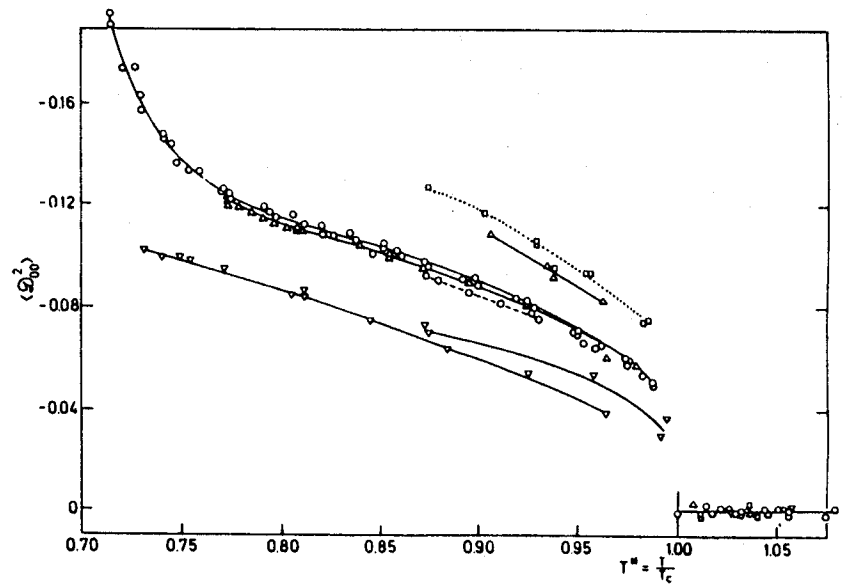

Fig. 20. Ordering parameter $\langle \mathscr{D}^2_{00} \rangle$ vs. reduced temperature $T^* \equiv T/T_c$ for PD-TEMPONE in several liquid crystals; ○, phase V solvent. [Reprinted with permission from Polnaszek and Freed, *J. Phys. Chem.* 79 (in press) (1975). Copyright by the American Chemical Society.]

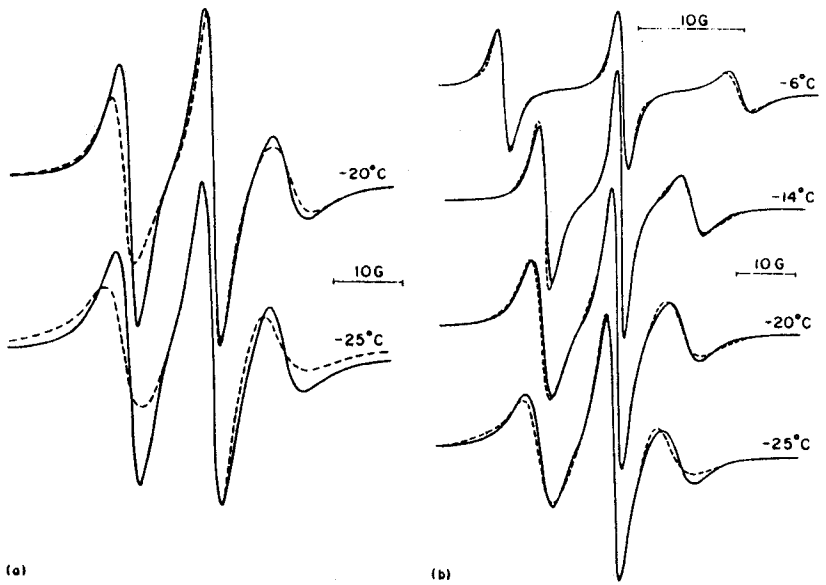

Fig. 21. Comparison of theoretical (——) and experimental (- - -) spectra for PD-TEMPONE in phase V liquid crystal at (a) $\varepsilon' = 1$ with $\tau_R = 2.5 \times 10^{-9}$ sec at $-20°C$ and $\tau_R = 3.6 \times 10^{-9}$ sec at $-25°C$ ($A' = 0$ G); (b) $\varepsilon'_{sec} = 1.2$, $\varepsilon'_{psec} = 20$. The values at $-6°$, $-14°$, $-20°$, and $-25°C$ are for τ_R: 0.9, 1.6, 2.5, and 3.6×10^{-9} sec, respectively, and for A': 0.55, 1.0, 1.45, and 1.75 G, respectively. The magnetic parameters are given in Table IV. [Reprinted with permission from Polnaszek and Freed, *J. Phys. Chem.* **79** (in press) (1975). Copyright by the American Chemical Society.]

there as well [i.e., the τ_R obtained from the B and C terms in Eq. (79) were no longer the same]. It was found possible to largely remove this discrepancy by the physically *unreasonable* model that anisotropic viscosity was developing such that while $\tau_{R_\perp}$ increased with η/T as is normal for a liquid, $\tau_{R_\parallel}$ remained virtually constant at $\sim 2 \times 10^{-10}$ sec. However, some alternative explanations have been proposed. To appreciate them, one must first examine Figs. 3 and 4 for isotropic liquids. There it is found that the nonsecular spectral densities for the rotational motion, which are expected to obey a Debye-type expression (cf. Chapter 2)

$$j(\omega_e) = \tau_R/(1 + \omega_e^2\tau_R^2) \tag{94}$$

were better fitted instead by the expression

$$j(\omega_e) = \tau_R/(1 + \varepsilon\omega_e^2\tau_R^2) \tag{94'}$$

with $\varepsilon \approx 5$. A similar correction was found to be the case in the work with nematic solvents both above and below the isotropic–nematic transition with a smaller one below the transition. Deviations from the simple Debye

formula would be expected to arise if the rotational reorientation is significantly coupled to other degrees of freedom of the molecule or its surroundings (e.g., the angular momentum of the molecule or internal rotational degrees of freedom). A detailed statistical mechanical theory in terms of fluctuating torques experienced by the spin probe in its liquid environment has been proposed by Hwang *et al.* (1975).

The pseudosecular terms reflect the nuclear spin-flip transitions $\omega_\pm \approx a_N/2$ for isotropic liquids and $\langle a_N \rangle/2$ for nematics. Thus one might try

$$j(\omega_\pm) = \tau_R/(1 + \varepsilon'\omega_\pm^2\tau_R^2) \tag{95}$$

It was found that a large value of ε' could account reasonably for the motional narrowing and slow tumbling spectra in the nematic (cf. Fig. 21b).

Actually, the analysis of this effect is fairly complex, involving incipient slow tumbling corrections from which it transpires that the secular spectral densities are now also characterized by nonzero frequencies and the pseudosecular spectral densities are modified. The proper analysis, which is complex, is discussed by Polnaszek and Freed (1975). It is found that the pseudosecular spectral densities require a correction of $\varepsilon'_{psec} \sim 15$–$20$ while for the secular spectral densities $\varepsilon'_{sec} \sim 1$–$2$. This yields satisfactory agreement with experiment (cf. Fig. 21b). Another approach to this problem, in terms of slowly fluctuating torques, has been introduced by Polnaszek and Freed (1975). It is based upon the concept of a local structure or ordering which is relaxing more slowly than the probe molecule. This structure is expected to result from the surrounding rodlike nematic solvent molecules, which reorient more slowly than the smaller spin probe. [Such effects are not included in the Meier–Saupe (1958) mean field analysis that leads to the effective pseudopotential.] A simple analysis of the spin relaxation effects of such a mechanism shows that it has many of the proper trends. We may let Ψ be the slowly relaxing set of Euler angles between the local structure and the lab frame, then for an axially symmetric potential of the spin probe relative to the local structure, rough estimates of $S_l^2 \equiv \langle \mathcal{D}_{00}^2(\Omega) \rangle^2 \sim 0.1$ and $\tau_x/\tau_R \sim 10$ are obtained from the simple model, where τ_x is the local structure relaxation time. If such a hypothesis were correct, further careful studies including larger spin probes of different shapes could shed further light on this phenomenon.

Some preliminary experimental spectra of the rodlike cholesteric spin label 3-doxyl-5α-cholestone in the viscous nematic phase of phase V are shown in Fig. 22 (Polnaszek, 1975a). The system is highly ordered and the apparent splitting constants do not change appreciably with temperature. The observed $\langle \mathcal{D}_{00}^2 \rangle$ values calculated from a motional narrowing theory analysis (cf. Chapter 8) are -0.35, -0.39, and -0.46 for $T = 26$, 3, and $-26°C$, respectively. The two splittings are not equal at the lowest tempera-

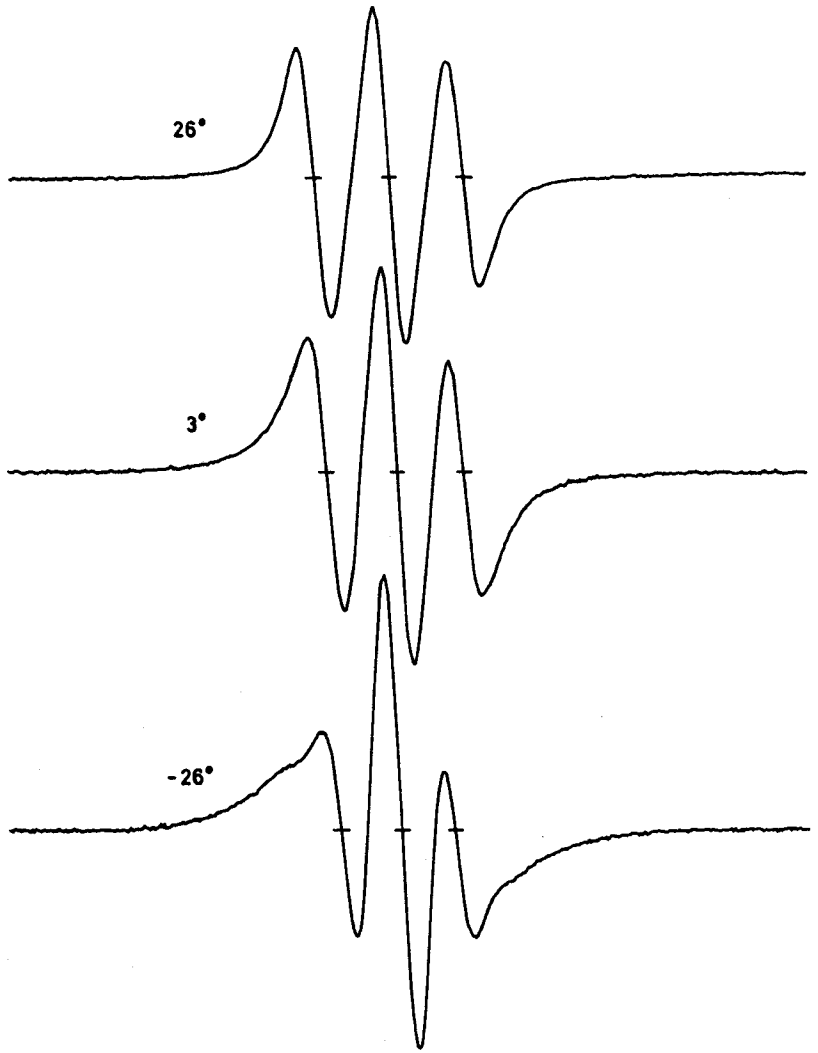

Fig. 22. Experimental spectra of the cholesteric spin label 3-doxyl-5α-cholestone in phase V at different temperatures. [From Polnaszek (1975a).]

tures, and, as already noted, this is indicative of slow motion (as is the exceedingly large value of $\langle \mathscr{D}^2_{00} \rangle$). The estimated τ_R for $-26°C$ is $\sim 4 \times 10^{-8}$ sec. These spectra compare favorably with the theoretical spectra simulated for high order ($\lambda = -7.5$) in Fig. 16a, although the actual ordering of the experimental spectra in Fig. 22 is somewhat less than that of the theoretical spectra.

F. Saturation and Nonlinear Effects

The general slow tumbling theory presented in Section I can also applied to saturation phenomena (Freed *et al.*, 1971; Goldman *et al.*, 19 Goldman, 1973; Bruno, 1973). A careful study of saturation and slow tu bling for PADS in viscous media has shown that the stochastic Liouv approach can be effectively employed to predict slow tumbling spec (Goldman *et al.*, 1973). This is illustrated in Fig. 23. Note that the simu tions were performed for axial nitroxide parameters, so the agreeme should not be expected to be perfect.

In the discussion of Section II.B on simplified methods of estimating from features of the outer hyperfine extrema, it was found that in the regi where $\tau_R > 10^{-8}$ sec they are quite insensitive to all parameters other th $\tau_{R_\perp}$, A_z, and A (the intrinsic width), while the central region is affected by t other magnetic tensor components. It is therefore reasonable to expect th simulations based on axial parameters should agree quite well with t saturation behavior of the outer extrema but not necessarily with the cent extrema. Such a comparison is shown in Fig. 24, which shows the ratios the $d_{\max}(\tilde{M}) = \frac{1}{2} |\gamma_e| H_{1,\max}(\tilde{M})$ [where $H_{1,\max}(\tilde{M})$ is the microwave fi strength at which the $\tilde{M} = -1, 0$, or $+1$ regions of the spectra maximi where these regions correspond, respectively, to the low field, central, a high-field extrema]. In particular, for $\tau_R > 10^{-8}$ sec, there is rather go agreement between experiment and prediction for $d_{\max}(+1)/d_{\max}(-1)$. It possible to use such a ratio (which depends only on relative values of B_1 a not on its absolute magnitude) as a means of estimating τ_R, but this has r yet been studied in detail. In particular, we are adding the new parame W_e, the electron-spin relaxation rate, into the analysis. Also note the ratl small changes in the ratio for large changes in τ_R.

At the heart of all saturation and nonlinear phenomena is the fact th the eigenfunction expansion coefficients for the density matrix elements r resenting population differences {cf. Eq. (27), the terms $[C_m^{(0)}]_\lambda - [C_m^{(0)}$ where $n = 0$} are relaxed at rates that depend on

$$2W_e + B_L RL(L+1) \qquad (9$$

when (1) an orientation-independent W_e is used and (2) isotropic reorient tion is assumed. There is, of course, coupling among the different ES transitions due to the nuclear spin-flip transitions induced by the p dosecular terms in $\mathscr{H}_1(\Omega)$. Thus while the expansion coefficients for L representing the population difference for the proper isotropic average o orientations, is relaxed by $T_{1,e} = (2W_e)^{-1}$, the coefficients for $L > 0$ a relaxed by the rotational motion as well. Furthermore, when $R \gg W_e$ (ty cal values of W_e are $\sim 10^{-5}$ sec), then (1) the rotational motion is ve

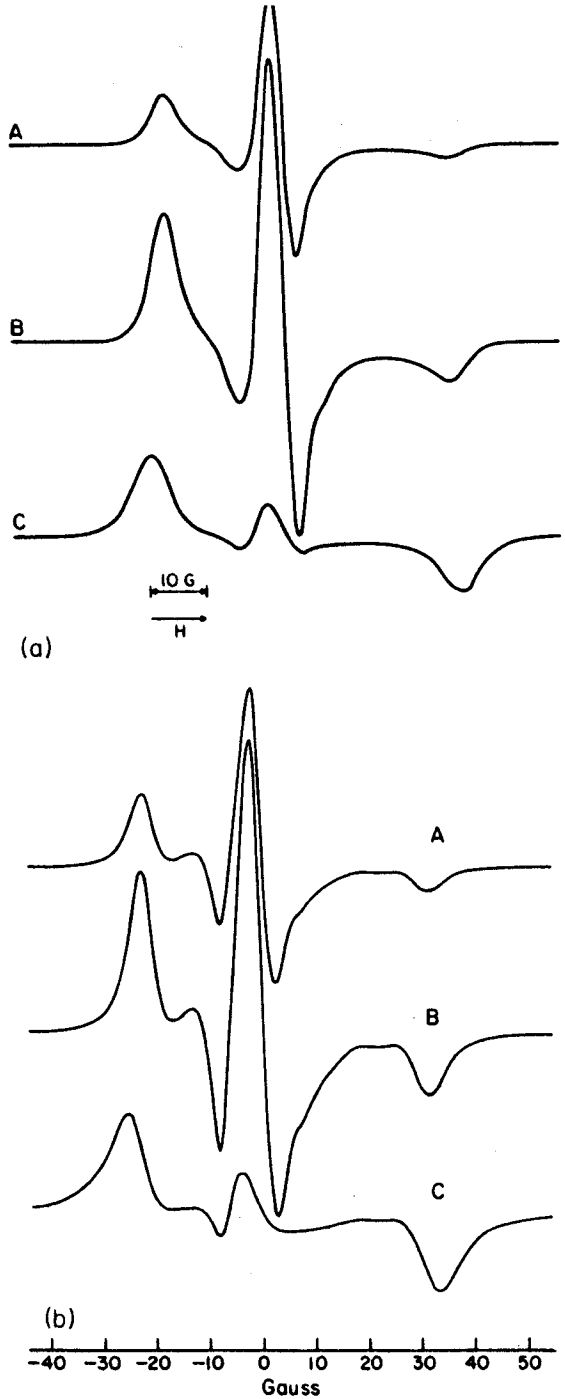

Fig. 23. (a) Experimental saturation spectra for PADS in 85% glycerol-H_2O at $T = -41°C$ and A, $d_e = 0.025$ G; B, $d_e = 0.079$ G; and C, $d_e = 0.45$ G. (b) Spectra simulated for free diffusion with $\tau_R = 2 \times 10^{-8}$ sec, $\delta = 1.2$ G, $W_e = 6.2 \times 10^4$ sec^{-1}, and A, $d_e = 0.03$ G; B, $d_e = 0.08$ G; and C, $d_e = 0.47$ G. Axial magnetic parameters were used in the simulations. $d_e = \frac{1}{2}\gamma_e H_1$. [From Goldman (1973).]

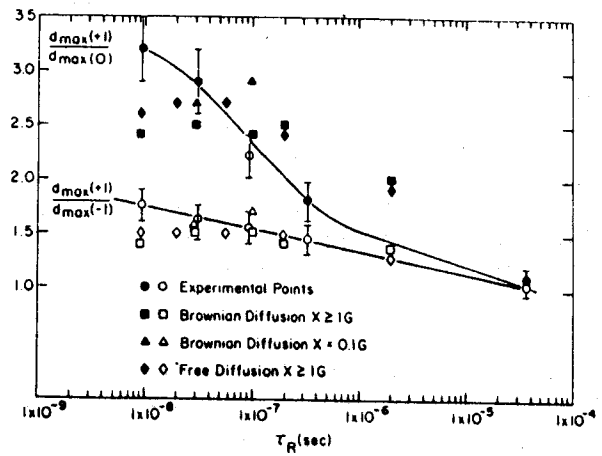

Fig. 24. Variation of $d_{max}(+1)/d_{max}(0)$ and $d_{max}(+1)/d_{max}(-1)$ with τ_R. Solid lines are drawn through the experimental points for the system PADS in 85% glycerol-H_2O. [From Goldman *et al.* (1973).]

effective in spreading the saturation throughout the spectrum, and (2) only the $L = 0$ component is effectively saturated. These ideas and the implications they have for pulsed saturation recovery studies are explored elsewhere (Freed, 1974). It is found in that work that the saturation recovery times (or at least the slowest relaxing mode) are often well approximated by $T_{1,e} \simeq (2W_e)^{-1}$ over a wide range of conditions, including the slow tumbling region.

Such considerations suggest that slow tumbling ELDOR experiments could be very interesting (Bruno, 1973; Bruno and Freed, 1974a; Smigel *et al.*, 1974). In such experiments, we saturate with a pump microwave field at a particular resonant frequency corresponding to a particular orientation (and nuclear spin) of the nitroxide and then observe at another position corresponding to a different orientation. Then the indirect saturation at the observing position will depend on the rotational motion of the molecule. We therefore expect that the ratio R/W_e will determine the relative importance of transmission of saturation to different environments (a form of "spin diffusion") versus simple ESR spin relaxation. The application of the stochastic Liouville theory to such experiments is discussed in detail elsewhere (Bruno, 1973; Bruno and Freed, 1974a; Smigel *et al.*, 1974).

Finally, we note the existence of a great variety of nonlinear phenomena, such as the modulation-frequency dependence of adiabatic rapid-passage effects explored by Hyde and Dalton (1972). This latter, more complex phenomenon can also be dealt with by stochastic Liouville methods and is

discussed elsewhere (Dalton, 1973; Leniart, 1972; Thomas and McConnell, 1974). The rather striking spectral effects observed have been calibrated with typical samples by the use of the S parameter and extrapolation of τ_R with known values of η/T to yield estimates of $\tau_R \gtrsim 10^{-6}$ sec (Hyde and Dalton, 1972).

In the discussion of saturation and nonlinear effects there is an important distinction to be made with respect to intrinsic widths, which was not important in the theory for unsaturated spectra. Note that in Eqs. (28) and (29) intrinsic widths were introduced by replacing ω_λ by $\omega_\lambda + iT_2^{-1}$ with no distinction made as to whether these widths are due to homogeneous or inhomogeneous broadening. It is possible to show, from the general form of the solutions in terms of superpositions of "complex Lorentzians" (cf. Appendix A), that this is entirely adequate for the case of a Lorentzian distribution of inhomogeneous broadening and *no saturation* (Abragam, 1961; Goldman *et al.*, 1973). If the inhomogeneous widths may not be approximated as Lorentzian, then we must convolute the line shapes obtained from the slow tumbling theory given here with a more appropriate inhomogeneous line-shape function (e.g., a Gaussian). This can become a real problem when unresolved proton extra hyperfine structure is a dominant source of broadening (in which case rigorous line-shape simulations require adequate knowledge of the proton splittings and their orientation dependence). It is well known, however, that in the case of saturation, homogeneous and Lorentzian inhomogeneous lines are no longer formally equivalent (Abragam, 1961). Then Eqs. (28) and (29) are only appropriate for the homogeneous broadening. Again, inhomogeneous broadening could be accounted for by convolution methods, but for Lorentzian inhomogeneous broadening there is a simpler method. The solutions for saturated cases require both the coefficients $C^L_{KM}(i)$ of Eq. (27) and their complex conjugates $C^L_{KM}(i)^*$, to which they are coupled by the saturating terms. For homogenous broadening we replace $\omega_\lambda \to \omega_\lambda + iT_2^{-1}$ for the former, as already noted, but $\omega_\lambda \to \omega_\lambda - iT_2^{-1}$ for the latter. But for Lorentzian inhomogeneous broadening, we can merely let $\omega_\lambda \to \omega_\lambda + iT_2^{-1}$ for both types of terms (Goldman *et al.*, 1973). The computer simulations of Fig. 23b were made for the case of homogeneous broadening.

APPENDIX A. GENERAL SOLUTIONS AND DISCUSSION OF THE COMPUTER PROGRAM FOR NITROXIDES

The equations upon which the computer program given in Appendix B for the ESR spectrum of a nitroxide in an isotropic fluid are based are (Bruno, 1973)

$$
\begin{aligned}
&[(\omega - \omega_e + 2b) - i(T_{2,a}^{-1} + \tau_{L,K}^{-1})]\bar{C}^L_{K,0}(1) \\
&\quad - (F_0 + D' + iT_{2,b}^{-1}) \sum_{L'} N(L, L') \begin{pmatrix} L & 2 & L' \\ -K & 0 & K \end{pmatrix} \begin{pmatrix} L & 2 & L' \\ 0 & 0 & 0 \end{pmatrix} \bar{C}^{L'}_{K,0}(1) \\
&\quad - (F_2 + D^{(2)\prime}) \sum_{L'} N(L, L') \begin{pmatrix} L & 2 & L' \\ 0 & 0 & 0 \end{pmatrix} \\
&\quad \times \left[\begin{pmatrix} L & 2 & L' \\ -K & -2 & K+2 \end{pmatrix} \bar{C}^{L'}_{K+2,0}(1) \right. \\
&\quad \left. + \begin{pmatrix} L & 2 & L' \\ -K & 2 & K-2 \end{pmatrix} \bar{C}^{L'}_{K-2,0}(1) \right] \\
&\quad + D \sum_{L'} N(L, L') \begin{pmatrix} L & 2 & L' \\ -K & 0 & K \end{pmatrix} \begin{pmatrix} L & 2 & L' \\ 0 & -1 & 1 \end{pmatrix} \\
&\quad \times \bar{C}^{L'}_{K,1}(4, 5) + D^{(2)} \sum_{L'} N(L, L') \begin{pmatrix} L & 2 & L' \\ 0 & -1 & 1 \end{pmatrix} \\
&\quad \times \left[\begin{pmatrix} L & 2 & L' \\ -K & -2 & K+2 \end{pmatrix} \bar{C}^{L'}_{K+2,1}(4, 5) \right. \\
&\quad \left. + \begin{pmatrix} L & 2 & L' \\ -K & 2 & K-2 \end{pmatrix} \bar{C}^{L'}_{K-2,1}(4, 5) \right] = 2^{1/2} q \omega_1 d_1 \delta(L, 0) \delta(K, 0) \qquad \text{(A.1)} \\
&[(\omega - \omega_e) - i(T_{2,a}^{-1} + \tau_{L,K}^{-1})]\bar{C}^L_{K,0}(2) \\
&\quad - (F_0 + iT_{2,b}^{-1}) \sum_{L'} N(L, L') \begin{pmatrix} L & 2 & L' \\ -K & 0 & K \end{pmatrix} \begin{pmatrix} L & 2 & L' \\ 0 & 0 & 0 \end{pmatrix} \bar{C}^{L'}_{K,0}(2) \\
&\quad - F_2 \sum_{L'} N(L, L') \begin{pmatrix} L & 2 & L' \\ 0 & 0 & 0 \end{pmatrix} \left[\begin{pmatrix} L & 2 & L' \\ -K & -2 & K+2 \end{pmatrix} \bar{C}^{L'}_{K+2,0}(2) \right. \\
&\quad \left. + \begin{pmatrix} L & 2 & L' \\ -K & 2 & K-2 \end{pmatrix} \bar{C}^{L'}_{K-2,0}(2) \right] + D \sum_{L'} N(L, L') \begin{pmatrix} L & 2 & L' \\ 0 & -1 & 1 \end{pmatrix} \\
&\quad \times \begin{pmatrix} L & 2 & L' \\ -K & 0 & K \end{pmatrix} [\bar{C}^{L'}_{K,1}(4, 5) + \bar{C}^{L'}_{K,1}(6, 7)] + D^{(2)} \sum_{L'} N(L, L') \\
&\quad \times \begin{pmatrix} L & 2 & L' \\ 0 & -1 & 1 \end{pmatrix} \\
&\quad \times \left\{ \begin{pmatrix} L & 2 & L' \\ -K & -2 & K+2 \end{pmatrix} [\bar{C}^{L'}_{K+2,1}(4, 5) + \bar{C}^{L'}_{K+2,1}(6, 7)] \right. \\
&\quad \left. + \begin{pmatrix} L & 2 & L' \\ -K & 2 & K-2 \end{pmatrix} [\bar{C}^{L'}_{K-2,1}(4, 5) + \bar{C}^{L'}_{K-2,1}(6, 7)] \right\} \\
&\quad = 2^{1/2} q \omega_2 d_2 \delta(L, 0) \delta(K, 0) \qquad \text{(A.2)}
\end{aligned}
$$

$$
\begin{aligned}
&[(\omega-\omega_e-2b)-i(T_{2,a}^{-1}+\tau_{L,K}^{-1})]\bar{C}^{L'}_{K,0}(3)\\
&\quad-(F_0-D'+iT_{2,b}^{-1})\sum_{L'}N(L,L')\begin{pmatrix}L&2&L'\\-K&0&K\end{pmatrix}\begin{pmatrix}L&2&L'\\0&0&0\end{pmatrix}\bar{C}^{L'}_{K,0}(3)\\
&\quad-(F_2-D^{(2)\nu})\sum_{L'}N(L,L')\begin{pmatrix}L&2&L'\\0&0&0\end{pmatrix}\\
&\quad\times\left[\begin{pmatrix}L&2&L'\\-K&-2&K+2\end{pmatrix}\bar{C}^{L'}_{K+2,0}(3)\right.\\
&\quad\left.+\begin{pmatrix}L&2&L'\\-K&2&K-2\end{pmatrix}\bar{C}^{L'}_{K-2,0}(3)\right]\\
&\quad+D\sum_{L'}N(L,L')\begin{pmatrix}L&2&L'\\-K&0&K\end{pmatrix}\begin{pmatrix}L&2&L'\\0&-1&1\end{pmatrix}\\
&\quad\times\bar{C}^{L'}_{K,1}(6,7)+D^{(2)}\sum_{L'}N(L,L')\begin{pmatrix}L&2&L'\\0&-1&1\end{pmatrix}\\
&\quad\times\left[\begin{pmatrix}L&2&L'\\-K&-2&K+2\end{pmatrix}\right.\\
&\quad\left.\times\bar{C}^{L'}_{K+2,1}(6,7)+\begin{pmatrix}L&2&L'\\-K&2&K-2\end{pmatrix}\bar{C}^{L'}_{K-2,1}(6,7)\right]\\
&\quad=2^{1/2}q\omega_3 d_3\delta(L,0)\delta(K,0)
\end{aligned}
\tag{A.3}
$$

$$
\begin{aligned}
&[(\omega-\omega_e+b)-i(T_{2,a}^{-1}+\tau_{L,K}^{-1})]\bar{C}^{L}_{K,1}(4,5)\\
&\quad+(F_0+\tfrac{1}{2}D'+iT_{2,b}^{-1})\sum_{L'}N(L,L')\begin{pmatrix}L&2&L'\\-K&0&K\end{pmatrix}\\
&\quad\times\begin{pmatrix}L&2&L'\\-1&0&1\end{pmatrix}\bar{C}^{L'}_{K,1}(4,5)\\
&\quad+(F_2+\tfrac{1}{2}D^{(2)\nu})\sum_{L'}N(L,L')\begin{pmatrix}L&2&L'\\-1&0&1\end{pmatrix}\\
&\quad\times\left[\begin{pmatrix}L&2&L'\\-K&-2&K+2\end{pmatrix}C^{L'}_{K+2,1}(4,5)\right.\\
&\quad\left.+\begin{pmatrix}L&2&L'\\-K&2&K-2\end{pmatrix}\bar{C}^{L'}_{K-2,1}(4,5)\right]+D\sum_{L'}N(L,L')\begin{pmatrix}L&2&L'\\-1&1&0\end{pmatrix}\\
&\quad\times\begin{pmatrix}L&2&L'\\-K&0&K\end{pmatrix}[\bar{C}^{L'}_{K,0}(1)+\bar{C}^{L'}_{K,0}(2)]\\
&\quad+D^{(2)}\sum_{L'}N(L,L')\begin{pmatrix}L&2&L'\\-1&1&0\end{pmatrix}
\end{aligned}
$$

(equation continues)

$$
\begin{aligned}
&\quad\times\left\{\begin{pmatrix}L&2&L'\\-K&-2&K+2\end{pmatrix}[\bar{C}^{L'}_{K+2,0}(1)+\bar{C}^{L'}_{K+2,0}(2)]\right.\\
&\quad+\begin{pmatrix}L&2&L'\\-K&2&K-2\end{pmatrix}[\bar{C}^{L'}_{K-2,0}(1)\\
&\quad\left.+\bar{C}^{L'}_{K-2,0}(2)]\right\}-2^{-1/2}D\sum_{L'}N(L,L')\begin{pmatrix}L&2&L'\\-K&0&K\end{pmatrix}\begin{pmatrix}L&2&L'\\-1&-1&2\end{pmatrix}\\
&\quad\times\bar{C}^{L'}_{K,2}(8,9)-2^{-1/2}D^{(2)}\sum_{L'}N(L,L')\begin{pmatrix}L&2&L'\\-1&-1&2\end{pmatrix}\\
&\quad\times\left[\begin{pmatrix}L&2&L'\\-K&-2&K+2\end{pmatrix}\right.\\
&\quad\left.\times\bar{C}^{L'}_{K+2,2}(8,9)+\begin{pmatrix}L&2&L'\\-K&2&K-2\end{pmatrix}\bar{C}^{L'}_{K-2,2}(8,9)\right]=0
\end{aligned}
\tag{A.4}
$$

$$
\begin{aligned}
&[(\omega-\omega_e-b)-i(T_{2,a}^{-1}+\tau_{L,K}^{-1})]C^{L}_{K,1}(6,7)\\
&\quad+(F_0-\tfrac{1}{2}D'+iT_{2,b}^{-1})\sum_{L'}N(L,L')\begin{pmatrix}L&2&L'\\-K&0&K\end{pmatrix}\\
&\quad\times\begin{pmatrix}L&2&L'\\-1&0&1\end{pmatrix}\bar{C}^{L'}_{K,1}(6,7)\\
&\quad+(F_2-\tfrac{1}{2}D^{(2)\nu})\sum_{L'}N(L,L')\begin{pmatrix}L&2&L'\\-1&0&1\end{pmatrix}\\
&\quad\times\left[\begin{pmatrix}L&2&L'\\-K&-2&K+2\end{pmatrix}\bar{C}^{L'}_{K+2,1}(6,7)\right.\\
&\quad\left.+\begin{pmatrix}L&2&L'\\-K&2&K-2\end{pmatrix}C^{L'}_{K-2,1}(6,7)\right]+D\sum_{L'}N(L,L')\begin{pmatrix}L&2&L'\\-K&0&K\end{pmatrix}\\
&\quad\times\begin{pmatrix}L&2&L'\\-1&1&0\end{pmatrix}[\bar{C}^{L'}_{K,0}(2)+\bar{C}^{L'}_{K,0}(3)]\\
&\quad+D^{(2)}\sum_{L'}N(L,L')\begin{pmatrix}L&2&L'\\-1&1&0\end{pmatrix}\\
&\quad\times\left\{\begin{pmatrix}L&2&L'\\-K&-2&K+2\end{pmatrix}[\bar{C}^{L'}_{K+2,0}(2)+\bar{C}^{L'}_{K+2,0}(3)]\right.\\
&\quad\left.+\begin{pmatrix}L&2&L'\\-K&2&K-2\end{pmatrix}[\bar{C}^{L'}_{K-2,0}(2)+\bar{C}^{L'}_{K-2,0}(3)]\right\}\\
&\quad-2^{-1/2}D\sum_{L'}N(L,L')\begin{pmatrix}L&2&L'\\-K&0&K\end{pmatrix}\begin{pmatrix}L&2&L'\\-1&-1&2\end{pmatrix}\bar{C}^{L'}_{K,2}(8,9)
\end{aligned}
$$

(equation continues)

$$- 2^{-1/2}D^{(2)} \sum_{L'} N(L, L')\begin{pmatrix} L & 2 & L' \\ -1 & -1 & 2 \end{pmatrix}$$
$$\times \left[\begin{pmatrix} L & 2 & L' \\ -K & -2 & K+2 \end{pmatrix}\bar{C}^{L'}_{K+2,2}(8,9) + \begin{pmatrix} L & 2 & L' \\ -K & 2 & K-2 \end{pmatrix}\bar{C}^{L'}_{K-2,2}(8,9)\right] = 0 \quad \text{(A.5)}$$

$$[(\omega - \omega_e) - i(T^{-1}_{2,a} + \tau^{-1}_{L,K})]\bar{C}^{L}_{K,2}(8,9)$$
$$- (F_0 + iT^{-1}_{2,b}) \sum_{L'} N(L, L')\begin{pmatrix} L & 2 & L' \\ -K & 0 & K \end{pmatrix}$$
$$\times \begin{pmatrix} L & 2 & L' \\ -2 & 0 & 2 \end{pmatrix}\bar{C}^{L'}_{K,2}(8,9)$$
$$- F_2 \sum_{L'} N(L, L')\begin{pmatrix} L & 2 & L' \\ -2 & 0 & 2 \end{pmatrix}\left[\begin{pmatrix} L & 2 & L' \\ -K & -2 & K+2 \end{pmatrix}\bar{C}^{L'}_{K+2,2}(8,9) + \begin{pmatrix} L & 2 & L' \\ -K & 2 & K-2 \end{pmatrix}\bar{C}^{L'}_{K-2,2}(8,9)\right] - 2^{-1/2}D \sum_{L'} N(L, L')$$
$$\times \begin{pmatrix} L & 2 & L' \\ -K & 0 & K \end{pmatrix}$$
$$\times \begin{pmatrix} L & 2 & L' \\ -2 & 1 & 1 \end{pmatrix}[\bar{C}^{L'}_{K,1}(4,5) + \bar{C}^{L'}_{K,1}(6,7)]$$
$$- 2^{-1/2}D^{(2)} \sum_{L'} N(L, L')\begin{pmatrix} L & 2 & L' \\ -2 & 1 & 1 \end{pmatrix}$$
$$\times \left\{\begin{pmatrix} L & 2 & L' \\ -K & -2 & K+2 \end{pmatrix}[\bar{C}^{L'}_{K+2,1}(4,5) + \bar{C}^{L'}_{K+2,1}(6,7)] + \begin{pmatrix} L & 2 & L' \\ -K & 2 & K-2 \end{pmatrix}[\bar{C}^{L'}_{K-2,1}(4,5) + \bar{C}^{L'}_{K-2,1}(6,7)]\right\} = 0 \quad \text{(A.6)}$$

Many of the terms in Eqs. (A.1)–(A.6) have been defined in Eqs. (75) and (76). ω_e is the electron-spin Larmor frequency and $b = -\frac{1}{2}a_N|\gamma_e|$.

The absorption is given by

$$\overline{Z''_1} + \overline{Z''_2} + \overline{Z''_3} = \text{Im} \sum_{i=1}^{3} C^0_{0,0}(i) \quad \text{(A.7)}$$

The following definitions have also been introduced:

$$\bar{C}^{L}_{K,M}(i) = 2^{-1/2}[C^{L}_{K,M}(i) \pm C^{L}_{-K,M}(i)], \qquad K \geqq 0 \quad \text{(A.8)}$$

where the plus sign is used for even L and the minus sign for odd L. For even L, i refers to all transitions; for odd L, i refers only to transitions 4, 5, 6, 7, 8, and 9;

$$\bar{C}^{L}_{K,1}(i,j) = 2^{-1/2}[\bar{C}^{L}_{K,1}(i) \mp \bar{C}^{L}_{K,-1}(j)] \quad \text{(A.9)}$$

where (i, j) are either (4, 5) or (6, 7), and the minus (plus) sign is for even (odd) L; and

$$\bar{C}^{L}_{K,2}(8,9) = 2^{-1/2}[\bar{C}^{L}_{K,2}(8) \pm \bar{C}^{L}_{K,-2}(9)] \quad \text{(A.10)}$$

where the plus (minus) sign is for even (odd) L. Also,

$$N(L, L') = [(2L+1)(2L'+1)]^{1/2} \quad \text{(A.11)}$$

and

$$T^{-1}_{2,a} = \alpha + \tfrac{1}{3}\beta \quad \text{(A.12a)}$$
$$T^{-1}_{2,b} = \tfrac{2}{3}\beta \quad \text{(A.12b)}$$

The quantity $\begin{pmatrix} L & 2 & L' \\ 0 & 0 & 0 \end{pmatrix}$ is a $3j$ symbol, whose values are tabulated or given by formulas (Rotenberg *et al.*, 1959; Edmonds, 1957). These are used to evaluate the integrals on the LHS of Eq. (27), utilizing

$$\int d\Omega \mathscr{D}^{L_1}_{m_1,m_1'}(\Omega)\mathscr{D}^{L_2}_{m_2,m_2'}(\Omega)\mathscr{D}^{L_3}_{m_3,m_3'}(\Omega) = 8\pi^2\begin{pmatrix} L_1 & L_2 & L_3 \\ m_1 & m_2 & m_3 \end{pmatrix}\begin{pmatrix} L_1 & L_2 & L_3 \\ m_1' & m_2' & m_3' \end{pmatrix} \quad \text{(A.13)}$$

with the relationship

$$\mathscr{D}^{L^*}_{m,m'}(\Omega) = (-)^{m-m'}\mathscr{D}^{L}_{-m,-m'}(\Omega) \quad \text{(A.14)}$$

There are a number of symmetry relations (Edmonds, 1957) in a $3j$ symbol $\begin{pmatrix} L_1 & L_2 & L_3 \\ m_1 & m_2 & m_3 \end{pmatrix}$. Among the more useful ones are: (1) The sum of the m values must be zero. (2) Naturally, L must be positive and the absolute value of m_i must not be greater than the corresponding L_i in a given column. (3) the columns can be permuted without changing the value of the $3j$ symbol if the sum of L values is even. If the sum of L values is odd, then a permutation of the columns results in a change in sign for the value of the $3j$ symbol. (4) If the sum of L values is even, then all the m values can change sign without changing the value of the $3j$ symbol. If the sum of L values is odd, then a change in sign for all m values results in a change in sign for the value of the $3j$ symbol. (5) The triangular property holds whereby the sum of any two L values must be equal to or greater than the third L value. Properties (4) and (5) result in the equations in L being coupled only to the equations in L and $L \pm 2$, for the three allowed transitions; but the forbidden transitions (only

when there are asymmetric magnetic parameters) result in a coupling to equations in $L \pm 1$ as well. The coupling of odd L values is important only for slow motions when $\tau_R \geq 5 \times 10^{-8}$ sec. The required $3j$ symbols are automatically calculated in the computer program in Appendix B.

The solutions in Eqs. (A.1)–(A.6) can be expressed by the matrix equation

$$\mathscr{J}\mathbf{C} = \mathbf{U} \tag{A.15}$$

where $\mathbf{C}$ is an r-dimensional column vector consisting of the independent variables [i.e., the expansion coefficients $C^L_{K,M}(i)$], which are to be solved for, $\mathbf{U}$ is an r-dimensional column vector of constants given by the RHS of Eqs. (A.1)–(A.6), and $\mathscr{J}$ is an $r \times r$ square matrix formed by the coefficients of the $C^L_{KM}(i)$ variables in Eqs. (A.1)–(A.6). For purposes of computer programming efficiency, it is best that the coefficient matrix $\mathscr{J}$ be complex symmetric.

The above equations, except for saturation, are "naturally" symmetric because orthonormal expansions as well as a properly "normalized" linear combination of terms were used. [Actually, one must first replace the $\tilde{C}^L_{0,M}(i)$ in Eqs. (A.1)–(A.6) by $C^L_{0,M}(i)$ to be able to render $\mathscr{J}$ symmetric.]

The diagonalization method for obtaining a spectrum is especially applicable, since Eq. (A.15) can be written in the form

$$(\mathscr{J}' + k\mathbf{1})\mathbf{C} = \mathbf{U} \tag{A.15'}$$

where $\mathscr{J}'$ does not contain the "sweep variable" (e.g., ω_e for a field-swept spectrum), $\mathbf{1}$ is the unit matrix, and k is a constant containing the sweep variable [i.e., $k = (\omega - \omega_e) - iT^{-1}_{2,a}$].

For a nondegenerate complex symmetric matrix $\mathscr{J}'$, a complex orthogonal matrix $\mathbf{O}$ exists such that

$$\mathbf{O}^{tr}\mathscr{J}'\mathbf{O} = \mathscr{J}_d \tag{A.16}$$

where $\mathscr{J}_d$ is a diagonal matrix and $\mathbf{O}^{tr}$ is the transpose of $\mathbf{O}$. Premultiplication of Eq. (A.15') by $\mathbf{O}^{tr}$, use of Eq. (A.16), and noting that $\mathbf{O}^{tr} = \mathbf{O}^{-1}$ leads to

$$(\mathscr{J}_d + k\mathbf{1})\mathbf{O}^{tr}\mathbf{C} = \mathbf{O}^{tr}\mathbf{U} \tag{A.17}$$

or

$$\mathbf{C} = \mathbf{O}(\mathscr{J}_d + k\mathbf{1})^{-1}\mathbf{O}^{tr}\mathbf{U} \tag{A.17'}$$

Note that the absorption $\overline{Z''}$ is given by

$$\overline{Z''} = \mathrm{Im}[\mathbf{DC}] \tag{A.18}$$

where

$$\mathbf{D} = Y\mathbf{U} \tag{A.19a}$$

with

$$Y = [2^{-1/2}q\omega_e d_e]^{-1} \tag{A.19b}$$

where we use the fact that $\omega_1 \cong \omega_2 \cong \omega_3 \cong \omega_e$ in high fields and $d_1 = d_2 = d_3 = d_e$. It follows from Eqs. (A.17) and (A.18) that

$$\overline{Z''} = \mathrm{Im}[(\mathbf{DO})(\mathscr{J}_d + k\mathbf{1})^{-1}(\mathbf{O}^{tr}\mathbf{U})] \tag{A.20}$$

which can be written for the r dimensions as

$$\overline{Z''} = Y\,\mathrm{Im}\left[\sum_{i=1}^{r} \frac{(\mathbf{O}^{tr}\mathbf{U})_i^2}{(\mathscr{J}_d)_{ii} + (\omega - \omega_e) - iT^{-1}_{2,a}}\right] \tag{A.21}$$

and for the first derivative of an absorption field-swept spectrum

$$\frac{d\overline{Z''}}{d\omega_e} = Y\,\mathrm{Im}\left[\sum_{i=1}^{r} \frac{(\mathbf{O}^{tr}\mathbf{U})_i^2}{[(\mathscr{J}_d)_{ii} + (\omega - \omega_e) - iT^{-1}_{2,a}]^2}\right] \tag{A.22}$$

Thus only a single diagonalization is required to calculate an absorption line shape or the nth derivative of the absorption. Another advantage is that $\mathscr{J}$ and $\mathbf{O}$ are not functions of $T^{-1}_{2,a}$, so that spectral line shapes can be calculated for different values of $T^{-1}_{2,a}$ without performing additional diagonalizations.

The diagonalization subroutine used for the slow tumbling computer program in Appendix B is due to Gordon and Messenger (1972). This subroutine had the fastest execution time of all diagonalization subroutines tried. Besides its speed in diagonalizing a matrix, it has characteristics that make it especially useful in solving the slow motional equations. First, the subroutine takes advantage of the symmetry of $\mathscr{J}$, so that only the elements to one side of the diagonal are stored. Second, the subroutine retains the banded nature of the equations, so that only the subdiagonals containing nonzero elements are stored. Third, the subroutine performs the operation $(\mathbf{O}^{tr}\mathbf{U})$ "instantaneously" for each step of the diagonalization, so that only a single column vector $(\mathbf{O}^{tr}\mathbf{U})$ need be stored rather than the construction and storage of the entire $r \times r$ $\mathbf{O}^{tr}$ matrix. A modified version of this subroutine which can be used to obtain all the eigenvectors, is given by Bruno (1973).

Anisotropic Liquids

Because $\tilde{\Gamma}_\Omega$ for anisotropic liquids is composed of a simple sum of terms in $\mathscr{D}^L_{K,M}(\Omega)$ plus the isotropic liquid Γ_Ω, there is much similarity between the equations for anisotropic liquids and those for isotropic liquids. In fact, the resulting equations for anisotropic liquids can be obtained by simple modifications of the isotropic liquid equations (A.1)–(A.6). These modifications can be specified by the following definitions for the simple

case of a Meier-Saupe potential, in which **n** is completely aligned by the magnetic field (Polnaszek *et al.* (1973):

$$C_A(j) = -i\frac{2}{15}R\lambda^2 C^L_{K,M}(j) + i2R\lambda\left(1 - \frac{\lambda}{21}\right)(-)^{K-M} \times \sum_{L'} N(L, L')\begin{pmatrix} L & 2 & L' \\ -K & 0 & K \end{pmatrix}\begin{pmatrix} L & 2 & L' \\ -M & 0 & M \end{pmatrix} C^{L'}_{K,M}(j) + i\frac{8}{35}R\lambda^2 \times (-)^{K-M} \sum_{L'} N(L, L')\begin{pmatrix} L & 4 & L' \\ -K & 0 & K \end{pmatrix}\begin{pmatrix} L & 4 & L' \\ -M & 0 & M \end{pmatrix} C^{L'}_{K,M}(j) \tag{A.23}$$

and

$$U^L_A = q\omega_e d_e \delta(K, 0)\delta(M, 0)\frac{(2L+1)^{1/2}}{I''_0}\int_{-1}^{1} \mathscr{D}^L_{0,0}(0, \beta, 0)\exp\left(\frac{1}{2}x^2\lambda\right) dx \tag{A.24}$$

with $I''_0 = \int_{-1}^{1} \exp(\frac{1}{2}x^2\lambda)\, dx$ and λ given by Eq. (60a). The addition of the term $C_A(j)$ to the left-hand side and the replacement of the right-hand side by the term U^L_A for each of the respective isotropic equations (A.1)–(A.6) gives the desired set of equations for the anisotropic liquid.

The equations for Brownian axially symmetric rotational diffusion and for anisotropic (axially symmetric) viscosity are obtained by using Eqs. (61a), (61b), and (62a)–(62f) and Eqs. (63), (64), and (65a)–(65f), respectively.

The absorption is, from Eq. (23) or Eq. (13), proportional to

$$\overline{Z''} = \mathrm{Im}\sum_{j=1}^{3}\sum_{L}\left\{\frac{(2L+1)^{1/2}}{I''_0}\left[\int_{-1}^{1} dx\, \mathscr{D}^L_{0,0}(0, \beta, 0)\exp\left(\frac{1}{2}x^2\lambda\right)\right] C^L_{0,0}(j)\right\} \tag{A.25}$$

If the anisotropic liquid equations are written in the matrix notation of Eq. (A.15), then from Eqs. (A.24) and (A.25) the absorption can again be written as proportional to

$$\overline{Z''} = Y\,\mathrm{Im}[\mathbf{U}\cdot\mathbf{C}] \tag{A.26}$$

In the numerical evaluation of the terms in U^L_A the following recursion formulas are useful:

$$\mathscr{D}^L_{0,0}(x) = [(2L-1)x\mathscr{D}^{L-1}_{0,0}(x) - (L-1)\mathscr{D}^{L-2}_{0,0}(x)]/L \tag{A.27a}$$

and

$$I_n = \int_{-1}^{1} x^n \exp(x^2\lambda_2)\, dx = \lambda_2^{-1}[\exp(\lambda_2) - \tfrac{1}{2}(n-1)I_{n-2}] \tag{A.27b}$$

for n even. Appropriate expressions for the more complicated cases are given by Polnaszek (1975a).

Convergence for isotropic spectra has been discussed in Section II.E in terms of an n_L. The effect of having $\lambda \neq 0$ means that the ordering affects the convergence of the solutions. For example, in the motionally narrowed region where $n_L = 2$ is sufficient for isotropic liquids, then for $\lambda = -0.5$ (weak ordering) one needs $n_L = 4$ and for $\lambda = -3.5$ (moderately strong ordering) $n_L = 6$. It appears safe, for the slow motional region, to use as n_L the sum of the value required for isotropic liquids and $n'_L - 2$, where n'_L is required for convergence for that value of λ in the motional narrowing region, although usually smaller values of n_L may be used.

Computer programs are given by Polnaszek (1975a) for calculating nitroxide line shapes when (1) the asymmetric potential defined by Eq. (58) describes the orientation of a nitroxide radical for which the principal magnetic (x''', y''', z''') and orientation (x', y', z') axes are coincident, and (a) Eqs. (61a), (61b), and (62a)–(62f) apply or (b) Eqs. (64) and (65a)–(65f) apply; (2) a Meier-Saupe potential is used; but the z' and z''' axes are titled by angle β (3) different reorientational models are used for a Meier-Saupe potential. All these programs contain the correction terms for nonsecular contributions to the resonant frequency shifts.

All the programs, including that given in Appendix B, have been written in FORTRAN IV language for an IBM 360/65 computer.

APPENDIX B. COMPUTER PROGRAM FOR SLOW TUMBLING NITROXIDES IN ISOTROPIC LIQUIDS

The following program was written in FORTRAN IV and is listed with 72 print positions per line. One of the subroutines in this program has been taken from Gordon and Messenger (1972), pp. 376–381, and has been reproduced with 60 print positions per line. The Gordon and Messenger subroutine is used with permission of Plenum Press.

```
                 NITROXIDE FREE RADICALS

                       I=1,S=1/2
     ASYMMETRIC  G  AND  A  TENSORS
     ISOTROPIC OR AXIALLY SYMMETRIC ROTATIONAL REORIENTATION
     MODELS OF ROTATIONAL REORIENTATION
     K,L(ODD),L(DOUBLY FORBIDDEN TRANSITION)  TRUNCATION

THIS PROGRAM SIMULATES ESR SPECTRAL LINESHAPES FOR THE
ROTATIONAL MODULATION OF AN UNPAIRED ELECTRON INTERACTING
      WITH A NUCLEUS OF SPIN I=1. THE HYPERFINE LINES
      ARISE BY COMPLETELY ASYMMETRIC G-TENSOR AND
      (ELECTRON-NUCLEAR DIPOLAR TENSOR). ROTATIONAL
      MOTION MAY BE ISOTROPIC OR AXIALLY SYMMETRIC ABOUT
   PRINCIPAL AXIS OF THE  G  AND  A  TENSOR (ASSUMED TO
   ... OPTION OF ROTATIONAL REORIENTATION MODELS
    OF BROWNIAN DIFFUSION,SIMPLE 'FREE' DIFFUSION, OR
   JUMP REORIENTATION (STRONG OR INTERMEDIATE). OUTPUT MAY BE
 DISPERSION, ABSORPTION, OR THEIR FIRST DERIVATIVES.

   IN DERIVATION OF THE EQUATIONS THAT ARE USED, THE
 FOLLOWING SIMPLIFICATIONS WERE MADE:
   1. THE PRINCIPAL AXES FOR THE  G  AND  A  TENSORS WERE
      ASSUMED TO COINCIDE.
   2. THE NUCLEAR ZEEMAN TERM WAS SET TO ZERO.
   3. NON-SECULAR AND SATURATION TERMS WERE NEGLECTED.
 THESE SIMPLIFICATIONS ARE USUALLY APPROPRIATE FOR
 NITROXIDE FREE RADICALS.

   ... ON THE TERMINATING VALUES  (KTERM,LDOUB,LODD)  FOR
   ... TYPES OF COEFFICIENT TERMS MAY BE MADE. THE
 ASYMMETRIC EXPANSION TERMS DUE TO THE DIFFERENCES IN THE X
   ...   PRINCIPAL AXIS COMPONENTS OF THE  A  AND  G
   ...   MAY BE TRUNCATED AT A SEPARATE VALUE (DESIGNATED
 BY KTERM). THE EXPANSION TERMS FOR THE 'DOUBLY FORBIDDEN'
 TRANSITIONS MAY BE TRUNCATED AT A SEPARATE VALUE
 (DESIGNATED BY  LDOUB). ALSO THOSE EXPANSION TERMS WITH
 ODD  L  VALUES MAY BE TRUNCATED AT A SEPARATE VALUE
 DESIGNATED BY  LODD).

 FOR THEORY, SEE  FREED,BRUNO,POLNASZEK(J.PHYS.CHEM.75,
 ...(1971)) AND GOLDMAN,BRUNO,POLNASZEK,FREED(J.CHEM.PHYS
 ...(1972)). THE DIAGONALIZATION METHOD IS USED TO
 ... THE APPROPRIATELY SYMMETRIZED EQUATIONS GIVEN IN
 BRUNO THESIS,EQ.(II.C.37) .

                 LIST OF INPUT VARIABLES
           (IN ORDER OF APPEARANCE IN PROGRAM)

 NPT = NUMBER OF PLOTS OR SETS OF PLOTS WHICH DIFFER IN
       G-TENSOR,A-TENSOR, OR ROTATIONAL REORIENTATION
       PARAMETERS (SPECIFICALLY  AX,AY,AZ,GX,GY,GZ,R,RZ,
       IROT,RTAU,BCEN,L,KTERM,LDOUB,LODD). PLOTS DIFFERING
       ONLY IN  T2IN  ARE NOT INCLUDED. (SEE BELOW FOR
       DEFINITIONS)

 LMAX = MAXIMUM  L  VALUE  TO BE USED FOR ANY PLOT

 NDIM = DIMENSION GIVEN IN THE DIMENSION STATEMENT OF THE
        MAIN PROGRAM FOR MATRICES  CSYM(NDIM,JDIM),
        CSYM1(NDIM,CSYM2(NDIM),VALUE(NDIM),AMP(NDIM).

 JDIM = DIMENSION GIVEN IN THE DIMENSION STATEMENT OF THE
        MAIN PROGRAM FOR MATRIX  CSYM(NDIM,JDIM)

 NSY = DIMENSION GIVEN IN DIMENSION STATEMENT OF MAIN
       PROGRAM FOR MATRIX  SY(NSY,8).

 NSY2 = DIMENSION GIVEN IN THE DIMENSION STATEMENT OF THE
        MAIN PROGRAM FOR MATRIX  SY2(NSY2,3).

 TITLE = TITLE FOR EACH OF THE  NPT  SETS OF PLOTS.

 AX,AY,AZ = VALUES OF THE A-TENSOR (ELECTRON-NUCLEAR
            DIPOLAR TENSOR PLUS FERMI-CONTACT TERM)
            COMPONENTS ALONG THE  X,Y,Z  PRINCIPAL AXES,
            RESPECTIVELY.
            -VALUE IN GAUSS.  (TYPICAL NITROXIDE SPIN
             LABEL VALUES FOR Z-AXIS ALONG THE NITROGEN
             2P-PI ORBITAL ARE  (6,5,32) RESPECTIVELY).

 GX,GY,GZ = G-TENSOR COMPONENTS ALONG THE  X,Y,Z
            PRINCIPAL AXES, RESPECTIVELY.

 R,RZ = ROTATIONAL DIFFUSION RATE CONSTANT ABOUT THE  X,Y
        AXES AND THE  Z  AXIS, RESPECTIVELY.
        -VALUE IS IN RADIANS PER SECOND.  (FOR ISOTROPIC
          BROWNIAN ROTATIONAL DIFFUSION, ROTATIONAL
          CORRELATION TIME IS  1/(6R) ).

 IROT = VALUE SPECIFIES ROTATIONAL REORIENTATION MODEL-
        1 BROWNIAN
        2 SIMPLE 'FREE'
        3 STRONG JUMP
        4 ... JUMP
        5 INTERMEDIATE JUMP WITH GAUSSIAN DISTRIBUTION
          FOR THE JUMP ANGLE
        6 INTERMEDIATE JUMP WITH EXPONENTIAL DISTRIBUTION
          FOR THE JUMP ANGLE

 RTAU = PRODUCT  R*TAU  TO BE GIVEN FOR THE INTERMEDIATE
        JUMP REORIENTATION OR SIMPLE 'FREE' DIFFUSION. R
        IS THE ROTATIONAL DIFFUSION CONSTANT (IN UNITS OF
        RADIANS PER SECOND) AND  TAU  IS EITHER THE TIME
        (IN UNITS OF SECONDS PER RADIAN) AT A FIXED
        ORIENTATION (INTERMEDIATE JUMP MODEL) OR THE TIME
        DURING WHICH THE MOLECULAE FREELY ROTATES (SIMPLE
        'FREE' DIFFUSION MODEL).

 BCEN = MAGNETIC FIELD VALUE AT CENTER OF SPECTRUM.
        -VALUE IN GAUSS.  (RESONANCE FIELD VALUE FOR THE
         ELECTRON ZEEMAN TERM WITH  G=(GX+GY+GZ)/3. FOR
         X-BAND TYPICAL VALUE IS 3300).

 L = TERMINATING  L  VALUE IN EXPANSION. L  MUST BE AN
     EVEN NUMBER. L=2  FOR THE FAST MOTIONAL LIMIT
     SPECTRUM. (L=10  IS TYPICAL FOR INTERMEDIATE SLOW
     MOTIONAL SPECTRUM WHILE  L=20  FOR A 'RIGID' LIKE
     SPECTRUM).

 TRUNC = .FALSE. -MAXIMUM TERMINATING VALUES SPECIFIED BY
                  L  ARE TO BE USED. THUS
                  KTERM = L; LDOUB = L ; LODD = L-1
         .TRUE. -TERMINATING VALUES  (KTERM,LDOUB,LODD)
                  ARE TO BE GIVEN

 KTERM = TERMINATING VALUE OF  K  FOR THE ASYMMETRIC
         EXPANSION TERMS DUE TO DIFFERENCES IN THE  X  AND
         Y  PRINCIPAL AXIS COMPONENTS OF THE  A  AND  G
         TENSORS. TO BE GIVEN WHEN  TRUNC  IS  .TRUE.
         VALUE MUST BE EVEN AND LESS THAN OR EQUAL TO  L.
         KTERM=0  IS FOR AN AXIALLY SYMMETRIC NITROXIDE
         FREE RADICAL.  (FOR Z AXIS ALONG THE 2P-PI
         NITROGEN ORBITAL, KTERM=4  IS TYPICAL FOR
         INTERMEDIATE SLOW MOTION AND  KTERM=8  FOR
         'RIGID' LIKE SPECTRUM).

 LODD = TERMINATING  L  VALUE FOR THOSE EXPANSION TERMS
        WITH ODD  L  VALUES. TO BE GIVEN WHEN  TRUNC  IS
        .TRUE.  VALUE MUST BE ODD, LESS THAN  L  AND
        GREATER OR EQUAL  1. IF  LODD=1  ALL ODD  L  TERMS
        ARE TRUNCATED.

 LDOUB = TERMINATING  L  VALUE FOR 'DOUBLY FORBIDDEN'
         TRANSITION EXPANSION TERMS. TO BE GIVEN WHEN
         TRUNC  IS  .TRUE.  VALUE MUST BE EVEN, NO GREATER
         THAN  L  AND NO LESS LESS THAN  2.

 NSET = NUMBER OF SPECTRA VARYING ONLY  T2IN  (OR  BI,BF,
        DISP) FOR A GIVEN SET OF VALUES FOR  TITLE,AX,AY,
        AZ,GX,GY,GZ,R,RZ,IROT,RTAU,BCEN,L,TRUNC,KTERM,
        LODD,LDOUB,WAMPEV,PAMPEV.

 WAMPEV = .TRUE. -PRINT OUT EIGENVALUES OF MATRIX  CSYM
                  AND COLUMN VECTOR  AMP.

 PAMPEV = .TRUE. -PUNCH OUT EIGENVALUES OF MATRIX  CSYM
                  AND THE COLUMN VECTOR  AMP.

 IPLOT = VALUE SPECIFIES TYPE OF PLOT-
           -1  ABSORPTION OR DISPERSION
            0  ABSORPTION OR DISPERSION AND ITS RESPECTIVE
               FIRST DERIVATIVE
           +1  FIRST DERIVATIVE OF THE ABSORPTION OR
               DISPERSION

 XPUNCH = .TRUE. -SPECTRAL POINTS PUNCHED OUT

 XPLOT = .TRUE. -SPECTRAL POINTS PRESENTED AS LINE PLOT

 DISP = .TRUE. -DISPERSION TYPE OUTPUT
        .FALSE. -ABSORPTION TYPE OUTPUT

 YLEN = FOR LINE PLOT OUTPUT, LENGTH OF ABSORPTION-
        DISPERSION/FIRST DERIVATIVE AXIS
        -VALUE IN INCHES

 XLEN = FOR LINE PLOT OUTPUT (XPLOT=.TRUE.), LENGTH OF
        FIELD SWEEP AXIS.
        -VALUE IN INCHES

 T2IN = ROTATIONALLY INVARIANT LORENTZIAN P-P FIRST
        DERIVATIVE LINEWIDTH
        -VALUE IN GAUSS.  (TYPICAL VALUE FOR NITROXIDE
         SPIN LABEL IS A FEW GAUSS).

 BI,BF = INITIAL AND FINAL FIELD SWEEP VALUES,
         RESPECTIVELY, WITH RESPECT TO CENTER OF SPECTRUM.
         -VALUE IN GAUSS

 NB = NUMBER OF POINTS FOR SPECTRUM, SPACED EQUIDISTANT
      APART ALONG THE SWEEP AXIS


THE STRUCTURE OF THE PROGRAM HAS AN INNER AND OUTER DO
LOOP. THE OUTER ONE IS EXECUTED  NPT  TIMES WHILE THE
INNER DO LOOP  IS EXECUTED  NSET  TIMES FOR EACH CYCLE OF
THE OUTER DO LOOP


      IMPLICIT REAL*8(A-H,O-Z)
      COMPLEX*16 CSYM,CSYM1,CSYM2,VALUE,AMP,ABSP,XAB
      REAL C,BFLD,DERAB,TITLE,YLEN,XLEN,ABMAX,ABMIN,DMAX,DMIN,X,Y,DXY
      LOGICAL XPUNCH,XPLOT,XPLEND,PAMPEV,WAMPEV,DISP,TRUNC
      DIMENSION SY(33,8),SY2(108,3),CSYM(108,34),VALUE(108),AMP(108),CSY
     1M1(108),CSYM2(108),C(401),DERAB(401),BFLD(401),TITLE(20),DROT(2)


               DIMENSIONING OF MATRICES

      DIMENSION SY(NSY,8),SY2(NSY2,3),CSYM(NDIM,JDIM),VALUE(
     2NDIM),AMP(NDIM),CSYM1(NDIM),CSYM2(NDIM),C(NPNT),DERAB(
     2NPNT),BFLD(NPNT),TITLE(20),DROT(2)

 LIMITS IMPOSED BY THE DIMENSIONS ABOVE:

   1.MAXIMUM NUMBER OF POINTS FOR ONE SPECTRUM
     -GIVEN BY  NPNT

   2.MAXIMUM VALUE FOR  L (=LMAX,SEE ABOVE)
     -DETERMINED FROM  NSY,NSY2
       NSY = 3*(L + 1)
       NSY2 = (3*(L+2)*(L+2))/4
      NO VALUE OF  L  SHOULD YIELD  NSY,NSY2  GREATER
      THAN THOSE SPECIFIED IN DIMENSION STATEMENT

   3.COMBINATION OF VALUES FOR  L,KTERM,LODD,LDOUB  FOR A
     SINGLE PLOT
     -DETERMINED FROM  NDIM,JDIM

     A.FOR  TRUNC = .FALSE.  (KTERM=L,LDOUB=L,LODD=L-1)
       NDIM = ((9*L*L) + (30*L) + 24)/8
       JDIM = (9*(L/2)) + 7
       JDIM = 13                  WHEN  L=2

     B.FOR  LDOUB > LODD > KTERM
       NDIM=((20*L) + 24 + (10*L*KTERM) + (2*LDOUB*KTERM)
            + (4*LODD*KTERM) + (4*LDOUB) -(9*KTERM*KTERM)
            + (12*KTERM))/8

       JDIM = (9*(KTERM/2)) + 16
       JDIM = 10                  WHEN  KTERM=0
       JDIM = 7                   WHEN  KTERM=0  AND  L=2

     C.FOR  LDOUB > OR = KTERM > LODD
       NDIM=((20*L) + 21 + (10*L*KTERM) + (2*LDOUB*KTERM)
            + (3*LODD*LODD) + (4*LDOUB) - (6*KTERM*KTERM)
            + (12*KTERM))/8

       JDIM = (3*KTERM) + 16
       JDIM = (3*KTERM) + 15    WHEN  KTERM=LDOUB
       JDIM = (3*KTERM) + 10    WHEN  KTERM=L
       JDIM = 13                WHEN  L=2 AND KTERM=2
     OR
       JDIM = (9*((LODD-1)/2)) + 16
       JDIM = 13                WHEN  L=2 AND KTERM=2
      (JDIM  EQUALS THE GREATER OF THE TWO VALUES)

     D.FOR  LODD > LDOUB > OR = KTERM
       NDIM=((20*L) + 24 + (10*L*KTERM) + (4*LDOUB*KTERM)
            + (4*LODD*KTERM) + (4*LDOUB) -(9*KTERM*KTERM)
            + (10*KTERM))/8

       JDIM = (9*(KTERM/2)) + 16
       JDIM = (4*KTERM) + 15        WHEN  LDOUB=KTERM
       JDIM = (9*(KTERM/2)) + 7     WHEN  LDOUB=KTERM  AND  KTERM>16
       JDIM = 10                    WHEN  KTERM=0

     E.FOR  LODD> KTERM > LDOUB
       NDIM=((20*L) + 24 + (10*L*KTERM) + (4*LODD*KTERM)
            + (2*LDOUB*LDOUB) + (4*LDOUB)-(7*KTERM*KTERM)
            + (10*KTERM))/8

       JDIM = (7*(KTERM/2)) + 14
     OR
       JDIM = (4*LDOUB) + 15
       JDIM = (9*(LDOUB/2)) + 7     WHEN  LDOUB>16
      (JDIM  EQUALS THE GREATER OF THE TWO VALUES)

     F.FOR  KTERM > LDOUB > LODD
       NDIM=((20*L) + 21 + (10*L*KTERM) + (LDOUB*LDOUB)
            + (3*LODD*LODD) + (6*LDOUB) - (5*KTERM*KTERM)
            + (10*KTERM))/8

       JDIM = (5*(KTERM/2)) + 14
     OR
       JDIM = (3*LDOUB) + 15
     OR
       JDIM = (9*((LODD-1)/2)) + 16
      (JDIM  EQUALS THE GREATEST OF THE THREE VALUES)

     G.FOR  KTERM > LODD > LDOUB
       NDIM=((20*L) + 22 + (10*L*KTERM) + (2*LDOUB*LDOUB)
            + (2*LODD*LODD) + (4*LDOUB) - (5*KTERM*KTERM)
            + (10*KTERM))/8

       JDIM = (5*(KTERM/2)) + 14
       JDIM = (5*(KTERM/2)) + 9     WHEN  KTERM=L
     OR
       JDIM = (7*((LODD-1)/2)) + 14
     OR
       JDIM = (4*LDOUB) + 15
       JDIM = (9*(LDOUB/2)) + 10    WHEN  LDOUB>10
      (JDIM EQUALS THE GREATEST OF THE THREE VALUES)

     NO SET OF VALUES FOR  L,KTERM,LODD,LDOUB  SHOULD
     YIELD A VALUE FOR  NDIM,JDIM  GREATER THAN THOSE
     SPECIFIED IN DIMENSION STATEMENT


      EQUIVALENCE (CSYM1(1),CSYM(1,1)),(CSYM2(1),CSYM(1,2))
      XPLEND = .FALSE.

************************************************************
* READ INPUT DATA - ONE READ STATEMENT                     *
************************************************************
-NOTE THIS INPUT STATEMENT WILL BE READ ONLY ONCE

      READ(5,1) NPT,LMAX,NDIM,JDIM,NSY,NSY2
    1 FORMAT(I2,3X,I2,3X,I3,2X,I3,2X,I3,2X,I3)
      LMAX1 = LMAX + 1
      LMAX2 = (3*LMAX) + 1
      LMAX3 = 1 + LMAX
      LMAX4 = 3*(LMAX + 1)
      LMAX5 = (3*((LMAX + 2)**2))/4
      IF((NSY.LT.LMAX4).OR.(NSY2.LT.LMAX5)) GO TO 2

CALCULATION OF  3-J  SYMBOL VALUE.
VALUES STORED IN MATRICES  SY,SY2. FORMULAE FOR THESE
CALCULATIONS BASED UPON EQUATION 1.5 IN 'THE 3-J AND
6-J SYMBOLS' BY ROTENBERG,BIVINS,METROPOLIS,WOOTEN
AND FORMULAE GIVEN IN 'ANGULAR MOMENTUM IN QUANTUM
MECHANICS' BY EDMONDS.

      SY(1,1) = 0.D0
      SY(1,2) = 0.D0
      SY(2,1) = 1.D0/DSQRT(5.D0)
      SY(2,2) = 2.D-1
      DO 3 I=3,LMAX1,2
      XI = DFLOAT(I) - 1.D0
      XXI = 2.D0*XI
      SY(I,1) = -DSQRT((XI*(XI + 1.D0))/((XXI + 3.D0)*(XXI + 1.D0)*(XXI
     1 - 1.D0)))
      SY(I,2) = SY(I,1)*SY(I,1)
      SY(I+1,1) = DSQRT((3.D0*(XI + 2.D0)*(XI + 1.D0))/(2.D0*(XXI + 5.D0
     1)*(XXI + 3.D0)*(XXI + 1.D0)))
    3 SY(I+1,2) = SY(I+1,1)*SY(I+1,1)
      DO 4 I=3,8
      DO 4 J=1,3
    4 SY(J,I) = 0.D0
      SY(3,3) = -1.D0/DSQRT(5.D0)
      XODD = -1.D0
      DO 5 I=4,LMAX2,3
      XI = (DFLOAT(I) - 1.D0)/3.D0
      XXI = 2.D0*XI
      SY(I,3) = XODD*DSQRT(3.D0/(2.D0*(XXI + 3.D0)*(XXI + 1.D0)*(XXI - 1
     1.D0)))
      SY(I+1,3) = -XODD*DSQRT(XI/((XXI + 3.D0)*(XXI + 1.D0)*2.D0))
      SY(I+2,3) = -XODD*DSQRT(((XI + 1.D0)*(XI + 3.D0))/((XXI + 5.D0)*(X
     1XI + 3.D0)*(XXI + 1.D0)))
      SY(I,4) = XODD*(((XI*(XI + 1.D0)) - 3.D0)/DSQRT((XXI + 3.D0)*(XXI +
     11.D0)*(XXI + 1.D0)*XI*(XXI - 1.D0)))
      SY(I+1,4) = XODD*DSQRT(3.D0/((XXI + 3.D0)*(XI + 1.D0)*(XXI + 1.D0)
     1))
      SY(I+2,4) = -XODD*DSQRT((3.D0*(XI + 3.D0)*XI)/(2.D0*(XXI + 5.D0)*(
     1XXI + 3.D0)*(XXI + 1.D0)))
      SY(I,5) = SY(I,3)
      SY(I+1,5) = -XODD*DSQRT((XI + 2.D0)/(2.D0*(XXI + 3.D0)*(XXI + 1.D0
     1)))
      SY(I+2,5) = XODD*DSQRT(((XI + 2.D0)*XI)/((XXI + 5.D0)*(XXI + 3.D0)
     1*(XXI + 1.D0)))
      SY(I,6) = -XODD*3.D0*DSQRT((3.D0*(XI + 2.D0)*(XI - 1.D0))/((XXI +
     1 3.D0)*(XI + 1.D0)*(XXI + 1.D0)*XXI*(XXI - 1.D0)))
      SY(I+1,6) = XODD*(XI - 2.D0)*DSQRT((XI + 3.D0)/((XXI + 3.D0)*(XI +
     1 1.D0)*(XXI + 1.D0)*XXI))
      SY(I+2,6) = XODD*DSQRT((XI*(XI + 4.D0)*(XI + 3.D0))/((XXI + 5.D0)*
     1(XI + 1.D0)*(XXI + 1.D0)*(XXI + 3.D0)))
      SY(I,7) = XODD*((12.D0 - (XI*(XI + 1.D0)))/DSQRT((XXI + 3.D0)*(XI
     1 + 1.D0)*(XXI + 1.D0)*XI*(XXI - 1.D0)))
      SY(I+1,7) = -XODD*2.D0*DSQRT((3.D0*(XI + 3.D0)*(XI - 1.D0))/((XI
     1 + 2.D0)*(XXI + 3.D0)*(XXI + 1.D0)*XI*(XI + 1.D0)))
      SY(I+2,7) = XODD*DSQRT(((XI + 4.D0)*(XI + 3.D0)*XI*(XI - 1.D0)*3.D
     10)/((XXI + 5.D0)*(XI + 2.D0)*(XXI + 3.D0)*(XXI + 2.D0)*(XXI + 1.D0
     2)))
      SY(I,8) = SY(I,6)
      SY(I+1,8) = XODD*(XI + 4.D0)*DSQRT((XI - 1.D0)/((XI + 2.D0)*(XXI +
     1 3.D0)*(XXI + 2.D0)*(XXI + 1.D0)))
      SY(I+2,8) = -XODD*DSQRT((XI*(XI + 3.D0)*(XI - 1.D0))/((XXI + 5.D0)
     1*(XI + 2.D0)*(XXI + 3.D0)*(XXI + 1.D0)))
    5 XODD = -XODD
      SY(4,7) = 0.D0
      K = 1
      XODD = 1.D0
      DO 6 I=1,LMAX3
      XI = DFLOAT(I) - 1.D0
      XXI = 2.D0*XI
      JK = (I+1)/2
      DO 7 J=1,JK
      XJ = (2.D0*DFLOAT(J)) - 2.D0
      IF((I+J).EQ.2) GO TO 8
      SY2(K,1) = XODD*(((3.D0*XJ*XJ) - (XI*(XI + 1.D0)))/DSQRT((XXI + 3.
     1D0)*(XI + 1.D0)*(XXI + 1.D0)*XI*(XXI - 1.D0)))
      SY2(K+1,1) = -XODD*XJ*DSQRT((3.D0*(XI + XJ + 1.D0)*(XI - XJ + 1.D0
     1))/((XI + 2.D0)*(XXI + 3.D0)*(XI + 1.D0)*(XXI + 1.D0)*XI))
      SY2(K,2) = XODD*DSQRT((6.D0*(XI - XJ - 1.D0)*(XI - XJ)*(XI + XJ +
     1 1.D0)*(XI + XJ + 2.D0))/((XXI + 3.D0)*(XXI + 2.D0)*(XXI + 1.D0)*X
     2XI*(XXI - 1.D0)))
      SY2(K+1,2) =  XODD*DSQRT(((XI + XJ + 1.D0)*(XI + XJ + 2.D0)*(XI +
     1XJ + 3.D0)*(XI - XJ))/((XI + 2.D0)*(XXI + 3.D0)*(XI + 1.D0)*(XXI +
     2 1.D0)*XXI))
      SY2(K,3) = XODD*DSQRT(( 6.D0*(XI + XJ - 1.D0)*(XI + XJ)*(XI - XJ +
     1 1.D0)*(XI - XJ + 2.D0))/((XXI + 3.D0)*(XXI + 2.D0)*(XXI + 1.D0)*X
     2XI*(XXI - 1.D0)))
      SY2(K+1,3) = -XODD*DSQRT(((XI - XJ + 1.D0)*(XI - XJ + 2.D0)*(XI -
     1XJ + 3.D0)*(XI + XJ))/((XI + 2.D0)*(XXI + 3.D0)*(XI + 1.D0)*(XXI +
     2 1.D0)*XXI))
    8 SY2(K+2,1) = XODD*DSQRT((6.D0*(XI + XJ + 2.D0)*(XI + XJ + 1.D0)*(X
     1I - XJ + 2.D0)*(XI - XJ + 1.D0))/((XXI + 5.D0)*(XXI + 4.D0)*(XXI +
     2 3.D0)*(XXI + 2.D0)*(XXI + 1.D0)))
      SY2(K+2,2) = XODD*DSQRT(((XI + XJ + 1.D0)*(XI + XJ + 2.D0)*(XI + X
     1J + 3.D0)*(XI + XJ + 4.D0))/((XXI + 5.D0)*(XXI + 4.D0)*(XXI + 3.D0
     2)*(XXI + 2.D0)*(XXI + 1.D0)))
      SY2(K+2,3) = XODD*DSQRT(((XI - XJ + 1.D0)*(XI - XJ + 2.D0)*(XI -XJ
     1 + 3.D0)*(XI - XJ + 4.D0))/((XXI + 5.D0)*(XXI + 4.D0)*(XXI + 3.D0)
     2*(XXI + 2.D0)*(XXI + 1.D0)))
    7 K = K + 3
    6 XODD = -XODD
      DO 9 I=1,2
      DO 9 J=1,3
    9 SY2(I,J) = 0.D0
      DO 10 LPT=1,NPT

************************************************************
*  READ INPUT DATA - FIVE READ STATEMENTS                  *
************************************************************
 -NOTE THAT THE FOLLOWING SET OF  5  INPUT CARDS IS
  FOLLOWED BY A SET OF  2*NSET  INPUT CARDS. THESE SETS
  OF INPUT CARDS ARE THEN REPEATED A TOTAL OF  NPT  TIMES

      READ(5,11) TITLE
   11 FORMAT(20A4)
      READ(5,12) AX,AY,AZ
   12 FORMAT(D10.3,5X,D10.3,5X,D10.3)
      READ(5,13) GX,GY,GZ
   13 FORMAT(F8.5,7X,F8.5,7X,F8.5)
      READ(5,14) R,RZ,IROT,RTAU,BCEN
   14 FORMAT(D10.3,5X,D10.3,5X,I1,4X,D10.3,5X,D10.3)
      READ(5,15) L,TRUNC,KTERM,LODD,LDOUB,NSET,PAMPEV,WAMPEV
   15 FORMAT(I2,3X,L1,4X,I2,3X,I2,3X,I2,3X,I2,3X,L1,4X,L1)
      DELG0 = GZ - ((GX + GY)/2.D0)
      DELG2 = GX - GY
      G = (GX + GY + GZ)/3.D0
      FOAB = +8.286D+07
      F0 = (DELG0*BCEN*2.D0*9.2731D+6)/(1.054430D*3.D0)
      F2 = (DELG2*BCEN*9.2731D+6)/(DSQRT(6.D0)*1.054430D)
      D = (AX + AY - (2.D0*AZ))/(2.D0*DSQRT(6.D0))
      D2 = ((AY - AX)/4.D0)
      B = -((AX + AY + AZ)/6.D0)
      GAMMA = (G*9.2731D+6)/1.054430D
      IF(TRUNC) GO TO 16
      KTERM = L
      LODD = L - 1
      LDOUB = L
   16 KT = KTERM/2
      LO = (LODD - 1)/2
      LDB = LDOUB/2
      WRITE(6,17) TITLE,AX,AY,AZ,D,D2,B,GX,GY,GZ,F0,F2,R,RZ,L,KTERM,LODD
     1,LDOUB,BCEN
   17 FORMAT(1H1,20A4,///,' A(X), A-TENSOR COMPONENT ALONG  X  PRINCIPAL
     1 AXIS  ',D12.5,' GAUSS',/,' A(Y), A-TENSOR COMPONENT ALONG  Y  PRI
     2NCIPAL AXIS  ',D12.5,' GAUSS',/,' A(Z), A-TENSOR COMPONENT ALONG
     3Z  PRINCIPAL AXIS  ',D12.5,' GAUSS',/,9X,'CALCULATED VALUE OF  D(0
     4)  ',D12.5,' GAUSS',/,9X,'CALCULATED VALUE OF  D(2)  ',D12.5,' GAU
     5SS',/,9X,'CALCULATED VALUE OF  B  ',D12.5,' GAUSS',//,' G(X), G-TE
     6NSOR COMPONENT ALONG  X  PRINCIPAL AXIS  ',F8.5,/,' G(Y), G-TENSOR
     7 COMPONENT ALONG  Y  PRINCIPAL AXIS  ',F8.5,/,' G(Z), G-TENSOR COM
     8PONENT ALONG  Z  PRINCIPAL AXIS  ',F8.5,/,9X,'CALCULATED VALUE OF
     9 F(0)  ',D12.5,' RADIANS PER SECOND',/,9X,'CALCULATED VALUE OF  F(
```

```
     * ' ',D12.5,' RADIANS PER SECOND',//,' R,ROTATIONAL DIFFUSION CONS
     *TANT ABOUT  X,Y  AXES  ',D12.5,' RADIANS PER SECOND',/,' R(Z), ROT
     *ATIONAL DIFFUSION CONSTANT ABOUT  Z  AXIS  ',D12.5,' RADIANS PER S
     *ECOND',//,' THE TERMINATING  L  VALUE  IS ',I3,//,' THE TERMINATIN
     *G  =  VALUE IS  ',I3,//,' THE TERMINATING  LODD  VALUE ASSOCIATED
     *WITH THE ODD  L  COEFFICIENTS IS ',I3,//,' THE TERMINATING  LDOUB
     * VALUE ASSOCIATED WITH THE DOUBLY FORBIDDEN TRANSITION COEFFICIENT
     *S IS  ',I3,//,' THE CENTER OF THE SPECTRUM  ',D12.5,' GAUSS',/)
      R=R/FOAB
      RZ = RZ/FOAB
      GO TO (18,19,20,21,22,23), IROT
   18 CORRT = 1.D0/(6.D0*DSQRT(R*RZ)*FOAB)
      WRITE(6,24)
      GO TO 30
   19 CORRT = DSQRT(7.D0)/(6.D0*DSQRT(R*RZ)*FOAB)
      WRITE(6,25)
      GO TO 30
   20 CORRT = 1.D0/(DSQRT(R*RZ)*FOAB)
      WRITE(6,26)
      GO TO 30
   21 CORRT = (1.D0 + (6.D0*RTAU))/(6.D0*DSQRT(R*RZ)*FOAB)
      WRITE(6,27) RTAU
      GO TO 30
   22 CORRT = 5.D0/(6.D0*DSQRT(R*RZ)*FOAB*(1.D0/(1.D0 + (9.D0*RTAU*RTAU)
     1)+(4.D0/(1.D0 + (36.D0*RTAU*RTAU)))))
      WRITE(6,28) RTAU
      GO TO 30
   23 WRITE(6,29) RTAU
      CORRT = (5.D0*RTAU)/((2.D0*DSQRT(R*RZ)*FOAB)*(2.D0 - (DEXP(-(3.D0*
     1RTAU)) + DEXP(-(12.D0*RTAU)))))
   24 FORMAT(1H ,'BROWNIAN ROTATIONAL DIFFUSION',/)
   25 FORMAT(1H ,'SIMPLE''FREE'' ROTATIONAL DIFFUSION',/)
   26 FORMAT(1H ,'RANDOM JUMP ROTATIONAL REORIENTATION',/)
   27 FORMAT(1H ,'EGELSTAFF JUMP ROTATIONAL REORIENTATION ',/,' THE PROD
     1UCT  R*TAU  IS  ',D12.5,/)
   28 FORMAT(1H ,'JUMP ROTATIONAL REORIENTATION WITH AN EXPONENTIAL DIST
     1RIBUTION OF JUMP ANGLES',/,' THE PRODUCT  R*TAU  IS  ',D12.5,/)
   29 FORMAT(1H ,' JUMP ROTATIONAL REORIENTATION WITH A GAUSSIAN DISTRIB
     1UTION OF JUMP ANGLES',/,' THE PRODUCT  R*TAU  IS  ',D12.5,/)
   30 WRITE(6,31) CORRT
   31 FORMAT(1H ,/,' THE CALCULATED ROTATIONAL CORRELATION TIME IS  ',D1
     12.5,' SECONDS PER RADIAN',/)
      D = D*(GAMMA/FOAB)
      D2 = D2*(GAMMA/FOAB)
      B = B*(GAMMA/FOAB)
      DPR = -(D*DSQRT(8.D0/3.D0))
      D2PR = -(D2*DSQRT(8.D0/3.D0))
      F0 = F0/FOAB
      F2 = F2/FOAB
      IF((KTERM.GT.LODD).OR.(LODD.GT.LDOUB)) GO TO 301
      M = ((20*L) + 24 + (10*L*KTERM) + (2*LDOUB*KTERM) + (6*LODD*KTERM)
     1 + (4*LDOUB) - (9*(KTERM**2)) + (12*KTERM))/8
      M = (9*KT) + 16
      IF(KTERM.EQ.0) M=10
      GO TO 302
  301 IF((LODD.GT.KTERM).OR.(KTERM.GT.LDOUB)) GO TO 303
      M = ((20*L) + 21 + (10*L*KTERM) + (2*LDOUB*KTERM) + (3*(LODD**2))
     1+ (4*LDOUB) - (6*(KTERM**2))+ (12*KTERM))/8
      M = (3*KTERM) + 16
      IF(KTERM.EQ.LDOUB) M = M - 1
      IF(KTERM.EQ.L) M = (3*KTERM) + 10
      M1 = (9*LO) + 16
      IF(M1.GT.M) M = M1
      GO TO 302
  303 IF((KTERM.GT.LDOUB).OR.(LDOUB.GT.LODD)) GO TO 304
      M = ((20*L) + 24 + (10*L*KTERM) + (4*LDOUB*KTERM) + (4*LODD*KTERM)
     1 + (4*LDOUB) - (9*(KTERM**2))+ (10*KTERM))/8
      M = (9*KT) + 16
      IF(LDOUB.EQ.KTERM) M = (4*KTERM) + 15
      IF((LDOUB.EQ.KTERM).AND.(KTERM.GT.16)) M = (9*KT) + 7
      IF(KTERM.EQ.0) M=10
      GO TO 302
  304 IF((LDOUB.GT.KTERM).OR.(KTERM.GT.LODD)) GO TO 305
      M = ((20*L) + 24 + (10*L*KTERM) + (4*LODD*KTERM) + (2*(LDOUB**2))
     1 + (4*LDOUB) - (7*(KTERM**2)) + (10*KTERM))/8
      M = (7*KT) + 14
      M1 = (4*LDOUB) + 15
      IF(LDOUB.GT.16) M1 = (9*LOB) + 7
      IF(M1.GT.M) M = M1
      GO TO 302
  305 IF((LODD.GT.LDOUB).OR.(LDOUB.GT.KTERM)) GO TO 306
      M = ((20*L) + 21 + (10*L*KTERM) + (LDOUB**2) + (3*(LODD**2)) + (6*
     1LDOUB) - (5*(KTERM**2)) + (10*KTERM))/8
      M = (5*KT) + 14
      M1 = (3*LDOUB) + 15
      M2 = (9*LO) + 16
      IF(M1.GT.M) M = M1
      IF(M2.GT.M) M = M2
      GO TO 302
  306 M = ((20*L) + 22 + (10*L*KTERM) + (2*(LDOUB**2)) + (2*(LODD**2)) +
     1 (4*LDOUB) - (5*(KTERM**2)) + (10*KTERM))/8
      M = (5*KT) + 16
      IF(L.EQ.KTERM) M = M - 5
      M1 = (7*LO) + 14
      M2 = (4*LDOUB) + 15
      IF(LDOUB.GT.10) M2 = (9*LOB) + 10
      IF(M1.GT.M) M = M1
      IF(M2.GT.M) M = M2
  302 IF((L.EQ.2).AND.(KTERM.EQ.2)) M = 13
      IF((L.EQ.2).AND.(KTERM.EQ.0)) M = 7
      IF((N.GT.NDIM).OR.(M.GT.JDIM)) GO TO 814
C     CONSTRUCTING THE COEFFICIENT MATRIX (SYMMETRIZED) OF THE
C     VECTOR
      DO 32 I=1,N
      DO 32 J=1,M
   32 CSYM(I,J) = (0.D0,0.D0)
      CSYM(1,4) = (-1.D0,0.D0)*((F0 + DPR)*SY(2,2)*DSQRT(5.D0))
      CSYM(1,7) = (1.D0,0.D0)*(D*SY(2,1)*SY(3,3)*DSQRT(5.D0))
      CSYM(2,4) = (-1.D0,0.D0)*(F0*SY(2,2)*DSQRT(5.D0))
      CSYM(2,6) = CSYM(1,7)
      CSYM(2,7) = CSYM(2,6)
      CSYM(3,4) = (-1.D0,0.D0)*((F0 - DPR)*SY(2,2)*DSQRT(5.D0))
      CSYM(3,6) = CSYM(1,7)
      CSYM(1,1) = (1.D0,0.D0)*(2.D0*B)
      CSYM(3,1) = (-1.D0,0.D0)*(2.D0*B)
      IF(KTERM.EQ.0) GO TO 33
      CSYM(1,10) = (-1.D0,0.D0)*((F2 + D2PR)*SY(2,1)*SY2(3,2)*DSQRT(1.D+
     11))
      CSYM(1,13) = (1.D0,0.D0)*(D2*SY(3,3)*SY2(3,2)*DSQRT(1.D+1))
      CSYM(2,10) = (-1.D0,0.D0)*(F2*SY(2,1)*SY2(3,2)*DSQRT(1.D+1))
      CSYM(2,12) = CSYM(1,13)
      CSYM(2,13) = CSYM(2,12)
      CSYM(3,10) = (-1.D0,0.D0)*((F2 - D2PR)*SY(2,1)*SY2(3,2)*DSQRT(1.D+
     11))
      CSYM(3,12) = CSYM(2,13)
   33 AL = 2.D0
      IEND = (L/2)
      J = 4
      DO 34 I=1,IEND
      K = (9*I) + 7
      IF((LOB.EQ.I).AND.(LO.GE.I).AND.(KT.GE.I)) K = (8*I) + 7
      IF((LOB.LT.I).AND.(LO.GE.I).AND.(KT.GE.I)) K = (7*I) + 6
      IF((LOB.GE.I).AND.(LO.LT.I).AND.(KT.GE.I)) K = (6*I) + 7
      IF((LOB.GT.I).AND.(LO.GE.I).AND.(KT.LT.I)) K = (9*KT) + 7
      IF((LOB.EQ.I).AND.(LO.GE.I).AND.(KT.LT.I)) K = (8*KT) + 7
      IF((LOB.LT.I).AND.(LO.LT.I).AND.(KT.GE.I)) K = (5*I) + 6
      IF((LOB.LT.I).AND.(LO.GE.I).AND.(KT.LT.I)) K = (7*KT) + 6
      IF((LOB.GE.I).AND.(LO.LT.I).AND.(KT.LT.I)) K = (3*KTERM) + 7
      IF((LOB.LT.I).AND.(LO.LT.I).AND.(KT.LT.I)) K = (5*KT) + 6
      KD = 0
      IF(I.GE.LOB) KD = 1
      LL1 = (2*I) + 1
      LL21 = LL1 + 1
      LL2 = (6*I) + 1
      LL12 = LL2 + 1
      LL22 = LL2 + 2
      L1L12 = LL2 + 3
      L1L22 = LL2 + 4
      L1L32 = LL2 + 5
      LL3 = (3*I*(I + 1)) + 1
      LL13 = LL3 + 1
      LL23 = LL3 + 2
      J1 = J + 1
      J2 = J + 2
      J3 = J + 3
      J4 = J + 4
      J5 = J + 5
      JCOUNT = 0
      SFLL = (2.D0*AL) + 1.D0
      SFL1L1 = (2.D0*AL) + 3.D0
      SFLL2 = DSQRT((4.D0*AL*AL) + (1.2D+1*AL) + 5.D0)
      SFLL1 = DSQRT((4.D0*AL*AL) + (8.D0*AL) + 3.D0)
      SFL1L2 = DSQRT((4.D0*AL*AL) + (1.6D+1*AL) + 1.5D+1)
      SFL1L3 = DSQRT((4.D0*AL*AL) + (2.D+1*AL) + 2.1D+1)
      ALL = AL
      LJUMP = 2*I
      DO 36 IR=1,2
      GO TO (37,38,39,40,41,42),IROT
   37 DROT(IR) = R*ALL*(ALL + 1.D0)
      GO TO 36
   38 DROT(IR) = R*((ALL*(ALL + 1.D0))/DSQRT(1.D0 + (ALL*(ALL + 1.D0))))
      GO TO 36
   39 DROT(IR) = R
      GO TO 36
   40 DROT(IR) = (R*ALL*(ALL + 1.D0))/(1.D0 + (RTAU*ALL*(ALL + 1.D0)))
      GO TO 36
   41 DROT(IR) = 0.D0
      DO 43 IJUMP=1,LJUMP
   43 DROT(IR) = DROT(IR) + ((DFLOAT(IJUMP)**2)/(1.D0 + ((3.D0*RTAU*DFLO
     1AT(IJUMP))**2)))
      DROT(IR) = DROT(IR)*((6.D0*R)/((2.D0*ALL) + 1.D0))
      GO TO 45
   42 DROT(IR) = 0.D0
      DO 44 IJUMP=1,LJUMP
   44 DROT(IR) = DROT(IR) + DEXP(-(3.D0*RTAU*DFLOAT(IJUMP)*DFLOAT(IJUMP)
     1))
      DROT(IR) = ((2.D0*R)/(((2.D0*ALL) + 1.D0)*RTAU))*(DFLOAT(LJUMP) -
     1DROT(IR))
   45 LJUMP = LJUMP + 1
   36 ALL = ALL + 1.D0
      IF(IEND.EQ.I) GO TO 46
      CSYM(J,K) = (-1.D0,0.D0)*((F0 + DPR)*SY(LL21,2)*SFLL2)
      CSYM(J,K+3) = (1.D0,0.D0)*(D*SY(LL21,1)*SY(LL22,3)*SFLL2)
      CSYM(J1,K) = (-1.D0,0.D0)*(F0*SY(LL21,2)*SFLL2)
      CSYM(J1,K+2) = CSYM(J,K+3)
      CSYM(J1,K+3) = CSYM(J1,K+2)
      CSYM(J2,K) = (-1.D0,0.D0)*((F0 - DPR)*SY(LL21,2)*SFLL2)
      CSYM(J2,K+2) = CSYM(J1,K+3)
      CSYM(J3,K) = (1.D0,0.D0)*((F0 + (DPR/2.D0))*SY(LL21,1)*SY(LL22,4)*
     1SFLL2)
      CSYM(J3,K-3) = (1.D0,0.D0)*(D*SY(LL21,1)*SY(LL22,5)*SFLL2)
      CSYM(J3,K-2) = CSYM(J3,K-3)
      CSYM(J4,K) = (1.D0,0.D0)*((F0 - (DPR/2.D0))*SY(LL21,1)*SY(LL22,4)*
     1SFLL2)
      CSYM(J4,K-3) = CSYM(J3,K-3)
      CSYM(J4,K-2) = CSYM(J4,K-3)
      IF(I.GT.LOB) GO TO 35
      CSYM(J5,K-2) = (-1.D0,0.D0)*((D/DSQRT(2.D0))*SY(LL21,1)*SY(LL22,8)
     1*SFLL2)
      CSYM(J5,K-1) = CSYM(J5,K-2)
      IF(I.GE.LOB) GO TO 35
      CSYM(J5,K) = (-1.D0,0.D0)*(F0*SY(LL21,1)*SY(LL22,7)*SFLL2)
      CSYM(J3,K+2) = (-1.D0,0.D0)*((D/DSQRT(2.D0))*SY(LL21,1)*SY(LL22,6)
     1*SFLL2)
      CSYM(J4,K+1) = CSYM(J3,K+2)
   35 IF(KTERM.EQ.0) GO TO 47
      CSYM(J,K+6-KD) = (-1.D0,0.D0)*((F2 + D2PR)*SY(LL21,1)*SY2(LL23,2)*
     1SFLL2*DSQRT(2.D0))
      CSYM(J,K+9-KD) = (1.D0,0.D0)*(D2*SY(LL22,3)*SY2(LL23,2)*SFLL2*DSQR
     1T(2.D0))
      CSYM(J1,K+6-KD) = (-1.D0,0.D0)*(F2*SY(LL21,1)*SY2(LL23,2)*SFLL2*DS
     1QRT(2.D0))
      CSYM(J1,K+8-KD) = CSYM(J,K+9-KD)
      CSYM(J1,K+9-KD) = CSYM(J1,K+8-KD)
      CSYM(J2,K+6-KD) = (-1.D0,0.D0)*((F2 - D2PR)*SY(LL21,1)*SY2(LL23,2)
     1*SFLL2*DSQRT(2.D0))
      CSYM(J2,K+8-KD) = CSYM(J1,K+9-KD)
      CSYM(J3,K+6-KD) = (1.D0,0.D0)*((F2 + (D2PR/2.D0))*SY(LL22,4)*SY2(L
     1L23,2)*SFLL2*DSQRT(2.D0))
      CSYM(J3,K+3-KD) = (1.D0,0.D0)*(D2*SY(LL22,5)*SY2(LL23,2)*SFLL2*DSQ
     1RT(2.D0))
      CSYM(J3,K+4-KD) = CSYM(J3,K+3-KD)
      CSYM(J4,K+6-KD) = (1.D0,0.D0)*((F2 - (D2PR/2.D0))*SY(LL22,4)*SY2(L
     1L23,2)*SFLL2*DSQRT(2.D0))
      CSYM(J4,K+3-KD) = CSYM(J3,K+3-KD)
      CSYM(J4,K+4-KD) = CSYM(J4,K+3-KD)
      IF(I.GT.LOB) GO TO 100
      CSYM(J5,K+4-KD) = (-1.D0,0.D0)*(D2*SY(LL22,8)*SY2(LL23,2)*SFLL2)
      CSYM(J5,K+5-KD) = CSYM(J5,K+4-KD)
      CSYM(J5,K+6) = (-1.D0,0.D0)*(F2*SY(LL22,7)*SY2(LL23,2)*SFLL2*DSQRT
     1(2.D0))
      CSYM(J3,K+8) = (-1.D0,0.D0)*(D2*SY(LL22,6)*SY2(LL23,2)*SFLL2)
      CSYM(J4,K+7) = CSYM(J3,K+8)
  100 IF(I.GT.LO) GO TO 46
      K1 = K - (3*I)
      IF((I.LT.LOB).AND.(I.GT.KT)) K1 = K - (3*KT)
      IF((I.GE.LOB).AND.(I.LE.KT)) K1 = K - (2*I)
      IF((I.GE.LOB).AND.(I.GT.KT)) K1 = K - KTERM
      CSYM(J,K1) =  (1.D0,0.D0)*(D2*SY(LL12,3)*SY2(LL13,2)*SFLL1*DSQRT(2
     1.D0))
      CSYM(J1,K1-1) = CSYM(J,K1)
      CSYM(J1,K1) = CSYM(J,K1)
      CSYM(J2,K1-1) = CSYM(J,K1)
      CSYM(J3,K1-3) = (1.D0,0.D0)*((F2 + (D2PR/2.D0))*SY(LL12,4)*SY2(LL1
     13,2)*SFLL1*DSQRT(2.D0))
      CSYM(J4,K1-3) = (1.D0,0.D0)*((F2 - (D2PR/2.D0))*SY(LL12,4)*SY2(LL1
     13,2)*SFLL1*DSQRT(2.D0))
      IF(I.GT.LOB) GO TO 46
      CSYM(J5,K1-5) = (-1.D0,0.D0)*(D2*SY(LL12,8)*SY2(LL13,2)*SFLL1)
      CSYM(J5,K1-4) = CSYM(J5,K1-5)
      IF(I.GE.LOB) GO TO 46
      CSYM(J5,K1-3) = (-1.D0,0.D0)*(F2*SY(LL12,7)*SY2(LL13,2)*SFLL1*DSQR
     1T(2.D0))
      CSYM(J3,K1-1) = (-1.D0,0.D0)*(D2*SY(LL12,6)*SY2(LL13,2)*SFLL1)
      CSYM(J4,K1-2) = CSYM(J3,K1-1)
   46 IF(KTERM.EQ.0) GO TO 47
      KD = 0
      IF(I.GT.LOB) KD = 1
      CSYM(J,7-KD) = (-1.D0,0.D0)*((F2 + D2PR)*SY(LL1,1)*SY2(LL3,2)*SFLL
     1*DSQRT(2.D0))
      CSYM(J,10-KD) = (1.D0,0.D0)*(D2*SY(LL2,3)*SY2(LL3,2)*SFLL*DSQRT(2.
     1D0))
      CSYM(J1,7-KD) = (-1.D0,0.D0)*(F2*SY(LL1,1)*SY2(LL3,2)*SFLL*DSQRT(2
     1.D0))
      CSYM(J1,9-KD) = CSYM(J,10-KD)
      CSYM(J1,10-KD) = CSYM(J1,9-KD)
      CSYM(J2,7-KD) = (-1.D0,0.D0)*((F2 - D2PR)*SY(LL1,1)*SY2(LL3,2)*SFL
     1L*DSQRT(2.D0))
      CSYM(J2,9-KD) = CSYM(J1,10-KD)
      CSYM(J3,7-KD) = (1.D0,0.D0)*((F2 + (D2PR/2.D0))*SY(LL2,4)*SY2(LL3,
     12)*SFLL*DSQRT(2.D0))
      CSYM(J3,4-KD) = (1.D0,0.D0)*(D2*SY(LL2,5)*SY2(LL3,2)*DSQRT(2.D0)*S
     1FLL)
      CSYM(J3,5-KD) = CSYM(J3,4-KD)
      CSYM(J4,7-KD) = (1.D0,0.D0)*((F2 - (D2PR/2.D0))*SY(LL2,4)*SY2(LL3,
     12)*SFLL*DSQRT(2.D0))
      CSYM(J4,4-KD) = CSYM(J3,4-KD)
      CSYM(J4,5-KD) = CSYM(J4,4-KD)
      IF(I.GT.LOB) GO TO 47
      CSYM(J5,5) = (-1.D0,0.D0)*(D2*SY(LL2,8)*SY2(LL3,2)*SFLL)
      CSYM(J5,6) = CSYM(J5,5)
      IF(I.GE.LOB) GO TO 47
      CSYM(J5,7) = (-1.D0,0.D0)*(F2*SY(LL2,7)*SY2(LL3,2)*SFLL*DSQRT(2.D0
     1))
      CSYM(J3,9) = (-1.D0,0.D0)*(D2*SY(LL2,6)*SY2(LL3,2)*SFLL)
      CSYM(J4,8) = CSYM(J3,9)
   47 CSYM(J,4) = (1.D0,0.D0)*(D*SY(LL1,1)*SY(LL2,3)*SFLL)
      CSYM(J1,3) = CSYM(J,4)
      CSYM(J1,4) = CSYM(J,4)
      CSYM(J2,3) = CSYM(J,4)
      CSYM(J,1) = ((1.D0,0.D0)*((2.D0*B) - (SFLL*(F0 + DPR)*SY(LL1,2))))
     1 + ((0.D0,-1.D0)*DROT(1))
      CSYM(J1,1) = ((-1.D0,0.D0)*(SFLL*F0*SY(LL1,2))) + ((0.D0,-1.D0)*DR
     1OT(1))
      CSYM(J2,1) = ((1.D0,0.D0)*(-(2.D0*B) - (SFLL*(F0 - DPR)*SY(LL1,2))
     1)) + ((0.D0,-1.D0)*DROT(1))
      CSYM(J3,1) = ((1.D0,0.D0)*(B + (SFLL*(F0 + (DPR/2.D0))*SY(LL1,1)*S
     1Y(LL2,4)))) + ((0.D0,-1.D0)*DROT(1))
      CSYM(J4,1) = ((1.D0,0.D0)*(- B + (SFLL*(F0 - (DPR/2.D0))*SY(LL1,1)
     1*SY(LL2,4)))) + ((0.D0,-1.D0)*DROT(1))
      IF(I.GT.LOB) GO TO 101
      CSYM(J5,1) = ((-1.D0,0.D0)*(SFLL*F0*SY(LL2,7)*SY(LL1,1))) + ((0.D0
     1,-1.D0)*DROT(1))
      CSYM(J3,3) = (-1.D0,0.D0)*((D/DSQRT(2.D0))*SY(LL2,6)*SY(LL1,1)*SFL
     1L)
      CSYM(J4,2) = CSYM(J3,3)
      J = J + 1
  101 J = J + 5
      DO 48 II=1,I
      IF(II.GT.(KTERM/2)) GO TO 48
      J1 = J + 1
      J2 = J + 2
      J3 = J + 3
      J4 = J + 4
      J5 = J + 5
      JODD = J + (6*I) - (3*(II - 1))
      IF((I.LE.KT).AND.(I.EQ.LOB)) JODD = J + (6*I) - (4*II) + 4
      IF((I.LE.KT).AND.(I.GT.LOB)) JODD = J + (5*I) - (3*II) + 3
      IF((I.GT.KT).AND.(I.LT.LOB)) JODD = J + (3*KTERM) - (3*II) + 3
      IF((I.GT.KT).AND.(I.EQ.LOB)) JODD = J + (3*KTERM) - (4*II) + 4
      IF((I.GT.KT).AND.(I.GT.LOB)) JODD = J + (5*KT) - (3*II) + 3
      KD = 0
      IF(I.GT.LO) KD = (3*I)
      KLL20 = (9*I) + 7 - KD
      KLL21 = KLL20 - 6
      KLL22 = KLL20 + 6
      KLL10 = (6*I) - (3*II) + 4
      KLL11 = KLL10 - 3
      KLL12 = KLL10 + 3
      KL1L20 = 3*(I + II) + 7
      KL1L21 = KL1L20 - 6
      KL1L22 = KL1L20 + 6
      KL1L30 = (9*I) + 13
      KL1L31 = KL1L30 - 3
      KL1L32 = KL1L30 + 3
      IF((I.GT.KT).OR.(I.NE.LOB)) GO TO 102
      KD = 1
      IF(I.GT.LO) KD = 0
      KLL20 = KLL20 - II - KD
      KLL21 = KLL20 - 5
      KLL22 = KLL20 + 5
      KLL10 = KLL10 - (II - 1)
      KLL11 = KLL10 - 2
      KLL12 = KLL10 + 2
      KL1L20 = KL1L20 - I - 1
      KL1L21 = KL1L20 - 5
      KL1L22 = KL1L20 + 5
      GO TO 103
  102 IF((I.GT.KT).OR.(I.LE.LOB)) GO TO 103
      KD = 1
      IF(I.GT.LO) KD = 0
      KLL20 = KLL20 - I - 1 - KD
      KLL21 = KLL20 - 5
      KLL22 = KLL20 + 5
      KLL10 = KLL10 - 1
      KLL11 = KLL10 - 2
      KLL12 = KLL10 + 2
      KL1L20 = KL1L20 - I - 1
      KL1L21 = KL1L20 - 5
      KL1L22 = KL1L20 + 5
  103 IF((I.GE.KT).OR.((I+1).NE.LOB)) GO TO 104
      KL1L30 = KL1L30 - I + 1
      KL1L31 = KL1L30 - 2
      KL1L32 = KL1L30 + 2
      GO TO 105
  104 IF((I.GE.KT).OR.((I+1).LE.LOB)) GO TO 106
      KL1L30 = KL1L30 - (2*I) - 2
      KL1L31 = KL1L30 - 2
      KL1L32 = KL1L30 + 2
      GO TO 105
  106 IF((I.LE.KT).OR.(I.GE.LOB)) GO TO 107
      KD = 0
      IF(I.GT.LO) KD = 3*KT
      KLL20 = (9*KT) + 7 - KD
      KLL21 = KLL20 - 6
      KLL22 = KLL20 + 6
      KLL10 = 3*(KTERM - II) + 4
      KLL11 = KLL10 - 3
      KLL12 = KLL10 + 3
      KL1L20 = (3*KT) + (3*II) + 7
      KL1L21 = KL1L20 - 6
      KL1L22 = KL1L20 + 6
      GO TO 108
  107 IF((I.LE.KT).OR.(I.NE.LOB)) GO TO 109
      KD = KTERM
      IF(I.GT.LO) KD = 0
      KLL20 = (3*KTERM) - II + 7 + KD
      KLL21 = KLL20 - 5
      KLL22 = KLL20 + 5
      KLL10 = (3*KTERM) - (4*II) + 5
      KLL11 = KLL10 - 2
      KLL12 = KLL10 + 2
      KL1L20 = KTERM + (3*II) + 6
      KL1L21 = KL1L20 - 5
      KL1L22 = KL1L20 + 5
      GO TO 108
  109 IF((I.LE.KT).OR.(I.LE.LOB)) GO TO 108
      KD = KTERM
      IF(I.GT.LO) KD = 0
      KLL20 = (5*KT) + 6 + KD
      KLL21 = KLL20 - 5
      KLL22 = KLL20 + 5
      KLL10 = (5*KT) - (3*II) + 4
      KLL11 = KLL10 - 2
      KLL12 = KLL10 + 2
      KL1L20 = KTERM + (3*II) + 6
      KL1L21 = KL1L20 - 5
      KL1L22 = KL1L20 + 5
  108 IF((I.LT.KT).OR.((I+1).GE.LOB)) GO TO 110
      KL1L30 = (9*KT) + 7
      KL1L31 = KL1L30 - 3
      KL1L32 = KL1L30 + 3
      GO TO 105
  110 IF((I.LT.KT).OR.((I+1).NE.LOB)) GO TO 111
      KL1L30 = (9*KT) - II + 8
      KL1L31 = KL1L30 - 2
      KL1L32 = KL1L30 + 2
      GO TO 105
  111 IF((I.LT.KT).OR.((I+1).LE.LOB)) GO TO 105
      KL1L30 = (7*KT) + 6
      KL1L31 = KL1L30 - 2
      KL1L32 = KL1L30 + 2
  105 LL3 = (3*I*(I + 1)) + (3*II) + 1
      LL13 = LL3 + 1
      LL23 = LL3 + 2
      L1L13 = LL3 + (3*I) + 3
      L1L23 = L1L13 + 1
      L1L33 = L1L13 + 2
      XK = DFLOAT(2*II)
      DROTK1 = DROT(1) + ((DROT(1)/(R*AL*(AL + 1.D0)))*(RZ - R)*XK*XK)
      DROTK2 = DROT(2) + ((DROT(2)/(R*(AL + 1.D0)*(AL + 2.D0)))*(RZ - R)
     1*XK*XK)
      IF(IEND.EQ.I) GO TO 49
      IF(II.EQ.(KTERM/2)) GO TO 50
      CSYM(J,KLL22) = (-1.D0,0.D0)*((F2 + D2PR)*SY(LL21,1)*SY2(LL23,2)*S
     1FLL2)
      CSYM(J,KLL22+3) = (1.D0,0.D0)*(D2*SY(LL22,3)*SY2(LL23,2)*SFLL2)
      CSYM(J1,KLL22)   = (-1.D0,0.D0)*(F2*SY(LL21,1)*SY2(LL23,2)*SFLL2)
      CSYM(J1,KLL22+2) = CSYM(J,KLL22+3)
      CSYM(J1,KLL22+3) = CSYM(J,KLL22+3)
      CSYM(J2,KLL22) = (-1.D0,0.D0)*((F2 - D2PR)*SY(LL21,1)*SY2(LL23,2)*
     1SFLL2)
      CSYM(J2,KLL22+2) = CSYM(J,KLL22+3)
      CSYM(J3,KLL22) = (1.D0,0.D0)*((F2 + (D2PR/2.D0))*SY(LL22,4)*SY2(LL
     123,2)*SFLL2)
      CSYM(J3,KLL22-3) = (1.D0,0.D0)*(D2*SY(LL22,5)*SY2(LL23,2)*SFLL2)
      CSYM(J3,KLL22-2) = CSYM(J3,KLL22-3)
      CSYM(J4,KLL22) = (1.D0,0.D0)*((F2 - (D2PR/2.D0))*SY(LL22,4)*SY2(LL
     123,2)*SFLL2)
      CSYM(J4,KLL22-3) = CSYM(J3,KLL22-3)
      CSYM(J4,KLL22-2) = CSYM(J4,KLL22-3)
      IF(I.GT.LOB) GO TO 112
      CSYM(J5,KLL22-2) = (-1.D0,0.D0)*((D2/DSQRT(2.D0))*SY(LL22,8)*SY2(L
     1L23,2)*SFLL2)
      CSYM(J5,KLL22-1) = CSYM(J5,KLL22-2)
      IF(I.GE.LOB) GO TO 112
      CSYM(J5,KLL22) = (-1.D0,0.D0)*(F2*SY(LL22,7)*SY2(LL23,2)*SFLL2)
      CSYM(J3,KLL22+2) = (-1.D0,0.D0)*((D2/DSQRT(2.D0))*SY(LL22,6)*SY2(L
     1L23,2)*SFLL2)
      CSYM(J4,KLL22+1) = CSYM(J3,KLL22+2)
  112 IF(I.GT.LO) GO TO 50
      IF(II.EQ.1) GO TO 51
      CSYM(J,KLL12) = (1.D0,0.D0)*(D2*SY(LL12,3)*SY2(LL13,2)*SFLL1)
      CSYM(J1,KLL12-1) = CSYM(J,KLL12)
      CSYM(J1,KLL12) = CSYM(J,KLL12)
```

```
      CSYM(J2,KLL12-1) = CSYM(J,KLL12)
      CSYM(J3,KLL12-3) = (1.D0,0.D0)*((F2 + (D2PR/2.D0))*SYlLL12,4)*SY2(
     1LL13,3)*SFLL1)
      CSYM(J4,KLL12-3) = (1.D0,0.D0)*((F2 - (D2PR/2.D0))*SYlLL12,4)*SY2(
     1   )*SFLL1)
          GO TO 91
      CSYM(J5,KLL12-5) = (-1.D0,0.D0)*((D2/DSQRT(2.DO))*SYlLL12,8)*SY2(L
     1L13,2)*SFLL1)
      CSYM(J5,KLL12-4) = CSYM(J5,KLL12-5)
      IF(I.GE.LDB) GO TO 91
      CSYM(J2,KLL22-3) = (-1.D0,0.D0)*(F2*SYlLL12,7)*SY2(LLL13,2)*SFLL1)
      CSYM(J3,KLL12-1) = (-1.D0,0.D0)*((D2/DSQRT(2.DO))*SYlLL12,8)*SY2(L
     1LL13,3)*SFLL1)
      CSYM(J3,KLL22-2) = CSYM(J3,KLL12-1)
      CSYM(J4,KLL22-2) = (1.D0,0.D0)*((F2 + (D2PR/2.D0))*SYlLL22,4)*SY
     1   ,2)*SFLL2)
      CSYM(JDDD,KLL22-2) = CSYM(JDDD,KLL22-3)
      CSYM(JDDD+1,KLL22-  ) = (1.D0,0.D0)*((F2 - (D2PR/2.D0))*SYlLL22,4)
     1*SY2(LLL23,2)*SFLL2)
      CSYM(JDDD+1,KLL22-3) = CSYM(JDDD,KLL22-3)
      CSYM(JDDD+2,KLL22-2) = (-1.D0,0.D0)*((D2/DSQRT(2.DO))*SYlLL22,8)*
     1SY2(LLL23,2)*SFLL2)
      CSYM(JDDD+2,KLL22-2) = CSYM(JDDD+2,KLL22-2)
      IF(I.GE.LDB) GO TO 113
      CSYM(JDDD+2,KLL22) = (-1.D0,0.D0)*((F2*SYlLL22,7)*SY2(LLL23,2)*SF
     1LL2)
      CSYM(JDDD,KLL22+2) = (-1.D0,0.D0)*((D2/DSQRT(2.DO))*SYlLL22,8)*S
     1Y2(LLL23,2)*SFLL2)
      CSYM(JDDD+1,KLL22+2) = CSYM(JDDD,KLL22+2)
      IF(I.GE.LDB) GO TO 50
      CSYM(JDDD+2,KLL32-2) = (1.D0,0.D0)*((F2 + (D2PR/2.DO))*SYlLL32,4)*SY2
     1(LLL33,2)*SFLL3)
      CSYM(JDDD+1,KLL32-2) = (1.D0,0.D0)*((F2 - (D2PR/2.DO))*SYlLL32,4)*
     1SY2(LLL33,2)*SFLL3)
      IF(I.GE.LDB) GO TO 50
      CSYM(JDDD+2,KLL32-1) = CSYM(JDDD+2,KLL32-2)
      IF(I.GE.LDB) GO TO 50
      CSYM(JDDD+2,KLL32) = (-1.D0,0.D0)*((F2*SYlLL32,7)*SY2(LLL33,2)*SF
     1LL3)
      CSYM(JDDD,KLL32+2) = (-1.D0,0.D0)*((D2/DSQRT(2.DO))*SYlLL32,8)*S
     1Y2(LLL33,2)*SFLL3)
      CSYM(JDDD+1,KLL32+2) = CSYM(JDDD,KLL32+2)
48 AZ = 1.DO
      IF(I.EQ.1) AZ = DSQRT(2.DO)
      CSYM(J,KLL20) = (-1.D0,0.D0)*((F0 + DPR)*SYlLL21,1)*SY2(LLL23,1)*SF
     1LL2)
      CSYM(J,KLL21) = (-1.D0,0.D0)*((F2 + D2PR)*SYlLL21,1)*SY2(LLL23,3)*S
     1F(L2*AZ)
      CSYM(J,KLL20+3) = (1.D0,0.D0)*(D*SYlLL22,3)*SY2(LLL23,1)*SFLL2)
      CSYM(J,KLL21+3) = (1.D0,0.D0)*(D2*SYlLL22,3)*SY2(LLL23,3)*SFLL2*AZ)
      CSYM(J4,KLL20) = (-1.D0,0.D0)*(F0*SYlLL21,1)*SY2(LLL23,1)*SFLL2)
      CSYM(J3,KLL21) = (-1.D0,0.D0)*(F2*SYlLL21,1)*SY2(LLL23,3)*SFLL2*AZ)
      CSYM(J3,KLL20+3) = CSYM(J,KLL20+3)
      CSYM(J3,KLL21+3) = CSYM(J,KLL21+3)
      CSYM(J4,KLL21+3) = CSYM(J,KLL21+3)
      CSYM(J2,KLL20) = (-1.D0,0.D0)*((F0 - DPR)*SYlLL21,1)*SY2(LLL23,1)*S
     1F(L2)
      CSYM(J2,KLL21) = (-1.D0,0.D0)*((F2 - D2PR)*SYlLL21,1)*SY2(LLL23,3)*
     1F(L2*AZ)
      CSYM(J,KLL20+3) = CSYM(J,KLL20+3)
      CSYM(J,KLL21+3) = CSYM(J,KLL21+3)
      CSYM(J3,KLL20) = (1.D0,0.D0)*((F0 + (DPR/2.DO))*SYlLL22,4)*SY2(LL2
     1LL33,1)*SFLL3)
      CSYM(J3,KLL21) = (1.D0,0.D0)*((F2 + (D2PR/2.DO))*SYlLL22,4)*SY2(LL
     1LL33,3)*SFLL3)
      CSYM(J4,KLL20+3) = (1.D0,0.D0)*(D*SYlLL22,5)*SY2(LLL23,1)*SFLL2)
      CSYM(J4,KLL21+3) = CSYM(J3,KLL20+3)
      CSYM(J4,KLL21-3) = (1.D0,0.D0)*(D2*SYlLL22,5)*SY2(LLL23,3)*SFLL2*AZ
     1)
      CSYM(J2,KLL21-2) = CSYM(J3,KLL21-3)
      CSYM(J2,KLL20) = (1.D0,0.D0)*((F0 - (DPR/2.DO))*SYlLL22,4)*SY2(LLL2
     13,1)*SFLL2)
      CSYM(J4,KLL21) = (1.D0,0.D0)*((F2 - (D2PR/2.DO))*SYlLL22,4)*SY2(LLL
     123,3)*SFLL2*AZ)
      CSYM(J4,KLL20-3) = CSYM(J3,KLL20-3)
      CSYM(J4,KLL20-2) = CSYM(J4,KLL20-3)
      CSYM(J4,KLL21-3) = CSYM(J3,KLL21-3)
      CSYM(J4,KLL21-2) = CSYM(J3,KLL21-3)
      IF(I.GE.LDB) GO TO 114
      CSYM(J5,KLL20-2) = (-1.D0,0.D0)*((D/DSQRT(2.DO))*SYlLL22,8)*SY2(LL
     1L23,1)*SFLL2)
      CSYM(J5,KLL20-3) = CSYM(J5,KLL20-2)
      CSYM(J5,KLL21-2) = (-1.D0,0.D0)*((D2/DSQRT(2.DO))*SYlLL22,8)*SY2(L
     1L23,3)*SFLL2*AZ)
      CSYM(J5,KLL21-1) = CSYM(J5,KLL21-2)
      IF(I.GE.LDB) GO TO 114
      CSYM(J5,KLL20) = (-1.D0,0.D0)*((F0*SYlLL22,7)*SY2(LLL23,1)*SFLL2)
      CSYM(J5,KLL21) = (-1.D0,0.D0)*((F2*SYlLL22,7)*SY2(LLL23,3)*SFLL2*AZ)
      CSYM(J3,KLL20+2) = (-1.D0,0.D0)*((D/DSQRT(2.DO))*SYlLL22,8)*SY2(LL
     1L23,1)*SFLL2)
      CSYM(J3,KLL21+2) = CSYM(J3,KLL21+2)
      CSYM(J4,KLL20+1) = CSYM(J3,KLL20+2)
      CSYM(J4,KLL21+1) = CSYM(J3,KLL21+2)
      IF(I.GT.LDB) GO TO 114
      CSYM(J,KLL10) = CSYM(J,KLL10)
      CSYM(J,KLL10-1) = CSYM(J,KLL10)
      CSYM(J,KLL10-3) = CSYM(J,KLL10)
      CSYM(J2,KLL10-3) = (1.D0,0.D0)*((F0 + (DPR/2.DO))*SYlLL12,6)*SY2(LL
     1L13,1)*SFLL1)
      CSYM(J2,KLL10-2) = (1.D0,0.D0)*((F0 - (DPR/2.DO))*SYlLL12,6)*SY2(LL
     1L13,3)*SFLL1)
      IF(I.GE.LDB) GO TO 115
      CSYM(J3,KLL10-3) = (-1.D0,0.D0)*((D/DSQRT(2.DO))*SYlLL12,8)*SY2(LL
     1L13,1)*SFLL1)
      CSYM(J3,KLL10-2) = (-1.D0,0.D0)*((D2/DSQRT(2.DO))*SYlLL12,8)*SY2(L
     1LL13,3)*SFLL1)
      CSYM(J4,KLL10-3) = CSYM(J3,KLL10-2)
      CSYM(J4,KLL10-2) = CSYM(J4,KLL10-3)
      IF(I.GE.LDB) GO TO 115
      CSYM(J5,KLL10-3) = (-1.D0,0.D0)*((D/DSQRT(2.DO))*SYlLL12,8)*SY2(LL
     1L13,1)*SFLL1)
      CSYM(J5,KLL10-2) = CSYM(J5,KLL10-3)
      CSYM(J3,KLL10-1) = (-1.D0,0.D0)*((D2/DSQRT(2.DO))*SYlLL12,8)*SY2(LL
     1L13,3)*SFLL1)
      CSYM(J4,KLL10-1) = CSYM(J3,KLL10-2)
      CSYM(J4,KLL10-2) = CSYM(J4,KLL10-1)
      IF(I.GE.LDB) GO TO 115
      CSYM(J5,KLL10-1) = CSYM(J5,KLL10-2)
      CSYM(J5,KLL10-3) = (-1.D0,0.D0)*((D/DSQRT(2.DO))*SYlLL12,8)*SY2(LL
     1L13,1)*SFLL1)
      CSYM(J5,KLL10-2) = CSYM(J3,KLL10-1)
115 IF(I.EQ.1) GO TO 55
      CSYM(J,KLL11) = (1.D0,0.D0)*((D2+SYlLL12,3)*SY2(LLL13,3)*SFLL1)
      CSYM(J,KLL11-1) = CSYM(J,KLL11)
      CSYM(J,KLL11-2) = CSYM(J,KLL11)
      CSYM(J2,KLL11-1) = CSYM(J,KLL11)
      CSYM(J3,KLL11-3) = (1.D0,0.D0)*((F2 + (D2PR/2.DO))*SYlLL12,4)*SY2(
     1LL13,3)*SFLL1)
      CSYM(J4,KLL11-3) = (1.D0,0.D0)*((F2 - (D2PR/2.DO))*SYlLL12,4)*SY2(
     1LL13,3)*SFLL1)
      IF(I.GT.LDB) GO TO 55
      CSYM(J5,KLL11-5) = (-1.D0,0.D0)*((D2/DSQRT(2.DO))*SYlLL12,8)*SY2(L
     1LL13,3)*SFLL1)
      CSYM(J5,KLL11-4) = CSYM(J5,KLL11-5)
      IF(I.GE.LDB) GO TO 55
      CSYM(J5,KLL11-3) = (-1.D0,0.D0)*(F2*SYlLL12,7)*SY2(LLL13,3)*SFLL1)
      CSYM(J3,KLL11-1) = (-1.D0,0.D0)*((D2/DSQRT(2.DO))*SYlLL12,8)*SY2(L
     1LL13,3)*SFLL1)
      CSYM(J4,KLL11-2) = CSYM(J3,KLL11-1)
55 CSYM(JDDD,KLL12D1 = (1.D0,0.D0)*((F0 + (DPR/2.DO))*SYlLL22,4)*SY2
     1(LLL23,1)*SFLL2)
      CSYM(JDDD,KLL12D-3) = (1.D0,0.D0)*(D*SYlLL22,5)*SY2(LLL23,1)*SFLL
     1L2)
      CSYM(JDDD,KLL12D-2) = CSYM(JDDD,KLL12D-3)
      CSYM(JDDD+1,KLL12D) = (1.D0,0.D0)*((F0 - (DPR/2.DO))*SYlLL22,4)*S
     1Y2(LLL23,1)*SFLL2)
      CSYM(JDDD+1,KLL12D-3) = CSYM(JDDD,KLL12D-3)
      CSYM(JDDD+2,KLL12D-2) = (-1.D0,0.D0)*((D/DSQRT(2.DO))*SYlLL22,8)*
     1SY2(LLL23,1)*SFLL2)
      CSYM(JDDD+2,KLL12D-1) = CSYM(JDDD+2,KLL12D-2)
      IF(I.GF.LDB) GO TO 116
      CSYM(JDDD+2,KLL12D) = (-1.D0,0.D0)*((F0*SYlLL22,7)*SY2(LLL23,1)*SF
     1LL2)
      CSYM(JDDD,KLL12D+2) = (-1.D0,0.D0)*((D/DSQRT(2.DO))*SYlLL22,8)*S
     1Y2(LLL23,1)*SFLL2)
      CSYM(JDDD+1,KLL12D+2) = CSYM(JDDD,KLL12D+2)
116 AZ = 1.DO
      IF(II.EQ.1) AZ = DSQRT(2.DO)
      CSYM(JDDD,KLL12I) = (1.D0,0.D0)*((F2 + (D2PR/2.DO))*SYlLL22,4)*SY
     12(LLL23,3)*SFLL2*AZ)
      CSYM(JDDD,KLL12I-3) = (1.D0,0.D0)*(D2*SYlLL22,5)*SY2(LLL23,3)*SFL
     1LL2*AZ)
      CSYM(JDDD,KLL12I-2) = CSYM(JDDD,KLL12I-3)
      CSYM(JDDD+1,KLL12I) = (1.D0,0.D0)*((F2 - (D2PR/2.DO))*SYlLL22,4)*
     1SY2(LLL23,3)*SFLL2*AZ)
      CSYM(JDDD+1,KLL12I-3) = CSYM(JDDD,KLL12I-3)
      CSYM(JDDD+2,KLL12I-2) = (-1.D0,0.D0)*((D2/DSQRT(2.DO))*SYlLL22,8)*
     1SY2(LLL23,3)*SFLL2*AZ)
      CSYM(JDDD+2,KLL12I-1) = CSYM(JDDD+2,KLL12I-2)
      IF(I.GE.LDB) GO TO 117
      CSYM(JDDD+2,KLL12I) = (-1.D0,0.D0)*(F2*SYlLL22,7)*SY2(LLL23,3)*SF
     1LL2*AZ)
      CSYM(JDDD,KLL12I+2) = (-1.D0,0.D0)*((D2/DSQRT(2.DO))*SYlLL22,8)*S
     1Y2(LLL23,3)*SFLL2*AZ)
      CSYM(JDDD+1,KLL12I+2) = CSYM(JDDD,KLL12I+2)
117 CSYM(JDDD,KLL13D1 = (1.D0,0.D0)*((F0 + (DPR/2.DO))*SYlLL32,4)*SY2
     1(LLL33,1)*SFLL3)
      CSYM(JDDD+1,KLL13D) = (1.D0,0.D0)*((F0 - (DPR/2.DO))*SYlLL32,4)*S
     1Y2(LLL33,1)*SFLL3)
      IF(I.GT.LDB) GO TO 118
      CSYM(JDDD+2,KLL13D-2) = (-1.D0,0.D0)*((D/DSQRT(2.DO))*SYlLL32,8)*
     1SY2(LLL33,1)*SFLL3)
      CSYM(JDDD+2,KLL13D-1) = CSYM(JDDD+2,KLL13D-2)
      IF(I.GE.LDB) GO TO 118
      CSYM(JDDD+2,KLL13D) = (-1.D0,0.D0)*(F0*SYlLL32,7)*SY2(LLL33,1)*SF
     1LL3)
      CSYM(JDDD,KLL13D+2) = (-1.D0,0.D0)*((D/DSQRT(2.DO))*SYlLL32,8)*S
     1Y2(LLL33,1)*SFLL3)
      CSYM(JDDD+1,KLL13D+2) = CSYM(JDDD,KLL13D+2)
118 CSYM(JDDD,KLL13I) = (1.D0,0.D0)*((F2 + (D2PR/2.DO))*SYlLL32,4)*SY
     12(LLL33,3)*SFLL3)
      CSYM(JDDD+1,KLL13I) = (1.D0,0.D0)*((F2 - (D2PR/2.DO))*SYlLL32,4)*
     1SY2(LLL33,3)*SFLL3)
      IF(I.GE.LDB) GO TO 49
      CSYM(JDDD+2,KLL13I-2) = (-1.D0,0.D0)*((D2/DSQRT(2.DO))*SYlLL32,8)
     1*SY2(LLL33,3)*SFLL3)
      CSYM(JDDD+2,KLL13I-1) = CSYM(JDDD+2,KLL13I-2)
      IF(I.GE.LDB) GO TO 49
      CSYM(JDDD+2,KLL13I) = (-1.D0,0.D0)*/F2*SYlLL32,7)*SY2(LLL33,3)*SF
     1LL3)
      CSYM(JDDD,KLL13I+2) = (-1.D0,0.D0)*((D2/DSQRT(2.DO))*SYlLL32,8)*S
     1Y2(LLL33,3)*SFLL3)
      CSYM(JDDD+1,KLL13I+2) = CSYM(JDDD,KLL13I+2)
 49 IF(((I.EQ.1).OR.(I.EQ.KT)) GO TO 56
      KD = 0
      IF(I.GT.LDB) KD = 1
      CSYM(J,7-KD) = (-1.D0,0.D0)*((F2 + D2PR)*SYlLL1,1)*SY2(LLL3,2)*SFLL
     11)
      CSYM(J,10-KD) = (1.D0,0.D0)*(D2*SYlLL2,3)*SY2(LLL3,2)*SFLL)
      CSYM(J,7-KD) = (-1.D0,0.D0)*(F2*SYlLL1,1)*SY2(LLL3,2)*SFLL)
      CSYM(J1,9-KD) = CSYM(J,10-KD)
      CSYM(J1,10-KD) = CSYM(J,10-KD)
      CSYM(J2,7-KD) = (-1.D0,0.D0)*((F2 - D2I  )*SYlLL1,1)*SY2(LLL3,2)*SFL
     1L)
      CSYM(J2,9-KD) = CSYM(J,10-KD)
      CSYM(J3,7-KD) = (1.D0,0.D0)*((F2 + (D2PR/2.DO))*SYlLL2,4)*SY2(LLL3,
     12)*SFLL)
      CSYM(J3,4-KD) = (1.D0,0.D0)*(D2*SYlLL2,5)*SY2(LLL3,2)*SFLL)
      CSYM(J3,5-KD) = CSYM(J3,4-KD)
      CSYM(J4,7-KD) = (1.D0,0.D0)*((F2 - (D2PR/2.DO))*SYlLL2,4)*SY2(LLL3,
     12)*SFLL)
      CSYM(J4,4-KD) = CSYM(J3,4-KD)
      CSYM(J4,5-KD) = CSYM(J3,4-KD)
      IF(I.GT.LDB) GO TO 119
      CSYM(J3,9) = (-1.D0,0.D0)*((D2/DSQRT(2.DO))*SYlLL2,6)*SY2(LLL3,2)*S
     1FLL)
      CSYM(J4,8) = CSYM(J3,9)
      CSYM(J5,7) = (-1.D0,0.D0)*(F2*SYlLL2,7)*SY2(LLL3,2)*SFLL)
      CSYM(J5,5) = (-1.D0,0.D0)*((D2/DSQRT(2.DO))*SYlLL2,8)*SY2(LLL3,2)*S
     1FLL)
      CSYM(J5,6) = CSYM(J5,5)
119 IF(I.GT.LDD) GO TO 56
      KD = 0
      IF(I.GE.LDB) KD = 1
      CSYM(JDDD,4-KD) = (1.D0,0.D0)*((F2 + (D2PR/2.DO))*SYlLL12,4)*SY2(
     1LL13,2)*SFLL1)
      CSYM(JDDD+1,4-KD) = (1.D0,0.D0)*((F2 - (D2PR/2.DO))*SYlLL12,4)*SY
     12(LLL13,2)*SFLL1)
      IF(I.GE.LDB) GO TO 56
      CSYM(JDDD,6) = (-1.D0,0.D0)*((D2/DSQRT(2.DO))*SYlLL12,6)*SY2(LLL1
     13,2)*SFLL1)
      CSYM(JDDD+1,5) = CSYM(JDDD,6)
      CSYM(JDDD+2,4) = (-1.D0,0.D0)*(F2*SYlLL12,7)*SY2(LLL13,2)*SFLL1)
      CSYM(JDDD+2,2) = (-1.D0,0.D0)*((D2/DSQRT(2.DO))*SYlLL12,8)*SY2(LL
     1LL13,2)*SFLL1)
      CSYM(JDDD+2,3) = CSYM(JDDD+2,2)
56 CSYM(J,4) = (1.D0,0.D0)*(D*SYlLL2,3)*SY2(LLL3,1)*SFLL)
      CSYM(J1,3) = CSYM(J,4)
      CSYM(J1,4) = CSYM(J,4)
      CSYM(J2,3) = CSYM(J,4)
      CSYM(J,1) = ((1.D0,0.D0)*((2.D0*B) - (SFLL*(F0 + DPR)*SYlLL1,1)*SY
     12(LLL3,1)))) + ((D.DO,-1.D0)*DROTK1)
      CSYM(J1,1) =((-1.D0,0.D0)*(SFLL*F0*SYlLL1,1)*SY2(LLL3,1))) + ((D.DO
     1,-1.DO)*DROTK1)
      CSYM(J2,1) = ((1.D0,0.D0)*(-(2.DO*B) - (SFLL*(F0 - DPR)*SYlLL1,1)*
     1SY2(LLL3,1)))) + ((D.DO,-1.DO)*DROTK1)
      CSYM(J3,1) = ((1.DO,0.DO)*1B + (SFLL*(F0 + (DPR/2.DO))*SYlLL2,4)*S
     1Y2(LLL3,1)))) + ((D.DO,-1.DO)*DROTK1)
      CSYM(J4,1) = ((1.D0,0.D0)*(-B + (SFLL*(F0 - (DPR/2.DO))*SYlLL2,4)*
     1SY2(LLL3,1)))) + ((D.DO,-1.DO)*DROTK1)
      CSYM(J3,3) = (-1.D0,0.D0)*((D/DSQRT(2.DO))*SYlLL2,6)*SY2(LL3,1)*SF
     1LL)
      CSYM(J4,2) = CSYM(J3,3)
      CSYM(J5,1) = ((-1.D0,0.D0)*ISFLL*F0*SYlLL2,7)*SY2(LL3,1))) + ((D.D
     1O,-1.D0)*DROTK1)
      J = J + 1
      J = J + 5
120 IF(I.GT.LO) GO TO 46
      CSYM(JDDD,1) = ((1.D0,0.D0)*(B + (SFLLL1*(F0 + (DPR/2.DO))*SYlLLL
     12,4)*SY2(LLL13,1)))) + ((D.DO,-1.DO)*DROTK2)
      CSYM(JDDD+1,1) = ((1.D0,0.D0)*(-B + (SFLLL1*(F0 - (DPR/2.DO))*SYLL
     1LL12,4)*SY2(LLL13,1)))) + ((D.DO,-1.DO)*DROTK2)
      IF(I.GE.LDB) GO TO 121
      CSYM(JDDD,3) = (-1.D0,0.D0)*((D/DSQRT(2.DO))*SYlLL12,6)*SY2(LLL13
     1,1)*SFLL1)
      CSYM(JDDD+1,2) = CSYM(JDDD,3)
      CSYM(JDDD+2,1) = ((-1.D0,0.D0)*(SFLL1*F0*SYlLL12,7)*SY2(LL13,1))
     11) + ((D.DO,-1.DO)*DROTK2)
      JCOUNT = JCOUNT + 1
121 JCOUNT = JCOUNT + 2
 48 CONTINUE
      J = J + JCOUNT
 34 AL = AL + 2.DO
      DO 60 I=1,N
      AMP(I) = (0.D0,0.D0)
 60 VALUE(I) = (0.D0,0.D0)
      AMP(1) = (1.D0,0.D0)
      AMP(2) = (1.D0,0.D0)
      AMP(3) = (1.D0,0.D0)

 SUBROUTINES  CSQZ  AND  CQRT  DIAGONALIZE A COMPLEX
 SYMMETRIC MATRIX. THESE SUBROUTINES WERE DEVELOPED BY
 GORDON AND MESSINGER,'ESR RELAXATION IN LIQUIDS',ED.
 L.T.MUUS AND P.W.ATKINS(PLENUM,NEW YORK,1972).

      CALL CSQZ(CSYM,AMP,NDIM,JDIM,N,M,SQTOL)
      CALL CQRT(CSYM1,CSYM2,AMP,NDIM,N,20,TOL,VALUE)
      IF(.NOT.PAMPEV) GO TO 821
      WRITE(7,822) GAMMA,FOAB,N,(CSYM1(I),AMP(I),I=1,N)
822 FORMAT(D20.13,5X,D20.13,5X,I3,/,(6D13.6))
821 IF(.NOT.WAMPEV) GO TO 823
      WRITE(6,824)(CSYM1(I),AMP(I),I=1,N)
824 FORMAT(1H ,///,10X,'EIGENVALUE',26X,'AMP',25X,'EIGENVALUE',26X,'AMP
     1',//,1X,2014.5,4X,2014.5,4X,2014.5,4X,2014.5)
823 ISET=ISET+1
      DO 10 ISET=1,NSET
      IF(ISET.GT.1) WRITE(6,825)
825 FORMAT(1H1,'INPUT VALUES ARE THE SAME AS FOR PRECEDING SET OF INPU
     1T VALUES ',/,' EXCEPT FOR THE FOLLOWING:',//)

      ********************************************************
      *   READ INPUT DATA - TWO READ STATEMENTS              *
      ********************************************************
 -NOTE THESE TWO INPUT CARDS ARE REPEATED UNTIL THEY ARE
  READ A TOTAL OF  NSET  TIMES.

      READ(5,87) IPLOT,XPUNCH,XPLOT,DISP,YLEN,XLEN
 87 FORMAT(I2,3X,L1,4X,L1,4X,L1,4X,E10.3,5X,E10.3)
      READ(5,88) T2IN,B1,BF,NB
 88 FORMAT(D10.3,5X,D10.3,5X,D10.3,5X,I3)
      WRITE(6,89) T2IN,B1,BF,NB
 89 FORMAT(1H ,//,' ROTATIONALLY INVARIANT P-P FIRST DERIVATIVE LINEWI
     1DTH ',D12.5,' GAUSS',//,' INITIAL FIELD SWEEP VALUE RELATIVE TO CE
     2NTER ',D12.5,' GAUSS',/,' FINAL FIELD VALUE RELATIVE TO CENTER ',
     3D12.5,' GAUSS',//,' NUMBER OF POINTS FOR SPECTRUM ',I3,/)
      T2IN = T2IN*(DSQRT(3.D0)/2.D0)*(GAMMA/FOAB)
      B1 = B1*(GAMMA/FOAB)
      BF = BF*(GAMMA/FOAB)
      DEL = (BF - B1)/(DFLOAT(NB-1)
      XAB = (0.D0,-1.D0)
      IF(DISP) XAB = (1.D0,0.D0)
      IF(IPLOT.GT.0) GO TO 241

 CALCULATION OF THE ABSORPTION-DISPERSION VALUES. NOTE
 THE ABSORPTION-DISPERSION VALUES ARE STORED IN  C  MATRIX
 AND THE CORRESPONDING FIELD VALUES ARE IN  BFLD  MATRIX.

      RES = B1
      DO 235 I=1,NB
      ABSP = (0.D0,0.D0)
      DO 223 I=1,N
223 ABSP = ABSP + (AMP(I)*AMP(I))/(CSYM1(I) + ((-1.D0,0.D0)*RES) + ((
     10.D0,-1.D0)*T2IN))
      C(I) = XAB*(ABSP/(3.D0*3.14159D0))
      BFLD(I) = RES*(FOAB/GAMMA)
      RES = RES + DEL
235 CONTINUE
      IF(DISP) WRITE(6,906)
906 FORMAT(1H ,' DISPERSION PLOT',//)
      WRITE(6,242)(C(I),BFLD(I),I=1,NB)
242 FORMAT(1H ,///,47X,'COORDINATES FOR ABSORPTION PLOT',///,4X,'ABSORP
     1TION',6X,'FIELD',11X,'ABSORPTION',6X,'FIELD',11X,'ABSORPTION',6X,'
     2FIELD',11X,'ABSORPTION',6X,'FIELD',//,(1X,2E14.5,4X,2E14.5,4X,2E14.
     45,4X,2E14.5))
      IF(.NOT.XPUNCH) GO TO 243

 PUNCH OUTPUT - COORDINATES OF ABSORPTION-DISPERSION
                SPECTRUM PUNCHED ON CARDS

      WRITE(7,244)(C(I),BFLD(I),I=1,NB)
244 FORMAT(E13.6,2X,E13.6,7X,E13.6,2X,E13.6)
243 IF(.NOT.XPLOT) GO TO 241

 LINE PLOT FOR ABSORPTION-DISPERSION SPECTRUM (CORNELL
 U. PLOT SUBROUTINES)

      APMAX = MAXIMUM ABSORPTION-DISPERSION VALUE
      ABMIN = MINIMUM ABSORPTION-DISPERSION VALUE

 SUBROUTINES FOR PLOTTING-
      AXIS = DRAWS AND LABELS AXIS
      PLOT = MOVES PEN TO A SPECIFIED POINT (COORDINATES IN
             INCHES).
      PLTEND = SPECIFIES END OF ALL PLOTTING

      ABMAX = C(1)
      DO 245 I=1,NB
      IF(ABMAX.LT.C(I)) ABMAX = C(I)
245 CONTINUE
      ABMIN = C(1)
      DO 246 I=1,NB
      IF(ABMIN.GT.C(I)) ABMIN = C(I)
246 CONTINUE
      YLEN = (BFLD(NB) - BFLD(1))/XLEN
      CALL AXIS(0.0,1.0,5HGAUSS,-5,XLEN,0.0,BFLD(1),DXY)
      Y = 1.0 + (YLEN*((C(1) - ABMIN)/(ABMAX - ABMIN)))
      X = 0.0
      CALL PLOT(X,Y,3)
      DO 247 I=1,NB
      Y = 1.0 + (YLEN*((C(I) - ABMIN)/(ABMAX - ABMIN)))
      X = XLEN*((BFLD(I) - BFLD(1))/(BFLD(NB) - BFLD(1)))
247 CALL PLOT(X,Y,2)
      XPLEND = .TRUE.
      Y = 0.0
      X = X + 3.
      CALL PLOT(X,Y,-3)
241 IF(IPLOT.LT.0) GO TO 10

 CALCULATION OF FIRST DERIVATIVE VALUES.
      THE FIRST DERIVATIVE VALUES ARE STORED IN THE  DERAB
      MATRIX AND THE CORRESPONDING MAGNETIC FIELD VALUES ARE
      IN THE MATRIX  BFLD.

      RES = B1
      DO 260 I=1,NB
      ABSP = (0.D0,0.D0)
      DO 261 I=1,N
261 ABSP = ABSP + ((AMP(I)*AMP(I))/(1(CSYM1(I) + ((-1.D0,0.D0)*RES) + (
     1(0.D0,-1.D0)*T2IN)))**2))
      DERAB(I) = XAB*ABSP
      BFLD(I) = RES*(FOAB/GAMMA)
260 RES = RES + DEL
      IF(DISP) WRITE(6,906)
      WRITE(6,248)(DERAB(I),BFLD(I),I=1,NB)
248 FORMAT(1H ,///,43X,'COORDINATES FOR FIRST DERIVATIVE SPECTRUM',//,
     14X,'1ST DERIV',7X,'FIELD',11X,'1ST DERIV',7X,'FIELD',11X,'1ST DERI
     2V',7X,'FIELD',11X,'1ST DERIV',7X,'FIELD',//,(1X,2E14.5,4X,2E14.5,4
     3X,2E14.5,4X,2E14.5))
      IF(.NOT.XPUNCH) GO TO 249

 PUNCH OUTPUT - COORDINATES OF FIRST DERIVATIVE PUNCHED
                ON CARDS

      WRITE(7,250)(DERAB(I),BFLD(I),I=1,NB)
250 FORMAT(E13.6,2X,E13.6,7X,E13.6,2X,E13.6)
249 IF(.NOT.XPLOT) GO TO 10

 LINE PLOT FOR A FIRST DERIVATIVE SPECTRUM.
      SAME AS FOR ABSORPTION-DISPERSION PLOTS EXCEPT  DMAX,
      DMIN  REFER TO MAXIMUM AND MINIMUM VALUES,
      RESPECTIVELY, OF FIRST DERIVATIVE SPECTRUM.

      DMAX = DERAB(1)
      DO 251 I=1,NB
      IF(DERAB(I).LT.DERAB(I)) DMAX = DERAB(I)
251 CONTINUE
      DMIN = DERAB(1)
      DO 252 I=1,NB
      IF(DMIN.GT.DERAB(I)) DMIN = DERAB(I)
252 CONTINUE
      DXY = (BFLD(NB) - BFLD(1))/XLEN
      CALL AXIS(0.0,1.0,5HGAUSS,-5,XLEN,0.0,BFLD(1),DXY)
      Y = 1.0 + (YLEN*((DERAB(1) - DMIN)/(DMAX - DMIN)))
      X = 0.0
      CALL PLOT(X,Y,3)
      DO 253 I=1,NB
      Y = 1.0 + (YLEN*((DERAB(I) - DMIN)/(DMAX - DMIN)))
      X = XLEN*((BFLD(I) - BFLD(1))/(BFLD(NB) - BFLD(1)))
253 CALL PLOT(X,Y,2)
      XPLEND = .TRUE.
      Y = 0.0
      X = X + 3.
      CALL PLOT(X,Y,-3)
 10 CONTINUE
      GO TO 813
  2 WRITE(6,812) LMAX4,NSY,LMAX5,NSY2
812 FORMAT(1H1,' JOB IS TERMINATED BECAUSE DIMENSIONS OF  SY  OR  SY2
     1  ARE LESS THAN REQUIRED BY LMAX+/,/,' VALUE OF DIMENSION  N  FOR
     2MATRIX  SY(N,M)  SHOULD BE ',I3,/,' VALUE SPECIFIED IS',2X,I3,//,'
     3 VALUE OF DIMENSION  N  FOR MATRIX  SY2(M,3)  SHOULD BE  ',I3,/,'
     4 VALUE SPECIFIED IS  ',I3)
      GO TO 813
814 WRITE(6,815) N,NDIM,M,JDIM
815 FORMAT(1H1,' JOB TERMINATED BECAUSE BANDWIDTH OR ORDER OF MATRIX
     1 CSYM  IS GREATER THAN SPECIFIED',//,' VALUE FOR THE ORDER  N  FOR
     2 THE MATRIX  CSYM(N,M)  SHOULD BE ',I3,/,' VALUE SPECIFIED IS ',I3
     3,//,' VALUE FOR THE DIMENSION(BANDWIDTH)  M  OF MATRIX  CSYM(N,M)
     4 SHOULD BE ',I3,/,' VALUE SPECIFIED IS ',I3)
813 IF(XPLEND) CALL PLTEND
      STOP
      END
```

```
C            GORDON AND MESSENGER SUBROUTINES
C
      SUBROUTINE CSQZE(A,AMP,IDIM,JDIM,N,M,SQTOL)
      IMPLICIT REAL*8(A-H,O-Z)
C
C  SUBROUTINE  CSQZE  TRANSFORMS, BY A SERIES OF COMPLEX
C  JACOBI ROTATIONS, AN  N BY N  COMPLEX BAND MATRIX,  A, OF
C  BAND WIDTH  2M-1  INTO A COMPLEX SYMMETRIC TRIDIAGONAL
C  MATRIX.  T = TRANSPOSE(R)*A*R
C
C  ENTERING THE SUBROUTINE,  A(I,1)  CONTAINS THE  ITH
C  DIAGONAL ELEMENT AND  A(I,J+1)  CONTAINS THE  JTH
C  ELEMENT FROM THE DIAGONAL IN THE  ITH  ROW.  N  IS THE
C  LENGTH OF THE COLUMNS OF  A, AND  M  IS THE HALF BAND
C  WIDTH PLUS ONE.
C
C  LEAVING THE SUBROUTINE  A(I,1)  CONTAINS THE DIAGONAL
C  ELEMENTS AND  A(I,2)  CONTAINS THE NEW OFF-DIAGONAL
C  ELEMENTS CORDERED AS BEFORE.
C  ON ENTERING THE VECTOR TO BE ROTATED IS IN  AMP.  AT EXIT
C  AMP  CONTAINS THE ROTATED VECTOR.
C
      COMPLEX*16 A(IDIM,JDIM),AMP(IDIM),
     1 B, G, S, SA, C*G,CS,U,V,TEMP
      DIMENSION RG(2)
      EQUIVALENCE (G,RG(1))
      SQTOL = 0.D0
      GRASS = 0.D0
      DO 101 L=M+1,N
      GRASS = GRASS + 1.D0
  101 SQTOL = SQTOL+CDABS(A(L,M+1-L))**2+SQTOL
      SQTOL = 1.D-15*SQTOL/DSQRT(GRASS)
      NA = N - 2
C  EACH PASS THROUGH THIS LOOP WILL DESTROY A SET OF OFF-
C  DIAGONAL ELEMENTS  A(I,NQ)
      DO 20 K=1,NA
      NR=M-1
      NL=NR+1
      NQ=N-NR
C  THIS STATEMENT SAVE COMPUTATION WHEN THE BAND IS LARGER
C  THAN THE MATRIX
      IF(NR) 20,20,5
C  EACH PASS THROUGH THIS DE.TROYS ONE OFF-DIAGONAL ELEMENT
C  A(K,NQ)
    5 DO 15 I=1,NA
C  THE FIRST PASS THROUGH THIS LOOP DESTROYS AN OFF-DIAGONAL
C  ELEMENT  A(K,NQ)  AND CREATES ANOTHER ELEMENT  G  BY THE
C  JACOBI ROTATION OF COLUMN AND ROWS  I  AND  I+1.
C  SUBSEQUENT PASSES DESTROY THE ELEMENT  G  AND CREATE
C  ANOTHER UNTIL THE LAST PASS WHICH DESTROYS WITHOUT
C  CREATING.
      DO 25 J=1,NR,NR
      IF(J-NA) 4C,30,40
   9C IF(CDABS(A(I,NQ)) - SQTOL) 15,15,4C
   40 B = -A(I,NR)/A(I,NQ)
      GC TO 60
   40 IF(DABS(1.D+2*RG(2)**2-SQTOL**2) 15,15,70
   70 B= -A(I,J-1)/G
C  THESE FIVE STATEMENTS COMPUTE THE CORRECT SINE S AND
C  COSINE  C.
   80 SA = 1.D0/(1.D0 + B**2)
      S = CDSQRT(SA)
      C=B*S
      CA = C**2
      CS = C*S
      I= J+NR - 1
C  THESE THREE STATEMENTS ROTATE  AMP
      TEMP = AMP(I)
      AMP(I) = C*TEMP - S*AMP(I+1)
      AMP(I+1) = C*AMP(I+1) + S*TEMP
C  THESE FIVE STATEMENTS ROTATE THE CROSS ELEMENTS
      U = A(I,1)
      V=A(I+1,1)
      A(I,1) = CA*U-2.D0*CS*A(I,2)+SA*V
      A(I+1,1) = SA*U + 2.D0*CS*A(I,2) + CA*V
      A(I,2) = CS*(U-V) + (CA-SA)*A(I,2)
   45 I2 = I - 1
C  THIS LOOP TRANSFORMS THE APPROPRIATE COLUMNS
      DO 90 I2=1,I2
      IN = I-I2+1
      U = A(IN,I2)
      V = A(IN,I2+1)
      A(IN,I2) = C*U - S*V
   90 A(IN,I2+1) = S*U + C*V
   79 IF(J-NA) 95,85,95
   95 A(J-1,NQ) = C*A(J-1,NQ) - S*G
   85 IR = MIN0(NR,N-I)
      IF(IR-2)55,45,45
C  THIS LOOP TRANSFORMS THE APPROPRIATE ROWS
   45 DO 10 I2=2,IR
      U = A(I,I2+1)
      A(I,I2+1) = C*U-S*A(I+1,I2)
   10 A(I+1,I2)=S*U+C*A(I+1,I2)
   55 IF(I+NR-N) 30,25,25
   30 G = -S*A(I+1,NQ)
      A(I+1,NQ) = C*A(I+1,NQ)
   25 CONTINUE
C  END OF THE LOOP OVER  J, ONE OFF-DIAGONAL ELEMENT
C  DESTROYED
   15 CCNTINUE
C  END OF THE LOOP OVER  K, ONE SET OF OFF-DIAGONAL
C  ELEMENTS DESTROYED.
   20 CONTINUE
C  END OF THE LOOP OVER L, NA SETS OF OFF-DIAGONAL
C  ELEMENTS DESTROYED
      RETURN
      END
      SUBROUTINE CURTCA(A,B,AMP,IDIM,N,M,TOL,EIGVAL)
      IMPLICIT REAL*8(A-H,O-Z)
CCURT
C
C  CURT IS INTENDED TO PRODUCE THE EIGENVALUE OF A COMPLEX
C  SYMMETRIC (NOT HERMITIAN) TRIDIAGONAL MATRIX BY ITERATIVE
C  QR  TRANSFORMS AS DESCRIBED IN WILKINSON 'THE ALGEBRAIC
C  EIGENVALUE PROBLEM' , P.565.
C
C  ENTERING THE SUBROUTINE THE ARRAY  A  OF DIMENSION  N
C  CONTAINS THE DIAGONAL ELEMENTS, B  THE OFF-DIAGONAL
C  ELEMENTS. THE VECTOR TO BE ROTATED IS  AMP. N  IS THE
C  DIMENSION OF THE MATRIX AND THE LENGTH OF  AMP.
C  ITERATION ARE CONTINUED UNTIL ALL OFF-DIAGONAL ELEMENTS
C  HAVE BEEN REDUCED TO LESS THAN  *TOL*  IN MAGNITUDE.
C  M  IS THE MAXIMUM NUMBER OF ITERATIONS ALLOWED PER
C  EIGENVALUE. M*2D  HAS ALWAYS BEEN MORE THAN SUFFICIENT.
C  THE NUMBER OF ITERATIONS REQUIRED MAY BE REDUCED IF
C  ACCURATE ESTIMATES OF THE EIGENVALUES ARE ALREADY KNOWN.
C  THESE INITIAL GUESSES SHOULD BE PLACED IN THE ARRAY
C  'EIGVAL' , IF NO GUESSES ARE FURNISHED, EIGVAL(1)
C  SHOULD BE SET EQUAL TO A COMPLEX ZERO, (0.D0,0.D0), IN
C  THE CALLING PROGRAM. CURT  WILL GENERATE ITS OWN GUESSES.
C
C  THE MATRICES  A,B,AMP,  ARE TREATED AS REAL ARRAYS OF
C  DIMENSION  N*2  INSIDE THE SUBROUTINE, OUTSIDE THEY
C  ARE TREATED AS COMPLEX ARRAYS OF DIMENSION  N.
      INTEGER HELL
      DIMENSION A(1),B(1),AMP(1),SM(2),EIGVAL(1)
      COMPLEX*16 SC
C  THE EQUIVALENCING OF THE ARRAY  SM  TO THE COMPLEX NUMBER
C  SC  PERMITS THE USE OF THE COMPLEX SQUARE ROOT ROUTINE
C  CSQRT.
      EQUIVALENCE (SC,SM(1))
C  NX  WILL BE THE UPPER LIMIT FOR THE ITERATION, NI  WILL
C  BE  LOWER LIMIT AND BOTH MAY VARY BETWEEN ITERATIONS
      NX = 2*N
      NI=2
C  THE TOLERANCE--THAT IS, THE SIZE TO WHICH OFF-DIAGONAL
C  ELEMENTS ARE REDUCED--IS SET IN  CURT  ON THE BASIS OF
C  THE  NORM OF THE TRIDIAGONAL MATRIX.
      TOL = 0.D0
      GRASS = DFLOAT(N)
      DO 200 K1D=1,NX,2
  200 TOL = DSQRT(A(K1D)**2+A(K1D+1)**2)+TOL+ 2.D0*DSQRT(ABS
     C  (B(K1D)**2 + B(K
     1)D+1)**2)
      TOL = 1.D-15*TOL/DSQRT(3.D0*GRASS)
C  SHR  AND SHI  CONTAIN THE TOTAL SHIFT
      SHR = 0.D0
      SHI = 0.D0
C  K  WILL COUNT THE NUMBER OF ITERATIONS PER EIGENVALUE
      K = 0
C  IF A SET OF 'EIGVALS' IS AVAILABLE FOR USE AS INITIAL
C  SHIFTS --I.E. IF THE FIRST 'EIGVAL' IS NOT (0.DC,0.DC)--
C  THEN WE USE THE GUESSES IN 'EIGVAL' AS SHIFTS BY SETTING
C  'HELL'  EQUAL TO  101.
      ASSIGN 1CC TO HELL
      IF(DABS(EIGVAL(1))+DABS(EIGVAL(2)).NE.0.D0)ASSIGN 101
     C  TO HELL
      GO TO HELL,(100,101)
C  EACH NEW ITERATION BEGINS AT THIS STATEMENT OR AT
C  STATEMENT 101 --WHICHEVER  'HELL' IS.
  100 K=K+1
C  THESE SEVEN STATEMENTS SOLVE THE TWO BY TWO MATRIX IN
C  THE LOWER LEFT CORNER AND USE ONE ROOT AS THE SHIFT
      AT1=A(NX-1) + A(NX-3)
      AT1=A(NX) + A(NX-2)
      SM(1)=AT*A**2-AT1**2 +4.D0*(A(NX-1)*A(NA-3)-A(NX)*A(NX-
     C  2))-
     1  B(NX-3)**2*B(NX-2)**2)
      SM(2)=2.D0*AT*AT1-4.D0*(A(NX-1)*A(NX-2)+A(NX)*A(NX-3)
     C  -
     1   2.D0*B(NX-3)*B(NX-2))
      SL = CDSQRT(SC)
      STR=(AT*-SM(1))*0.5D0
      STI=(AT1-SM(2))*0.5D0
      STTR=(AT*+SM(1))*0.5D0
      STTI=(AT1+SM(2))*.5D0
      TEMP = CDABS(DCMPLX(A(NX-1)-STR,A(NX)-STI))
      TEMPO = CDABS(DCMPLX(A(NX-1)-STTR,A(NX)-STTI))
      IF(TEMPO.GT.TEMP) GO TO 102
      STR = STTR
      STI = STTI
      GO TO 102
  101 A=A+1
      IF(K .GE. M) GO TO 999
      STR = EIGVAL(A-1) - SHR
      STI=EIGVAL(A) - SHI
102 IF(A.LE.M) GO TO 104
999 WRITE(6,1C3) M
103 FORMAT(20H CURT HAS NOT CONVERGED IN,I3,11H ITERATIONS
     C  )
      CALL EXIT
C  THESE TWO STATEMENTS INCREASE THE SHIFT BY THE
C  TEMPORARY SHIFT
  104 SHR = SHR + STR
      SHI = SHI+STI
C  THIS LOOP SUBTRACTS THE TEMPORARY SHIFT FROM THE DIAGONAL
C  ELEMENTS.
      DC 20 I=2,NX,2
      A(I-1) = A(I-1)-STR
   20 A(I) = A(I) -STI
C  THESE FOUR STATEMENTS SUPPLY INITIAL VALUES FOR THE
```



```
C  ITERATION.
      CR=1.000
      CI=0.000
      CSR =0.CO
      CSI=0.CO
      UR =C.COO
      UI=0.00U
C  THIS LOOP COMPLETES ONE ITERATION, THAT IS, ONE  QR
C  TRANSFORM. I  IS DOUBLE THE  I  IN THE OTHER CURT  DO IN
C  CURTA
      DO 10 I=NI,NX,2
C  G  IS THE GAMMA IN WILKINSON.
      GR = A(I-1)-UR
      GI = A(I) - UI
C  Q  IS THE  P  IN WILKINSON.
      QR=CR*A(I-1)-CI*A(I)-CSR*B(I-3)+CSI*B(I-2)
      QI=CI*A(I-1)+CR*A(I)-CSI*B(I-3)-CSR*B(I-2)
C  THIS BRANCH AVOIDS UNNECESSARY COMPUTATION AT THE END
   10 IF(I.EQ.NX) GO TO 10
      SM(1) = QR**2-QI**2+B(I-1)**2-B(I)**2
      SM(2) =2.D0*(QR*QI+B(I-1)*B(I))
      SC= CDSQRT(SC)
      RR = SM(1)
      RI=SM(2)
      IF(I.EQ.NI) GO TO 18
C  THESE TWO STATEMENTS ROTATE AN OFF-DIAGONAL ELEMENT
      B(I-3) = SR*BP-SI*BI
      B(I-2) = SR*BI+SI*BR
   18 RS =1.DO/(RR**2+RI**2)
C  THESE TWO STATEMENTS COMPUTE THE NEW SINE FOR THE
C  JACOBI ROTATION.
      SR =(RR*B(I-1)+RI*A(I))*RS
      SI=(RR*B(I)-B(I-1)*RI)*RS
C  THESE TWO STORE THE PRODUCT OF THE NEW SINE AND THE OLD
C  COSINE.
      CSR = CR*SR-CI*SI
      CSI = CR*SI+CI*SR
C  THESE TWO COMPUTE THE NEW COSINE.
      CR=(RR*QR+RI*QI)*RS
      CI=(RR*QI-RI*QR)*RS
C  THESE SIX COMPUTE A NEW  U.
      TR = GR * A(I+1)
      TI=GI*A(I+2)
      SKR = SR**2-SI**2
      SAI = 2.D0*SR*SI
      UR = SKR*TR-SAI*TI
      UI=SAR*TI+SAI*TR
C  THESE TWO ROTATE THE DIAGONAL ELEMENT.
      A(I-1) = GR + UR
      A(I) = GI + UI
C  THESE NINE ROTATE  AMP.
      TAR = AMP(I-1)
      TAI = AMP(I)
      TBR = AMP(I+1)
      TBI = AMP(I+2)
      AMP(I-1)=TAR*CR-TAI*CI+TBR*SR -TBI*SI
      AMP(I) = TAI*CR+TAR*CI+TBI*SR+TBR*SI
      AMP(I+1) = TBR*CR-TBI*CI-TAR*SR+TAI*SI
      AMP(I+2)=TBI*CR+TBR*CI-TAI*SR-TAR*SI
   10 CONTINUE
C  THIS ENDS ONE ITERATION.
C  THESE TWO COMPUTE THE LAST OFF-DIAGONAL ELEMENT.
      B(NX-3) = SR*QP -SI*QI
      B(NX-2) = SR*QI+SI*QR
C  THESE TWO COMPUTE THE LAST DIAGONAL ELEMENT
      A(NX-1) = GR
      A(NX) = GI
C  AT THIS POINT WE BEGIN CHECKING UPWARD THROUGH THE OFF-
C  DIAGONAL ELEMENTS TO FIND THOSE LESS THAN  TOL.
   65 IT=NX
C  THESE THREE STATMENTS CONSTITUTE AN EFFECTIVE BACKWARD
C  LOOP
   30 ITC= IT-2
C  THIS LOOP IS LEFT WHEN AN ELEMENT LESS THAN  TOL  IS
C  FOUND.
      IF(DABS(B(IT-1)) + DABS(B(IT)).LE.TOL) GO TO 40
      IF(IT-NI) 100,100,30
C  IF NO OFF-DIAGONAL ELEMENT LESS THAN  TOL  ARE FOUND, WE
C  PERFORM ANOTHER ITERATION.
C  THIS CONDITIONAL BRANCHES ACCORDING TO WHETHER THE
C  MATRIX ISOLATED BY THE SMALL OFF-DIAGONAL ELEMENT IS OF
C  DIMENSION  ONE, TWO, OR GREATER THAN TWO
   40 IF(NX-IT-4) 50,60,70
C  THESE TWO STATEMENTS EXTRACT THE EIGENVALUE OF A ONE BY
C  ONE MATRIX, ADDING BACK THE SHIFT.
   50 A(NX-1) = A(NX-1) + SHR
      A(NX) = A(NX) + SHI
C  THIS DECREASES THE SIZE OF THE PORTION OF THE MATRIX
C  AFFECTED BY LATER ITERATIONS.
      NX = NX - 2
C  THIS RESETS THE ITERATION COUNTER.
      K = 0
      GC TO 80
C  THIS SECTION EXTRACTS THE EIGENVALUE FROM A TWO BY TWO
C  MATRIX SECTION WHICH HAS BECOME ISOLATED FROM THE REST.
C  IT ALSO PERFORMS THE COMPENSATING ROTATIONS ON  AMP.
C  THE FIRST TWENTY-NINE STATEMENTS COMPUTE THE PROPER
C  VALUES FOR THE SINE AND COSINE.
   60 ALR=-B(NX-3)
      ALI=-B(NX-2)
      AMR= C.5DO*(A(NX-3) - A(NX-1))
      AMI = 0.5DO*(A(NX-2) - A(NX))
      SM(1) = ALR**2-ALI**2+AMR**2-AMI**2
      SM(2) =2.DO*(ALR*ALI+AMR*AMI)
      SC = CDSQRT(SC)
      AMR=SM(1)
      AMI= SM(2)
      TAR = AMR + ANR
      TAI = AMI+ANI
      TBR=ANR-AMR
      TBI=ANI-AMI
      SIG = 1.UDU
C  THIS BRANCH CHOOSES THE ROOT OF THE EMPLETELY SOLVED
C  QUADRATIC SO THE COSINE HAS THE LARGER ABSOLUTE VALUE.
      IF(TAR**2+TAI**2.GT.TBR**2+TBI**2) GO TO 65
      TAR = TBR
      TAI = TBI
      SIG = -1.UDU
C  THESE SIX COMPUTE THE COSINE.
   65 TCR = U.5DO/(ANR**2+ANI**2)
      SM(1) = (ANR*TAR+ANI*TAI)*TCR
      SM(2) = (ANR*TAI-ANI*TAR)*TCR
      SC = CDSQRT(SC)
      CR=SM(1)
      CI = SM(2)
C  THESE FIVE COMPUTE THE SINE.
      TAR = ANR*CR-ANI*CI
      TAI=ANR*CI+ANI*CR
      TBR=0.5DO/(TAR**2+TAI**2)
      SNR=SIG*(TAR*AL R+TAI*ALI)*TBR
      SI= SIG*(TAR*ALI-ALR*TAI)*TBR
C  THESE SIXTEEN STORE DATA NEEDED IN THE ROTATION OF THE
C  MATRIX ELEMENTS.
      TAR = A(NX-3)
      TAI= A(NX-2)
      TCR=A(NX-1)
      TBI=A(NX)
      TCR=B(NX-3)
      TCI=B(NX-2)
      CAR=CR**2-CI**2
      CAI = 2.DO*CR*CI
      SAR=SR**2-SI**2
      SAI = 2.DO*SR*SI
      CSR=CR*SR-CI*SI
      CSI=CR*SI+CI*SR
      TR=CSR-SAI
      TI= CXI-SAI
      UR = 2.DO*(TCR*CSR - TCI*CSI)
      UI = 2.DO*(TCI*CSR + TCR*CSI)
C  THESE FOUR ROTATE THE DIAGONAL ELEMENTS
      A(NX-3) =TAR*CAR-TAI*CAI+TBR*SAR-TBI*SAI-UR+SNR
      A(NX-2)=TAR*CAI+TAI*CAR+TBR*SAI+TBI*SAR-UI+SNI
      A(NX-1)=TAR*SAR-TAI*SAI+TBR*CAR-TBI*CAI+UR+SNR
      A(NX) =TAR*SAI+TAI*SAR+TBR*CAI+TBI*CAR+UI+SNI
C  THESE TWO ROTATE THE OFF-DIAGONAL ELEMENTS
      B(NX-3) = 2.DO*(ANR*CSR-ANI*CSI)+TCR*TR-TCI*TI
      B(NX-2) = 2.DO*(ANR*CSI+ANI*CSR) + TCR*TI+TCI*TR
      I=NX-2
C  THESE NINE ROTATE  AMP.
C  NOTICE THAT THE SENSE OF ROTATION IS OPPOSITE TO THAT
C  OF THE FIRST ROTATION.
      TAR=AMP(I-1)
      TAI=AMP(I)
      TBR=AMP(I+1)
      TBI=AMP(I+2)
      AMP(I-1) = TAR*CR-TAI*CI-TBR*SR+TBI*SI
      AMP(I) =TAI*CR+TAR*CI-TBI*SR-TBR*SI
      AMP(I+1)=TBR*CR-TBI*CI+TAR*SR-TAI*SI
      AMP(I+2)=TBI*CR+TBR*CI+TAI*SR+TAR*SI
C  THIS RESETS THE ITERATION COUNT.
      A=0
C  THIS DECREASES THE SIZE OF THE PORTION OF THE MATRIX
C  AFFECTED BY THE LATER ITERATIONS.
      NX=NX-4
      GO TC 80
C  THIS STATEMENT IS REACHED WHEN THE PORTION OF THE MATRIX
C  ISOLATED IS GREATER THAN TWO BY TWO. IT CHANGES THE
C  LOWER LIMIT OF THE ITERATION SO THAT ONLY THIS PORTION
C  WILL BE  AFFECTED BY SUBSEQUENT ROTATIONS UNTIL ALL ITS
C  EIGENVALUES ARE FOUND.
   70 NI=IT+2
C  THIS STATEMENT TRANSFERS TO THE BEGINNING OF ANOTHER
C  ITERATION.
      GC TO HELL,(100,101)
C  THIS STATEMENT IS REACHED AFTER EITHER ONE OR TWO
C  EIGENVALUES HAVE JUST BEEN FOUND. IT TRANSFERS IF ALL
C  THE EIGENVALUES IN THIS PORTION OF THE MATRIX HAVE BEEN
C  FOUND.
   80 IF(NA.LT.NI) GO TO 90
C  THIS BRANCH TRANSFERS ACCORDING TO WHETHER ONE, TWO, OR
C  MORE EIGENVALUES REMAIN TO BE FOUND IN THIS PORTION.
   85 IF(NA-NI-2) 50,60,85
C  THIS CONDITIONAL IS REACHED WHEN ALL THE EIGENVALUES IN
C  THIS PORTION OF THE MATRIX HAVE BEEN FOUND. IT RETURNS IF
C  THIS IS THE LAST PORTION OF THE MATRIX
   90 IF(NI-2) RETURN
C  THIS ENLARGES THE PORTION OF THE MATRIX BEING TREATED TO
C  INCLUDE THE BEGINNING OF THE MATRIX.
      NI=2
      GO TC 65
      END
```

Acknowledgments

Support of this work by grants from the National Science Foundation, the Petroleum Research Fund (Grant No. 6818-AC6) administered by the American Chemical Society, and the Cornell University Materials Science center are gratefully acknowledged. The efforts of the past and present members of the Cornell Chemistry Department ESR group have been the basis for this chapter and their critical comments are greatly appreciated. Special thanks are due Dr. G. V. Bruno for developing the computer program given here and Dr. C. F. Polnaszek for his considerable help with it. This chapter was completed while the author was a guest professor at the Department of Physical Chemistry of Aarhus University (Spring semester, 1974), and he greatly appreciates the facilities made available to him.

References

Abragam, A. (1961). "The Principles of Nuclear Magnetism," pp. 49–51, Oxford Univ. Press, London and New York.

Bordeaux, O. *et al.* (1973). *J. Org. Mag. Res.* **5**, 47.

Bruno, G. V. (1973). Application of the Stochastic Liouville Method in Calculating ESR Line Shapes in the Slow Tumbling Region and An ESR-ELDOR Study of Exchange, Ph.D. Thesis, Cornell Univ.

Bruno, G. V., and Freed, J. H. (1974a). ESR lineshapes and saturation in the slow motional region: ELDOR, *Chem. Phys. Lett.* **25**, 328–332.

Bruno, G. V., and Freed, J. H. (1974b). Analysis of inertial effects on ESR spectra in the slow tumbling region, *J. Phys. Chem.* **78**, 935–940.

Birrell, G. B., Van, S. P., and Griffith, O. H. (1973). Electron spin resonance of spin labels in organic inclusion crystals. Models for anisotropic motion in biological membranes, *J. Amer. Chem. Soc.* **95**, 2451–2464.

Cukier, R. I., and Lakatos-Lindenberg, K. (1972). Rotational relaxation of molecules in fluids for reorientations of arbitrary angle, *J. Chem. Phys.* **57**, 3427–3435.

Dalton, L. (1973). Private communication.

Eastman, M. P., Kooser, R. G., Das, M. R., and Freed, J. H. (1969). Studies of Heisenberg spin exchange in ESR spectra, I. Linewidth and saturation effects, *J. Chem. Phys.* **51**, 2690–2709.

Eastman, M. P., Bruno, G. V., and Freed, J. H. (1970). Studies of Heisenberg spin exchange in ESR spectra II. Effects of radical charge and size, *J. Chem. Phys.* **52**, 2511–2522.

Edmonds, A. R. (1957). "Angular Momentum in Quantum Mechanics." Princeton Univ. Press, Princeton, New Jersey.

Egelstaff, P. A. (1970). Cooperative rotation of spherical molecules, *J. Chem. Phys.* **53**, 2590–2598.

Favro, L. D. (1965). Rotational Brownian motion, *In* "Fluctuation Phenomena in Solids" (R. E. Burgess, ed.), pp. 79–101. Academic Press, New York.

Freed, J. H. (1964). Anisotropic rotational diffusion and electron spin resonance linewidths, *J. Chem. Phys.* **41**, 2077–2083.

Freed, J. H. (1967). Theory of saturation and double resonance effects in electron spin resonance spectra. II. Exchange vs. dipolar mechanisms, *J. Phys. Chem.* **71**, 38–51.

Freed, J. H. (1972a). Ch. VIII, ESR relaxation and lineshapes from the generalized cumulant and relaxation matrix viewpoint, and Ch. XIV, ESR lineshapes and saturation in the slow motional region. The stochastic Liouville approach, *In* "Electron Spin Relaxation in Liquids" (L. T. Muus and P. W. Atkins, eds.), pp. 165–191, 387–409. Plenum, New York.

Freed, J. H. (1972b). Electron spin resonance, *Ann. Rev. Phys. Chem.* **23**, 265–310.

Freed, J. H. (1974). Theory of saturation and double resonance in ESR spectra VI: Saturation recovery, *J. Phys. Chem.* **78**, 1155–1167.

Freed, J. H., and Fraenkel, G. K. (1963). Theory of linewidths in electron spin resonance spectra, *J. Chem. Phys.* **39**, 326–348.

Freed, J. H., Bruno, G. V., and Polnaszek, C. F. (1971). Electron spin resonance lineshapes and saturation in the slow motional region, *J. Phys. Chem.* **75**, 3385–3399.

Glarum, S. H., and Marshall, J. H. (1966). ESR of the perinaphthenyl radical in a liquid crystal, *J. Chem. Phys.* **44**, 2884–2890.

Glarum, S. H., and Marshall, J. H. (1967). Paramagnetic relaxation in liquid-crystal solvents, *J. Chem. Phys.* **46**, 55–62.

Goldman, S. A. (1973). An ESR Study of Rotational Reorientation and Spin Relaxation in Liquid and Frozen Media, Ph.D. Thesis, Cornell Univ.

Goldman, S. A., Bruno, G. V., Polnaszek, C. F., and Freed, J. H. (1972a). An ESR study of anisotropic rotational reorientation and slow tumbling in liquid and frozen media, *J. Chem. Phys.* **56**, 716–735.

Goldman, S. A., Bruno, G. V., and Freed, J. H. (1972b). Estimating slow motional rotational correlation times for nitroxides by electron spin resonance, *J. Phys. Chem.* **76**, 1858–1860.

Goldman, S. A., Bruno, G. V., and Freed, J. H. (1973). ESR studies of anisotropic rotational reorientation and slow tumbling in liquid and frozen media II. Saturation and non-secular effects, *J. Chem. Phys.* **59**, 3071–3091.

Gordon, R. G., and Messenger, T. (1972). Ch. XIII, Magnetic resonance line shapes in slowly tumbling molecules, *In* "Electron Spin Relaxation in Liquids" (L. T. Muus and P. W. Atkins, eds.), pp. 341–381. Plenum, New York.

Griffith, O. H., *et al.* (1965). *J. Chem. Phys.* **43**, 2909.

Hamrick, P. J., *et al.* (1972). *J. Chem. Phys.* **57**, 5029.

Hubbell, W. L. and McConnell, H. M. (1969a). Motion of steroid spin labels in membranes, *Proc. Nat. Acad. Sci. U.S.* **63**, 16–22.

Hubbell, W. L., and McConnell, H. M. (1969b). Orientation and motion of amphiphilic spin labels in membranes, *Proc. Nat. Acad. Sci. U.S.* **64**, 20–27.

Hubbell, W. L., and McConnell, H. M. (1971). Molecular motion in spin labeled phospholipids and membranes, *J. Amer. Chem. Soc.* **93**, 314–326.

Hyde, J. S., and Dalton, L. (1972). Very slowly tumbling spin labels: Adiabatic rapid passage, *Chem. Phys. Lett.* **16**, 568–572.

Hwang, J. S., Mason, R., Hwang, L. P., and Freed, J. H. (1975). ESR studies of anisotropic rotational reorientation and slow tumbling in liquid and frozen media III: Perdeuterotempone and an analysis of fluctuating torques, *J. Phys. Chem.* **79**, 489–511.

Johnson, C. S. Jr. (1965). Chemical rate processes and magnetic resonance, *Advan. Magn. Res.* **1**, 33–102.

Kubo, R. (1962). A stochastic theory of line shape and relaxation, *In* "Fluctuation, Relaxation, and Resonance in Magnetic Systems" (D. ter Haar, ed.), pp. 23–67. Oliver and Boyd, London.

Kubo, R. (1969). A stochastic theory of lineshape, *In* "Stochastic Processes in Chemical Physics, Advances in Chemical Physics" (K. E. Shuler, ed.), Vol. XVI, pp. 101–127. Wiley, New York.

Leniart, D. S. (1972). Private Communication.

Libertini, L. J., and Griffith, O. H. (1970). *J. Chem. Phys.* **53**, 1359.

Mason, R., and Freed, J. H. (1974). Estimating microsecond rotational correlation times from lifetime broadening of nitroxide ESR spectra near the rigid limit, *J. Phys. Chem.* **78**, 1321–1323.

Mason, R., Polnaszek, C. F., and Freed, J. H. (1974). Comments on the interpretation of ESR spectra of spin labels undergoing very anisotropic rotational reorientation, *J. Phys. Chem.* **78**, 1324–1329.

McCalley, R. C., Shimshick, E. J., and McConnell, H. M. (1972). The effect of slow rotational motion on paramagnetic resonance spectra, *Chem. Phys. Lett.* **13**, 115–119.

McConnell, H. M., and McFarland, B. G. (1970). Physics and chemistry of spin labels, *Quart. Rev. Biophys.* **3**, 91–136.

McFarland, B. G., and McConnell, H. M. (1971). Bent fatty acid chains in lecithin bilayers, *Proc. Nat. Acad. Sci. U.S.* **68**, 1274–1278.

Meier, V. W., and Saupe, A. (1958). Eine einfache molekulare theorie des nematischen kristallinflüssigen zustandes, *Z. Naturforsch.* **13a**, 564–566.

Miesowicz, M. (1946). The three coefficients of viscosity of anisotropic liquids, *Nature (London)* **158**, 27.

Nordio, P. L., and Busolin, P. (1971). Electron spin resonance line shapes in partially oriented systems, *J. Chem. Phys.* **55**, 5485–5490.

Nordio, P. L., Rigatti, G., and Segre, U. (1972). Spin relaxation in nematic solvents, *J. Chem. Phys.* **56**, 2117–2123.

Ohnishi, S., Boeyens, J. C. A., and McConnell, H. M. (1966). Spin-labeled hemoglobin crystals, *Proc. Nat. Acad. Sci. U.S.* **56**, 809–813.

Pedersen, J. B., and Freed, J. H. (1973a). Theory of chemically-induced dynamic electron polarization. I., *J. Chem. Phys.* **58**, 2746–2762.

Pedersen, J. B., and Freed, J. H. (1973b). Theory of chemically-induced dynamic electron polarization. II., *J. Chem. Phys.* **59**, 2869–2885.

Polnaszek, C. F. (1975a). An ESR Study of Rotational Reorientation and Spin Relaxation in Liquid Crystal Media, Ph.D. Thesis, Cornell Univ.

Polnaszek, C. F. (1975b). The analysis and interpretation of electron spin resonance spectra of nitroxide spin probes in terms of correlation times for rotational reorientation and of order parameters, *Quart. Rev. Biophys.* (to be published).

Polnaszek, C. F., and Freed, J. H. (1975). ESR studies of anisotropic ordering, spin relaxation and slow tumbling in liquid crystalline solvents, *J. Phys. Chem.* **79** (in press).

Polnaszek, C. F., Bruno, G. V., and Freed, J. H. (1973). ESR lineshapes in the slow-motional region: Anisotropic liquids, *J. Chem. Phys.* **58**, 3185–3199.

Rose, M. E. (1957). "Elementary Theory of Angular Momentum." Wiley, New York.

Rotenberg, M., Bivins, R., Metropolis, N., and Wooten, J. K. (1959). "The 3*j*- and 6*j*-Symbols," Technology Press, M.I.T., Boston, Massachusetts.

Smigel, M., Dalton, L. R., Hyde, J. S., and Dalton, L. A. (1974). Investigation of very slowly tumbling spin labels by nonlinear spin response techniques: Theory and experiment for stationary electron-electron double resonance, *Proc. Nat. Acad. Sci. U.S.* **71**, 1925–1929.

Thomas, D. D., and McConnell, H. M. (1974). Calculation of paramagnetic resonance spectra sensitive to very slow rotational motion, *Chem. Phys. Lett.* **25**, 470–475.

Valiev, K. A., and Ivanov, E. N. (1973). Rotational Brownian motion, *Sov. Phys.-Usp.* **16**, 1–16.

Wee, E. L., and Miller, W. G. (1973). Studies on nitroxide spin-labeled poly-γ-benzyl-α,L-glutamate, *J. Phys. Chem.* **77**, 182–189.

McCalley, R. C., Shimshick, E. J., and McConnell, H. M. (1972). The effect of slow rotational motion on paramagnetic resonance spectra, *Chem. Phys. Lett.* **13**, 115–119.
McConnell, H. M., and McFarland, B. G. (1970). Physics and chemistry of spin labels, *Quart. Rev. Biophys.* **3**, 91–136.
McFarland, B. G., and McConnell, H. M. (1971). Bent fatty acid chains in lecithin bilayers, *Proc. Nat. Acad. Sci. U.S.* **68**, 1274–1278.
Meier, V. W., and Saupe, A. (1958). Eine einfache molekulare theorie des nematischen kristallinflüssigen zustandes, *Z. Naturforsch.* **13a**, 564–566.
Miesowicz, M. (1946). The three coefficients of viscosity of anisotropic liquids, *Nature (London)* **158**, 27.
Nordio, P. L., and Busolin, P. (1971). Electron spin resonance line shapes in partially oriented systems, *J. Chem. Phys.* **55**, 5485–5490.
Nordio, P. L., Rigatti, G., and Segre, U. (1972). Spin relaxation in nematic solvents, *J. Chem. Phys.* **56**, 2117–2123.
Ohnishi, S., Boeyens, J. C. A., and McConnell, H. M. (1966). Spin-labeled hemoglobin crystals, *Proc. Nat. Acad. Sci. U.S.* **56**, 809–813.
Pedersen, J. B., and Freed, J. H. (1973a). Theory of chemically-induced dynamic electron polarization. I., *J. Chem. Phys.* **58**, 2746–2762.
Pedersen, J. B., and Freed, J. H. (1973b). Theory of chemically-induced dynamic electron polarization. II., *J. Chem. Phys.* **59**, 2869–2885.
Polnaszek, C. F. (1975a). An ESR Study of Rotational Reorientation and Spin Relaxation in Liquid Crystal Media, Ph.D. Thesis, Cornell Univ.
Polnaszek, C. F. (1975b). The analysis and interpretation of electron spin resonance spectra of nitroxide spin probes in terms of correlation times for rotational reorientation and of order parameters, *Quart. Rev. Biophys.* (to be published).
Polnaszek, C. F., and Freed, J. H. (1975). ESR studies of anisotropic ordering, spin relaxation and slow tumbling in liquid crystalline solvents, *J. Phys. Chem.* **79** (in press).
Polnaszek, C. F., Bruno, G. V., and Freed, J. H. (1973). ESR lineshapes in the slow-motional region: Anisotropic liquids, *J. Chem. Phys.* **58**, 3185–3199.
Rose, M. E. (1957). "Elementary Theory of Angular Momentum." Wiley, New York.
Rotenberg, M., Bivins, R., Metropolis, N., and Wooten, J. K. (1959). "The 3*j*- and 6*j*-Symbols," Technology Press, M.I.T., Boston, Massachusetts.
Smigel, M., Dalton, L. R., Hyde, J. S., and Dalton, L. A. (1974). Investigation of very slowly tumbling spin labels by nonlinear spin response techniques: Theory and experiment for stationary electron-electron double resonance, *Proc. Nat. Acad. Sci. U.S.* **71**, 1925–1929.
Thomas, D. D., and McConnell, H. M. (1974). Calculation of paramagnetic resonance spectra sensitive to very slow rotational motion, *Chem. Phys. Lett.* **25**, 470–475.
Valiev, K. A., and Ivanov, E. N. (1973). Rotational Brownian motion, *Sov. Phys.-Usp.* **16**, 1–16.
Wee, E. L., and Miller, W. G. (1973). Studies on nitroxide spin-labeled poly-γ-benzyl-α,L-glutamate, *J. Phys. Chem.* **77**, 182–189.